BOSTON UNIVERSITY

SCHOOL OF MEDICINE

Dissertation

PROTEIN KINASE C δ IS A POTENTIAL THERAPEUTIC TARGET IN MALIGNANT MELANOMA WITH NRAS MUTATION OR B-RAF INHIBITOR-RESISTANCE

by

ASAMI TAKASHIMA

B.A., University of Tokyo, Tokyo, 2004

M.S., University of Tokyo, Tokyo, 2006

Submitted in partial fulfillment of the

requirements for the degree of

Doctor of Philosophy

2013

Approved by

First Reader [redacted]

Douglas V. Faller, Ph.D., M.D.
Karin Grunebaum Professor of Medicine, Biochemistry, Pediatrics, Microbiology, Pathology and Laboratory Medicine

Second Reader [redacted]

Sam Thiagalingam, Ph.D.
Associate Professor of Medicine, Genetics & Genomics and Pathology & Laboratory Medicine

ACKNOWLEDGEMENTS

First and foremost, I would like to thank Dr. Douglas V. Faller for being a great mentor to me for the past five years. He trained me to be able to think and write logically, and present data and ideas clearly. He also taught me the importance of seeing a big picture all the time even when I plan a small experiment. I would not be able to do what I can do today without his patient and considerate mentorship, and I believe these skills would be valuable no matter what I do in the future. I will always be proud of having been his graduate student.

I would also like to thank my thesis committees, Drs. David C. Seldin (Chair), Adam Lerner, Sam Thiagalingam (Second reader) and Maria V. Panchenko. They have challenged me and provided me advice in any committee meetings, and they have always been helpful and supportive. I looked forward to committee meetings for the exciting discussions with them.

I appreciate the support given by colleagues and friends in Cancer Research Center. Especially, Ms. Lora W. Forman and Dr. Sajal Ghosh not only helped me with experimental techniques based on their profound knowledge and experience, but also have been great friends.

I appreciate the opportunity to pursue a Ph.D. given by the Graduate Program in Molecular Medicine. It has been the great opportunity for me to study the approach of translational research, which was my desire to come to this program.

I was supported by many friends for the entire time of the graduate study. Their supports were indispensable to get me through the difficult times. I would particularly like to thank Hiroshi Tanaka, Yutaka Ikeuchi, Patricia F. Kao, Vivian Tu, Aurther Lambert and Teresa A. Colvin.

Finally, I would like to thank my parents for always being the biggest cheerleaders of my adventures in my entire life and enjoying the every step in this journey with me as much as I did.

PROTEIN KINASE C δ IS A POTENTIAL THERAPEUTIC TARGET IN MALIGNANT MELANOMA WITH NRAS MUTATION OR B-RAF INHIBITOR-RESISTANCE

(Order No.)

ASAMI TAKASHIMA

Boston University School of Medicine, 2013

Major Professor: Douglas V. Faller, M.D., Ph.D., Karin Grunebaum Professor of Medicine, Biochemistry, Pediatrics, Microbiology, Pathology and Laboratory Medicine

ABSTRACT

Metastatic melanoma is the major cause of skin cancer death, and the annual incidence of melanoma continues to increase. Despite the impressively high rates of response to BRAF inhibitors in patients with melanomas harboring BRAF mutations, most of these patients eventually relapse after developing resistance to the drug, due in part to secondary mutations in NRAS. Although NRAS mutation is the second most common genetic mutation in melanoma patients (after BRAF mutation), there is currently no treatment option that targets NRAS-mutated melanomas. Previous reports have demonstrated the sensitivity of cancer cell lines carrying RAS mutations to apoptosis initiated by inhibition of protein kinase C delta (PKCδ), suggesting the possible association between RAS mutational status and sensitivity to PKCδ inhibition. I therefore hypothesized that PKCδ inhibitors might also be cytotoxic in melanomas with primary or

acquired NRAS mutations. In this project, the effect of PKCδ inhibition, and the efficacy of a new PKCδ inhibitor, BJE6-106 (B106), in melanoma were investigated. Inhibition of PKCδ inhibited the growth of multiple human melanoma cell lines carrying NRAS mutations, and induced apoptosis mediated by terminal caspase activation. Analysis of the molecular mechanisms demonstrated activation of the JNK pathway after PKCδ inhibition, leading to the activation (phosphorylation) of H2AX, a histone H2A variant. Activation of H2AX was attenuated when JNK1/2 levels were repressed, indicating that H2AX activation is mediated by the JNK pathway in response to PKCδ inhibition. Consistent with recent reports on the apoptotic role of phospho-H2AX, knockdown of H2AX prior to PKCδ inhibition mitigated the induction of caspase-dependent apoptosis. To explore the potential of B106 further, melanoma cell lines harboring BRAF mutations that had evolved resistance to a BRAF inhibitor, PLX4032 (vemurafenib), were developed. B106 effectively induced cytotoxicity in these cells, suggesting the potential clinical application of targeting PKCδ in patients who have relapsed following treatment with PLX4032. Taken together, this work suggests that inhibition of PKCδ causes caspase-dependent apoptosis in melanomas with NRAS mutations and in PLX4032-resistant BRAF mutant melanomas. This apoptosis is mediated via activation of the JNK-H2AX pathway, which involves a novel role for phospho-H2AX in the execution of apoptosis.

TABLE OF CONTENTS

LIST OF TABLES

LIST OF FIGURES

ABBREVIATIONS

α	Alpha
AP-1	Activator protein-1
β	Beta
B-CLL	B cell chronic lymphocytic leukemia
°C	Degree Celsius
CDK	Cyclin-dependent kinase
cDNA	Complimentary DNA
Ct	Cycle Threshold
CTL	Cytotoxic T-lymphocytes
CTLA-4	Cytotoxic T-lymphocytes antigen 4
δ	Delta
DAG	Diacylglycerol
DMSO	Dimethyl sulfoxide
DNA	Deoxyribonucleic acid
E	Glutamic acid
EDTA	Ethylendiaminetetraacetic acid
EGFR	Epidermal growth factor receptor
EGTA	Ethylene glycol tetraacetic acid
EMT	Epithelial-mesenchymal transition
FDA	Food and Drug Administration
FLIP	FLICE-like inhibitory protein

GAPDH	Glyceraldehyde 3-phosphate dehydrogenase
GF	Growth factor
GSK-3	Glycogen synthase kinase-3
h	Hour(s)
H2AX	Histone H2A variant X
HER2	Human epidermal growth factor receptor 2
IAP	Inhibitor of apoptosis protein
IGF1R	Insulin-like growth factor 1 receptor
IR	Ionizing radiation
JNK	c-Jun N-terminal kinase
K	Lysine
kg	Kilogram(s)
L	Leucine
μM	Micro molar
μg	Microgram(s)
μl	Microliter(s)
MAPK	Mitogen activated protein kinase
min	Minute(s)
mg	Milligram(s)
$MgCl_2$	Magnesium chloride
ml	Milliliter(s)
mm	Millimeter(s)

MTS	3-(4,5-dimethylthiazol-2-yl)-5-(3-carboxymethoxyphenyl)-2-(4-sulfophenyl)-2H-tetrazolium
mRNA	Messenger RNA
n	Sample size
NaCl	Sodium chloride
NaF	Sodium fluoride
NFκB	Nuclear Factor-κ (kappa) B
NIH-BRAF	NIH-3T3 cells stably-transfected with BRAF-V600E mutant
NIH-NRAS	NIH-3T3 cells stably-transfected with NRAS-Q61K mutant
NSCLC	Non-small cell lung cancer
Q	Glutamine
PBS	Phosphate buffered saline
PDGFRβ	Platelet-derived growth factor receptor-β
PFS	Progression free survival
PI3K	Phosphatidylinositol 3-kinase
PKC	Protein kinase C
PKCδ	Protein kinase C delta
PLX-R	PLX-4032 resistant cells
R	Arginine
RBD	Ras binding domain
RNA	Ribonucleic acid
RNAi	RNA interference

ROS	Reactive oxygen species
RT	Room temperature
RTK	Receptor tyrosine kinase
RT-PCR	Real-time polymerase chain reaction
S, Ser	Serine
SAPK	Stress-activated protein kinase
SDS-PAGE	Sodium dodecyl sulfate-Polyacrylamide gel electrophoresis
sec	Second(s)
siRNA	small interference RNA
T, Thr	Threonine
TBS-T	Tris buffered saline-Tween 20
TRAIL	TNF-related apoptosis-inducing ligand
TTP	Time to progression
UV	Ultraviolet radiation
V	Valine
Y, Tyr	Tyrosine
ZVAD, Z-VAD-FMK	Carbobenzoxy-valyl-alanyl-aspartyl-[Omethyl]-fluoromethylketone

Introduction

Melanoma is one of the three major types of skin cancers that originate within the epidermis, which sustains the most damage from the sun. Skin cancers are subcategorized based on the types of cells that the cancers originated from: basal cell carcinomas, squamous cell carcinomas and melanomas. Basal cell and squamous cell carcinomas (collectively referred to as non-melanoma skin cancers) are more prevalent, but highly curable. Conversely, melanomas, originating in melanocytes, account for less than 5% of skin cancers; however, they are responsible for more than 75% of estimated skin cancer deaths in 2012, and more strikingly, the incidence rate has been increasing for the last 30 years (1). Although melanomas can be curable if detected at their earliest stages and treated properly, they are more metastatic than other skin cancer types: for localized melanoma (84% of cases), the 5-year survival rate is 98%; survival declines to 62% and 15% for regional and distant stage disease, respectively (1).

Advanced melanomas are treated with surgery, chemotherapy, and/or radiation therapy. Chemotherapy has not made a significant impact on survival in metastatic melanoma for decades, although some protocols achieved improved response rates. In addition to these conventional treatment options, the Food and Drug Administration (FDA) approved two targeted therapies for metastatic melanomas in 2011. Ipilimumab is an immunotherapy that activates cytotoxic T-lymphocytes (CTL), by blocking CTL antigen 4 (CTLA-4), for destruction of cancerous cells (2). Ipilimumab was targeted for melanoma because it is one of the most immunogenic cancers, as indicated by the presence of tumor infiltrating lymphocytes (2). Although the adverse effects of the

treatment are highly manageable, the clinical benefit remains relatively mild: the response rate (complete and partial responses) was limited to 10-15% and overall survival was extended only by an average of a few months (2).

The other FDA-approved therapy, vemurafenib (also known as PLX4032), was developed to target the genetic background of melanoma. Melanoma is highly-dependent on the Ras/Raf/MEK/ERK pathway, one of the three major pathways of mitogen-activated protein kinase (MAPK) pathways. Melanoma is therefore frequently the target disease area of investigational drugs targeting B-Raf and MEK which are currently in clinical trials (3). Physiologically, upon the arrival of extracellular stimuli, Ras GTPase family proteins (K-Ras, N-Ras and H-Ras) are activated and induce a series of kinase chain-reactions, including the Raf/MEK/ERK pathway (**Figure 1**). The activation of the Raf/MEK/ERK pathway evokes critical changes in cellular activities, such as cell proliferation and survival in normal cells; conversely, uncontrolled activity of the Ras proteins or the Raf/MEK/ERK pathway can result in aberrant proliferation, migration, morphological changes and epithelial-mesenchymal transition (EMT), leading to malignant transformation and progression of cancers. In melanoma, the most common genomic mutations occur in BRAF (one of the three Raf isoforms) which are observed in 50-70% of melanoma cases, while NRAS mutations, the second most frequent in melanoma, account for 15-30% (4-6). While BRAF and NRAS mutations are considered to be mutually exclusive, constitutive hyperactivation of ERK signaling is the common consequence since both molecules lie upstream of the ERK-MAPK pathway (6). Vemurafenib is a selective B-Raf inhibitor which preferentially inhibits the V600E

mutant form of B-Raf over wild-type and was approved for late-stage melanoma patients with BRAF-V600E mutation. In clinical trials, vemurafenib achieved significant response rates and tumor regression in patients with BRAF-V600E mutation compared to conventional treatment; however, responders eventually and inevitably become resistant to this drug and relapse (7). As discussed in Chapter 3 in more detail, one of the proposed mechanisms of acquired resistance to vemurafenib is development of secondary mutations in the NRAS gene and reactivation of ERK-MAPK signaling, whose suppression was originally the goal of vemurafenib action (8).

Although these first targeted therapies approved for melanoma present great potential, there are remaining obstacles to be addressed: low response rates to ipilimumab and recurrence due to drug resistance to vemurafenib. Another remaining problem in melanoma is the absence of targeted therapies for non-BRAF-mutant-melanomas. Vemurafenib was approved specifically for the patients with the BRAF-V600E mutation, while it is still difficult to predict who would respond to treatment with ipilimumab. Even with the emergence of these promising new drugs, these issues still place advanced melanomas among notoriously difficult cancers to treat and new treatment options are urgently needed. Moreover, mutation of BRAF was reported to be associated with enhanced and selective sensitivity to MEK inhibition in comparison to cells harboring either a wild-type BRAF or a RAS mutation, even though target of action of MEK inhibitors does not directly involve BRAF mutations (9). In fact, many investigational MEK inhibitors currently in clinical trials are being tested against BRAF-mutant type

melanomas. This current situation further underlines the need for new strategies, especially for non-BRAF-mutant-melanomas.

Previous reports demonstrated the sensitivity of pancreatic cancer cell lines carrying oncogenic KRAS mutations to apoptosis initiated by inhibition of protein kinase C delta (PKCδ) (10). Although PKCδ belongs to the PKC family of serine/threonine protein kinases, which is involved in the regulation of a wide variety of important cellular functions, PKCδ is not required for survival of normal, non-cancerous cells, making it a potential therapeutic target that can be selective against cancer cells (11). Considered together with the mutation profile of melanoma and the current obstacles to the melanoma therapies, these observations led me to the hypothesis that PKCδ can be a potential therapeutic target in melanomas with an original NRAS mutation or secondary mutation resulting from drug resistance, and that pharmacological inhibitors of PKCδ might provide a clinical benefit to those types of melanomas. This dissertation presents the effect of PKCδ inhibition on cell growth suppression and the efficacy of PKCδ inhibition in melanomas which remain insensitive to the currently-available targeted therapies, and proposes a molecular mechanism of apoptosis and cancer growth inhibition, which involves a novel role for phospho-H2AX.

The dissertation consists of three chapters. Chapter 1 introduces the PKCδ inhibitors used in the project, including BJE6-106 (B106), which has been developed in our lab, and their effects on cell growth inhibition in melanoma with NRAS mutations. It also demonstrates the mechanism of growth inhibition caused by inhibition of PKCδ: caspase-dependent apoptosis. Chapter 2 provides the molecular mechanism by which

PKCδ inhibition leads to apoptosis through activation of the stress response signaling JNK pathway. JNK activation provoked by inhibition of PKCδ is directly linked to the activation of histone H2A variant H2AX, which is a novel mechanism of apoptosis induction. Chapter 3 focuses on the effect of PKCδ inhibition on melanoma cell lines carrying BRAF mutations which developed resistance to vemurafenib, as well as the mechanisms of resistance in these particular sub cell lines. These PLX4032-resistant cells responded to B106 in manner similar to the NRAS-mutant melanoma cells, which might suggest a method to screen for types of cancers that are potentially susceptible to a therapy using PKCδ inhibitors, for future clinical application. The dissertation is concluded with the discussion including the significance of this work and future directions beyond the studies presented.

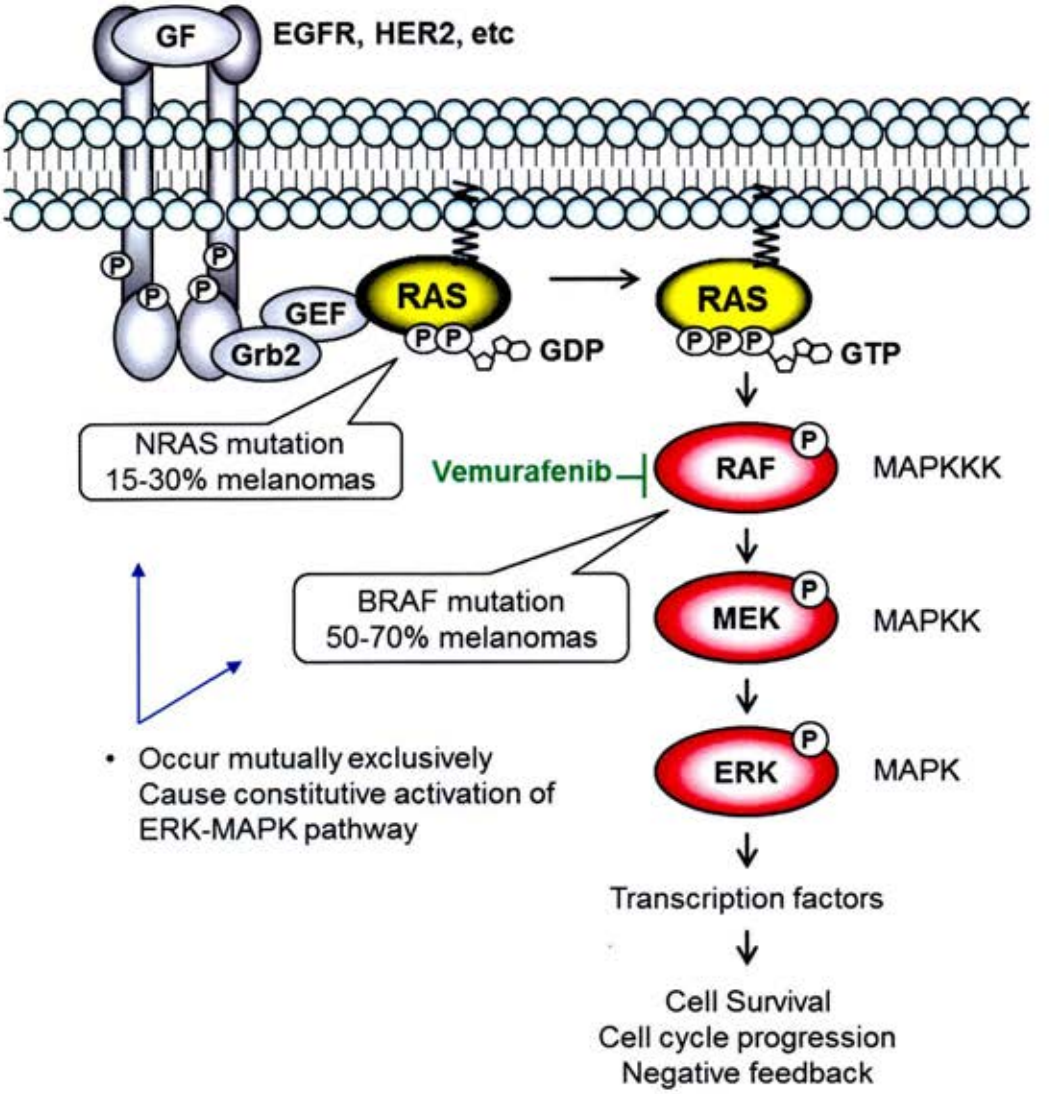

Figure 1: Ras/Raf/MEK/ERK pathway in melanoma. Melanoma is highly-dependent upon Ras/Raf/MEK/ERK signaling for survival. BRAF is the most frequently mutated gene in melanoma and genomic mutations in BRAF are observed in 50-70% of melanoma cases. NRAS mutations account for 15-30% of melanomas. These mutations occur mutually exclusively, but both cause constitutive activation of ERK signaling. Vemurafenib, approved by FDA in 2011 for metastatic melanomas, preferentially inhibits the V600E mutant form of B-Raf over wild-type, which provides cancer-selectivity to the therapy.

Materials and Methods

Reagents

BJE6-106 and BJE6-154 were designed by Dr. Douglas V. Faller with the scheme stated in Chapter 1and synthesized by Dr. Robert M Williams (Colorado State University, Fort Collins, CO). Rottlerin, PLX4032 (vemurafenib), U0126 and propidium iodine, RNase A were purchased from Axxora, LC Labs, Promega, Sigma and Fisher Bio Reagents respectively. Z-VAD-FMK was purchased from R&D Systems and Enzo Life Sciences. Antibodies against phospho-SAPK/JNK (Thr183/Tyr185) (#4668), SAPK/JNK (#9252), phospho-Histone H2A.X (Ser 139) (#2577), Histone H2A (#2578), phospho-SEK1/MKK4) (#4514), SEK1/MKK4 (#9152), phospho-MKK7 (Ser271/Thr275) (#4171), MKK7 (#4172), phospho-c-Jun (Ser63) (#9261), c-Jun (#9165), phospho-ERK1/2 (Thr202/Tyr204) (#4370), phospho-Akt (Ser473) (#4060), phospho-p38 (Thr180/Tyr182) (#4511), p38 (#9212), phospho-c-Raf (Ser338) (#9427) and phospho-B-Raf (Ser445) (#2696) were purchased from Cell Signaling Technologies. Antibodies against ERK1 (K-23), Akt1(B-1), B-Raf (C-19), Raf-1 (C-12) and N-Ras (F155) are purchased from Santa Cruz Biotechnology. Antibodies against Ras (#610001) and PKCδ (#610398) were purchased from BD Biosciences. Antibodies against α-Tubulin (#T6074), β-Actin (#A1978) and GAPDH (#G8795) were purchased from Sigma-Aldrich. Plasmids pBabe-N-Ras-61K and pBabe-Puro-BRAF-V600E were purchased from Addgene. ON-TARGETplus SMART pool siRNA against JNK1 (L-003514), JNK2

(L-003505) and H2AX (L-011682) were purchased from Dharmacon. Silencer Select siRNA against PKCδ (PRKCD) was purchased from Ambion.

Cell culture, siRNA transfection, plasmid stable transfection & PLX4032-resistant sub cell lines

SBcl2 was obtained from Department of Dermatology, Boston University School of Medicine (Boston, MA). A375 and SKMEL5 were obtained from Dr. Remco Spanjard. WM1366, WM1361A, WM852, FM28, FM6, SKMEL2 and SKMEL28 were obtained from Dr. Anurag Singh (Boston University School of Medicine, Boston, MA). NIH-3T3 was purchased from ATCC. SBcl2, and A375 and its derivative lines were maintained in Dulbecco's modified Eagle's medium (DMEM) supplemented with 10% fetal bovine serum. SKMEL5 was maintained in minimum essential medium (MEM) supplemented with 10% fetal bovine serum. NIH-3T3 and its derivative lines were maintained in DMEM supplemented with 10% donor calf serum. All media were additionally supplemented with L-glutamine 2mM, penicillin 100 units/ml, and streptomycin 100μg/ml. siRNA transfection was performed by reverse transcription using Lipofectamine RNAiMax (Invitrogen) according to the product protocol, and media was changed the following day of transfection. NIH-NRAS and NIH-BRAF cell sublines were established by stably transfection with pBabe-N-Ras-61K and pBabe-Puro-BRAF-V600E, respectively, and selection in puromycin-containing medium (2.5μg/ml). PLX4032-resistant cell sublines were established according to the method described in (8). Briefly, A375 and SKMEL5 cells were plated at low cell density and treated with

PLX4032 at 1μM or 0.5μM, respectively. The concentration of PLX4032 was gradually increased up to 4μM (A375) or 2μM (SKMEL5) over the course of 3-4 week period, and clonal colonies were picked up. Derived sublines of A375 and SKMEL5 have been maintained in PLX4032-containing medium at 1-2μM (A375) or 0.5μM (SKMEL5) since selection.

Cell proliferation & Caspase assays

Cell proliferation assays (MTS assay) and caspase assays were performed with CellTiter 96 AQueous Non-Radioactive Cell Proliferation Assay kit and Caspase-Glo 3/7 Assay Systems (Promega) according to the product protocols. Briefly, for the assays employing inhibitors, cells were plated in a 96-well plate (500-4000 cells per well depending on the cell lines and duration of the experiment), treated with inhibitors 24 hours later and cultured for the durations indicated in the individual figure legends. For the assays employing siRNA, cells were plated the day of siRNA transfection, cultured for the duration indicated in the figure legends, and if indicated, treated with inhibitors. After the indicated treatment time, assay reagent was added and cell plates were incubated for 1 hour at 37°C (MTS assay) or 30 minutes at RT (caspase assay). Absorbance at 490nm (MTS assay) or luminescence (caspase assay) were measured using microplate readers for quantification.

Clonogenic colony assay

For the experiments depicted in Figure 7, cells were treated with drugs for the time indicated in the figure, and then the same number of viable cells from each treatment was replated at the low cell density and cells were cultured in normal medium for 8 days, by which time colony formation was quantitated. For the experiments depicted in Figure 28, cells were plated at low density and treated with inhibitors 24 hours later. Cells were cultured in inhibitor-containing medium for the next 8 days. Cell colonies were stained with ethidium bromide for visualization on an ImageQuant LAS 4000 (GE Healthcare) and number of colonies counting.

DNA fragmentation

Cells were harvested and fixed in 1 ml of a 35% ethanol/DMEM solution at 4°C for 30 min. Cells were then stained with a solution containing 25μg/ml of propidium iodide/ml and 50μg/ml of RNase A in PBS and incubated in the dark at 37°C for 30 min for flow cytometric analysis. The proportion of cells in the sub-G1 population, which contain a DNA content of less than 2N (that is, fragmented DNA), was measured as an indicator of apoptosis.

Immunoblotting & Ras activity assay

Whole cell lysates were prepared in a buffer containing 20mM Hepes (pH 7.4), 10% glycerol, 2mM EDTA, 2mM EGTA, 50mM β-glycerophosphate and 1% Triton-X100, 1mM dithiothreitol (DTT) and 1mM sodium vanadate, supplemented with Halt Protease and Phosphatase Inhibitor Cocktail (100X) (Thermo Scientific). For Ras activity assay,

whole cell lysates were prepared in a buffer containing 25mM Hepes (pH 7.4), 150mM NaCl, 1mM EDTA, 10mM MgCl2, 25mM NaF, 10% glycerol, 0.25% sodium deoxycholate, 1% Nonidet P-40 and 1mM sodium vanadate, supplemented with Halt Protease and Phosphatase Inhibitor Cocktail (100X), and activated Ras proteins were pulled down from the whole cell lysates using 10μg of agarose-conjugated Raf-1 Ras binding domain peptide (#14-278, Millipore) according to the product protocol. Lysates were subjected to SDS-PAGE and transferred to nitrocellulose membranes. Membranes were blocked at RT for 1-1.5h with 5% BSA or 5% non-fat dry milk in TBS-T and probed with the appropriate primary antibodies (1:500-1:10,000) overnight. After washing, the blots were incubated with horseradish peroxidase-conjugated secondary antibodies (1:2000-1:10,000) and visualized using the ECL system (Amersham Biosciences) on an ImageQuant LAS 4000.

Quantitative real-time PCR

RNA is extracted with RNeasy Mini kit purchased (Qiagen) according to the product protocol. 1μg of RNA was used to synthesize cDNA in a 20μl reaction volume employing SuperScript III First-Strand Synthesis System (Invitrogen) or QuaniTect Reverse Transcription Kit (Qiagen) according to the product protocol. Quantitative real-time PCR was performed with SYBR Green PCR Master Mix (Applied Biosystems) according to the product protocol. Briefly, cDNA was diluted to a final concentration of 25ng per reaction, added to a primer set (5μM) and SYBR Green PCR Master Mix to a final volume of reaction mixture of 20μl, and run on an Applied Biosystems 7500 Fast

Real-Time PCR system using the following thermal cycling protocol: 50°C for 2 min, 95°C for 10 min, and 40 cycles of 95°C for 15 sec and 60°C for 1 min. The relative amount of an mRNA of interest was calculated by normalizing the Ct value of the mRNA to the Ct of the internal control. Primer sequences were: H2AX Forward: 5'-CAACAAGAAGACGCGAATCA-3', H2AX Reverse: 5'-CGGGCCCTCTTAGTACTCCT-3', β-actin Forward: 5'-GCTCGTCGTCGACAACGGCTC-3', β-actin Reverse: 5'-CAAACATGATCTGGGTCATCTTCTC-3'.

Mouse tumor xenograft model

Prior to the experiment to test B106 for anti-tumor efficacy in mice, tumors were grown and harvested from donor animals for future implantation. Athymic nude mice (Crl:NU(NCr)-Foxn1nu homozygous, Charles River) were injected subcutaneously with 3 x 10^6 cells of the SBcl2 cell line and tumors were grown. Approximately 3 months later, these tumors were harvested, dissected into small blocks (approximately 3 mm3) and frozen in 10% DMSO/medium. For the xenograft study, tumor blocks were implanted subcutaneously into 12 mice and 8 days later, when tumor growth was apparent, dosing was started. 6 mice were administered vehicle (DMSO) intraperitoneally and the other 6 mice were administered B106 (40mg/kg) daily for 12 consecutive days. Tumor size was documented daily and tumor growth rate was calculated.

Genomic mutation analysis

Genomic mutations in NRAS codon 61 and BRAF codon 600 in SBcl2, A375 and SKMEL5 and their drug-resistant sublines were analyzed by Genewiz (Figure 24A, Table 1). Genomic mutations in NRAS codon 61 in FM6, FM28, SKMEL2, WM1366, WM1361A and WM852 were analyzed by Dr. Anurag Sing's Lab (Boston University School of Medicine, Boston, MA).

Chapter 1: PKCδ inhibition causes growth inhibition in melanoma with NRAS mutation by inducing caspase-dependent apoptosis

1-1. Introduction

PKCδ belongs to the PKC family of serine/threonine protein kinases, which is involved in diverse cellular functions, such as cell proliferation, tumor promotion, differentiation and apoptotic cell death (12). The PKC family is categorized into three subfamilies based on structural, functional and biochemical differences, and activators: the classical/conventional PKCs (cPKCs: α, βI, βII, γ), the novel PKCs (nPKCs: δ, ε, θ, μ), and the atypical PKCs (aPKCs: ζ, λ). The novel PKCs that include PKCδ are characteristically activated by diacylglycerol (DAG) and are independent of the second messenger Ca^{2+}. PKCδ is a 77.5 kDa protein, consisting of 676 amino acids and widely expressed among tissues (12). In its inactive state, PKCδ is folded at the linker region between the N-terminal regulatory domain and the C-terminal catalytic domain and auto-inhibited. Upon the binding of DAG to the regulatory domain or phosphorylation on threonine/serine residues, PKCδ changes its conformation into the active state, in which the substrate binding site in the catalytic domain is fully exposed (13). Conversely, phosphorylation of certain other tyrosine residues exerts an inhibitory effect on its kinase activity: in some cases, phosphorylation of the same residue was reported to be either stimulatory or inhibitory depending on the context (12). While this apparent conflict implies a complexity in the regulation of this protein in different circumstances, it also

might be attributed to the fact that the structural information was primarily obtained from *in vitro* studies. It is possible that this might not completely reflect the physiological condition.

PKCδ functions as either a pro- and anti-apoptotic regulator, depending on cellular context, such as stimuli/tissue types or its subcellular localization. Most studies have described it as pro-apoptotic. The existing research on the pro-apoptotic functions of PKCδ can be categorized into three groups based on the following parameters: 1) proteolytic cleavage of PKCδ by caspase 3, 2) subcellular localization of PKCδ, and 3) induction/suppression of other molecules by PKCδ-dependent phosphorylation. The former two events were reported to activate PKCδ under pro-apoptotic environmental conditions, whereas the third category regulates certain downstream effectors of activated PKCδ, which activate the apoptotic cascade in the cell. Proteolytic cleavage of the linker region between the regulatory and catalytic domains by caspase 3, which exposes the substrate binding site in the catalytic domain, is another way of activating PKCδ, in addition to the conformational change introduced by DAG binding or phosphorylation as mentioned above: in contrast, however, proteolytic activation is exclusive to the pro-apoptotic function and irreversible, so that it is believed to occur when cells are destined for apoptosis (13). Translocation of cytosolic PKCδ to multiple subcellular organelles has been reported, possibly in a tissue- or stimulus dependent manner, but the mitochondria and nuclei appear to be the major destinations. Translocated PKCδ phosphorylates apoptotic regulators in those compartments. While translocation can occur with or without proteolytic cleavage by caspase 3, translocation can also trigger proteolytic

cleavage (13, 14) (**Figure 2**). There are various downstream targets of pro-apoptotic PKCδ reported which appear to also be subject to cellular contexts, including MAPK family (ERK, p38, JNK), Bcl-2 family(15-18), the inhibitor of apoptosis (IAP) family (19) or p53 (15, 20) (**Figure 2**). Among MAPK signaling pathways, stress-activated protein kinase/c-Jun N-terminal kinase (SAPK/JNK) and p38 are known to mediate the stress response signaling. PKCδ has been reported to provoke apoptosis through activation of p38 or JNK (17, 18, 21-27). On the other hand, both stimulation and suppression of ERK signaling, often known as a pro-survival signaling, downstream of activated PKCδ, was shown to cause apoptosis (28, 29). Tumor suppressor p53-mediated apoptosis and cell cycle arrest through increased expression of cyclin-dependent kinase (CDK) inhibitors $p21^{Cip1/WAF1}$ and $p27^{Kip1}$ have also been reported to occur downstream of activated PKCδ (20, 30-33).

Although PKCδ is mainly known as a pro-apoptotic regulator, the anti-apoptotic/pro-survival function of PKCδ has also been documented in multiple studies. Increased expression of PKCδ has been observed in various types of cancers (34-36). In B cell chronic lymphocytic leukemia (B-CLL) cells isolated from patient blood, PKCδ was activated and its inhibition strikingly induced apoptosis in contrast to normal peripheral blood B cells (37). The role of PKCδ in anti-apoptotic/pro-survival signaling has been reported in non-small cell lung cancer (NSCLC), pancreatic, breast and colon cancer cells, neutrophils, thyroid cells, inslin-secreting cells (35, 36, 38-42). In these studies, PKCδ was implicated as an early regulator in the anti-apoptotic/pro-survival signaling cascades through induction or suppression of downstream substrates (**Figure**

2). Pro-survival signaling pathways involving ERK, AKT or NF-κB were most frequently indicated as PKCδ downstream targets among these studies, whereas one group reported PKCδ downregulation increased ERK activity and caused apoptosis in a breast cancer cell line (37, 40-46). Knockdown of PKCδ was reported to induce JNK-mediated apoptosis via intermediate upregulation of PKCα and PKCβ in prostate cancer cell lines (47). Interestingly, glycogen synthase kinase-3 (GSK3) was implicated to be either an upstream or downstream regulator of PKCδ (40, 42). Expression of FLICE-like inhibitory protein (FLIP), an endogenous caspase inhibitor, and cIAP2, a member of inhibitor of apoptosis (IAP) family, were induced by activation of PKCδ (45, 46). PKCδ facilitates proliferation of insulin-secreting cells by promoting nuclear export of $p21^{Cip1/WAF1}$ (48).

PKCδ is also implicated in metastasis of melanoma. Overexpression of PKCδ increased the metastatic potential of murine BL16 mouse melanoma cells, and elevated expression of PKCδ and PKCα was shown to be responsible for integrin-mediated invasion of melanoma cells (49, 50). In addition, several studies demonstrated that inhibition of PKCδ sensitized cells to apoptosis induced by chemotherapeutic agents, such as trastuzumab, cisplatin or doxorubicin analogs, or TNF-related apoptosis-inducing ligand (TRAIL) through inhibition of ERK, AKT or NF-κB pathways (35, 44, 51, 52).

Our previous studies demonstrated the sensitivity of pancreatic cancer cell lines carrying oncogenic KRAS mutations to apoptosis initiated by inhibition of PKCδ by means of a chemical inhibitor or RNA interference (RNAi) (10). Oncogenic mutations of Ras proteins are found in up to 30% of all human tumors, and are particularly frequent in those types of cancers with the highest mortality rates, such as lung, colorectal and

pancreatic cancers and melanomas. For this reason, pharmacological interventions of oncogenic Ras proteins have long been sought; however, direct targeting of Ras proteins themselves was unexpectedly challenging and Ras proteins are now widely considered to be "undruggable" targets (please see my recent review (3)). Meanwhile, the emerging (or rediscovered) strategies variously termed "synthetic lethality" and "non-oncogene addiction" have produced a framework for the development of indirect approaches to targeting mutant Ras in cancer cells. Two genes are in a so-called "synthetic lethal" interaction if a mutation of either gene alone is compatible with viability but simultaneous mutations of both genes lead to cell death (53-55). Thus, inhibition of a synthetic lethal interactor of Ras theoretically kills only tumor cells with a mutated RAS gene without affecting normal cells. Similarly, "non-oncogene addiction" describes the situation in which transformation of a cell (whether by a known oncogene or unknown mechanisms) renders it dependent upon a normally non-essential protein for survival (56). These concepts have provided a new approach to target oncogenic Ras indirectly: that is, to discover synthetic lethal interactors, or critical "non-oncogenes," which are more druggable than Ras, and then develop therapeutic methods to target these interactors. Importantly for this new approach, PKCδ is not required for the proliferation or survival of normal cells, and PKCδ-null animals develop normally and are fertile, suggesting the potential tumor-specificity of a PKCδ-targeted approach (11). In the previous work mentioned above, inhibition of PKCδ induced apoptosis in pancreatic cancer cell lines with activating KRAS mutations at least in part through suppression of

AKT signaling, and "Ras-dependency" in the tumors was not required for the cytotoxic effects (10, 57).

In this chapter, the project hypothesis, which postulated potential cytotoxic effects of PKCδ inhibition in melanoma with NRAS mutation, was tested using multiple modalities of PKCδ inhibition, including chemical inhibitors, such as a commercially available PKCδ inhibitor and a novel inhibitor that has been developed in our lab, and siRNA in multiple melanoma cell lines with NRAS-Q61 mutations. Chapter 1 also demonstrates the efficacy of the new inhibitor and the mechanism of cell growth inhibition induced by PKCδ inhibition.

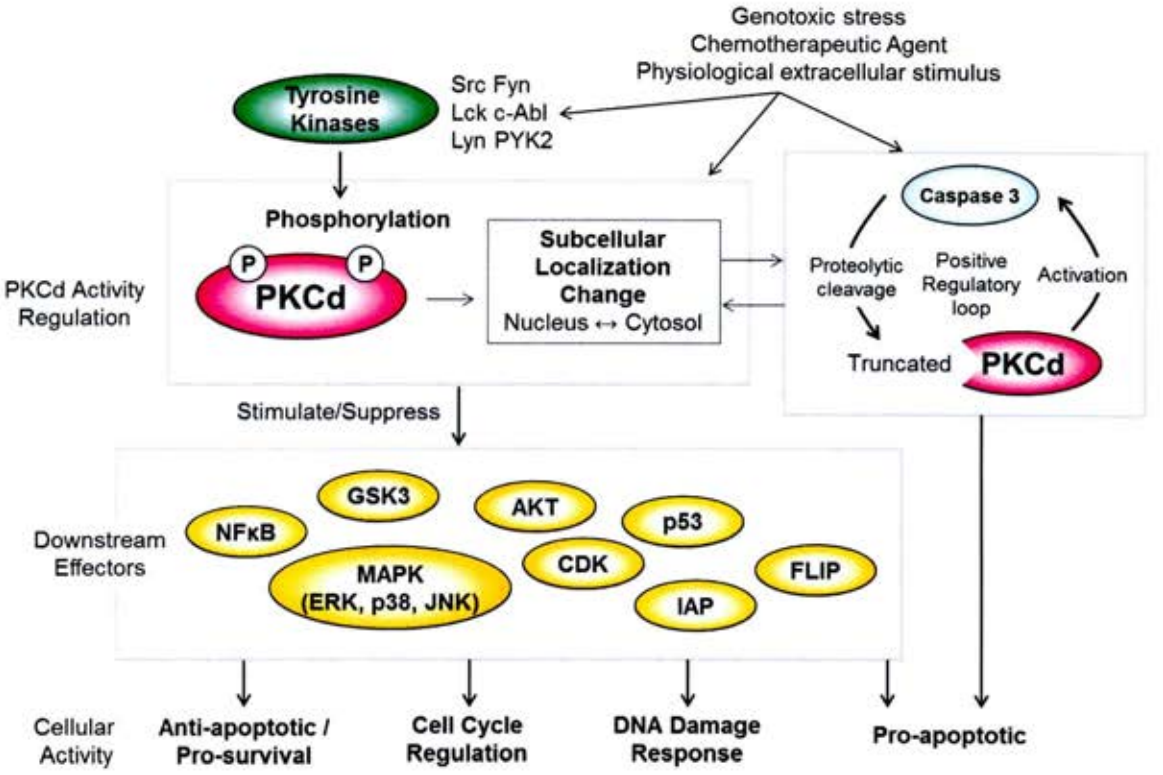

Figure 2: Complexity of PKCδ regulation, downstream effectors and outcome. PKCδ is activated by proteolytic cleavage, changes in subcellular localization or phosphorylation of tyrosine residues. Activation of PKCδ is involved in multiple cellular activities including apoptosis, cell cycle regulation or DNA-damage response through stimulation or suppression of a variety of signaling pathways.

1-2. Results

Characteristics of novel PKCδ inhibitor BJE6-106 (B106)

The rationale for PKCδ as a therapeutic target in cancer-targeted therapies is supported by the preceding reports: 1) its inhibition preferentially inhibits the growth of pancreatic cancer cells with KRAS mutation, which is prominent in many types of cancers with particularly high prevalence and mortality rates, and inhibits cells into which activated K-Ras or H-Ras have been introduced, as well as a variety of other tumor cell lines with RAS mutations (10, 58), and 2) PKCδ is not required for the proliferation or survival of normal cells (56). Although commercially-available rottlerin has been extensively utilized as a PKCδ-selective inhibitor in many fields of research , its exclusive specificity against PKCδ has been questioned in a recent study (59). Some PKC isozymes are required for normal physiological functions and inhibition of such isozymes by a non-selective PKCδ inhibitor could damage normal cells (60). We therefore pursued development of a more potent PKCδ inhibitor with higher PKCδ selectivity. In the effort to seek next generation PKCδ-selective inhibitors, a number of compounds were designed based on the structure of rottlerin (for isozyme specificity) and the pan-PKC inhibitor staurosporine (for potency). Among 36 novel compounds synthesized, BJE6-106 (B106), showed the greatest potency in different types of cancer cell lines including melanoma, prostate cancer, triple-negative breast cancer, and pancreatic cancer (data not shown). **Figure 3** shows the chemical structures of the PKCδ inhibitors used in this study (rottlerin and B106). BJE6-154 (B154) was among the least potent of 36 compounds

studied and is being used as the negative control with minimal inhibitory activity against PKCδ. *In vitro* kinase assays demonstrated IC_{50} value of 50nM for B106 against PKCδ, and verified a 1000-fold PKCδ selectivity over PKCα (**Table 1**). To further validate the target specificity of B106, *in vitro* kinase assays in which B106 is tested against a panel of kinases are being planned in the near future. All three compounds were dissolved in DMSO for the following studies.

Changes in cell morphology induced by rottlerin or B106 treatment in SBcl2, a melanoma cell line with NRAS-Q61K mutation, were compared (**Figure 4**). Morphological changes were observed as early as 5 hours after the initiation of B106 treatment; some cells started to round up and floating cells were observed. By 24 hours of treatment, the majority of cells were detached or detaching from the surface of the cell culture plate. In contrast, rottlerin treatment did not dramatically affect the appearance of the cells even after 24 hours of treatment. Few floating cells were observed with rottlerin treatment, although the number of cells on the cell culture plate was fewer than that of cells treated with vehicle (DMSO) or B154, a negative control compound for PKCδ inhibition. B154 treatment did not change the cell morphology at any treatment time.

Inhibition of PKCδ activity induces cell growth inhibition in melanoma cell lines with NRAS mutations

To investigate the effect of PKCδ inhibition on tumor cell growth, I began by assessing survival of melanoma cells in the presence of rottlerin or B106. In order to ensure the consistency among different cell lines and exclude the possibility of cell line-

specific effects, multiple melanoma cell lines with NRAS mutations were tested: SBcl2, FM6, WM1366, WM1361A, WM852, FM28 and SKMEL2. The presence of genomic mutations in the NRAS gene was confirmed by sequencing analysis (**Table 2**). Cells were treated with rottlerin (2 or 5μM) or B106 (0.1, 0.2 or 0.5μM) and the quantity of viable cells was measured at 24, 48 and 72 hours after treatment by a MTS assay (**Figure 5**). A MTS assay determines the mass of viable cells by the amount of MTS metabolite generated, as measured by the amount of 490nm absorbance, and this is directly proportional to the number of living cells in culture. Rottlerin consistently inhibited proliferation of all cell lines at 5μM and intermediate inhibitory effects were observed at 2μM. The new PKCδ inhibitor B106 effectively inhibited growth of all cell lines tested at 0.5μM, or 0.2μM in some cell lines, which is at least 10 times lower than the concentration of rottlerin required to exert the same degree of effect. B154 treatment at 2μM produced a proliferation curve similar to vehicle (DMSO) treatment in all cell lines, indicating cell growth inhibition induced by B106 indeed resulted from the inhibition of PKCδ activity. These assays demonstrated the greater potency of B106 on tumor cell growth inhibition in comparison to rottlerin, with activity at nano molar concentrations.

Subsequently, a clonogenic colony assay was performed in SBcl2 cells to test the kinetics of irreversible actions of PKCδ inhibitors on the growth and proliferative characteristics of the cells. In contrast to a MTS assay which highlights the temporary survival ability of cells under drug treatment, a clonogenic assay illustrates more relevant clinical benefit. In the clinical setting, patients receive treatment for a certain amount of time, but anti-cancer effect of a drug is expected to sustain after the treatment is

terminated. In this assay, cells were treated with rottlerin or B106 for 12, 24 and 48 hours and then cells were replated in normal medium without drugs (washout). This assay assesses the timeframe required for the compounds to inflict irreversible damage to cells by measuring the difference in colony-forming ability of cultures grown under vehicle control and inhibitor treatment. Both rottlerin and B106 treatment significantly decreased the number of colonies formed in SBcl2 cells after as short as 12 hours of treatment, and approximately 40-fold reduction in the number of colonies was observed with 48 hours of drug treatment (**Figure 6**). This experiment demonstrated an irreversible cytotoxic effect of PKCδ inhibitors on tumor cell growth.

As kinase inhibitors inevitably generate off-target effects, the effect of PKCδ-selective inhibition on cell growth was confirmed by knocking down protein expression of PKCδ using siRNA in multiple melanoma cell lines with NRAS mutations (**Figure 7**). Cells were transfected with siRNA targeting PKCδ or scrambled control siRNA at 50 or 5nM depending on the cell line-specific optimal transfection conditions, and MTS assays were conducted on each day starting 3 or 4 days after siRNA transfection to measure the number of viable cells. Treatment with rottlerin or transfection reagent alone (without siRNA) served as a positive control of cell growth inhibition and a vehicle control, respectively. Downregulation of PKCδ, confirmed by immunoblotting, significantly inhibited proliferation of melanoma cells with NRAS mutation, particularly SBcl2, FM28 and FM6. Although transfection with scrambled control siRNA produced slight cytotoxicity in some cell lines, the resulting proliferation curve did not greatly differ from that of vehicle control in these cell lines. Interestingly, the degree of protein knockdown,

quantified by densitometric analyses, did not appear to be the sole factor in determining the degree of growth inhibitory effect by siRNA transfection, as they were not correlated throughout cell lines. It is possible that some cell lines are more susceptible to cell growth inhibition resulting from PKCδ downregulation, regardless the degree of knockdown. These assays verified that cell growth inhibition can be induced by selective downregulation of PKCδ in melanoma cells with NRAS mutations, as was observed with the inhibition of PKCδ activity by chemical compounds.

Collectively, these experiments supported PKCδ as a potential therapeutic target in melanoma with NRAS mutation, a subtype which is not susceptible to the currently-available targeted therapies in melanoma. The new PKCδ inhibitor B106 demonstrated great potency for effective cancer cell growth inhibition, active at nano molar concentrations, and may serve as a lead compound for *in vivo* application in melanoma.

Inhibition of PKCδ activity triggers caspase-dependent apoptosis

Next, I sought to determine how PKCδ inhibition results in suppression of tumor cell growth in melanoma. Induction of apoptosis is one of the most desirable mechanisms for chemotherapeutic action since, theoretically, it selectively kills cells in which an apoptotic signal is introduced without adversely affecting surrounding cells and hence creates fewer chances to induce inflammation or tissue scarring (61). Apoptosis, which can be initiated by various stimuli, intrinsic or extrinsic inducers, is mediated in many cases by a proteolytic cascade of caspases, a family of cysteine proteases (62). There are two subtypes of caspases: initiator caspases and effector caspases. Activated by early

apoptotic events, initiator caspases (e.g. caspase-8, caspase-9) proteolytically activate effector procaspases (e.g. caspase-3, caspase-7). Activated caspase 3 and caspase 7, the ultimate executioners of apoptosis, trigger proteolytic cleavage of crucial key apoptotic proteins, which in turn leads to the late apoptotic events, including DNA fragmentation (62). To explore the possible involvement of apoptosis in the cell growth inhibition induced by PKCδ inhibition, the activity of caspase 3 and 7 was assessed in cells treated with PKCδ inhibitors. **Figure 8** demonstrated that 24 hours of treatment of SBcl2 cells with rottlerin (2μM) or B106 (0.2 and 0.5μM) significantly increased the activity of caspase 3/7 compared to vehicle (DMSO) treatment. The effect of B106 on caspase 3/7 activation was more extensive than that of rottlerin: 10-fold increase at 0.2μM and 12.5-fold increase at 0.5μM of B106 treatment, in contrast to 5-fold increase by rottlerin treatment at 5μM. The negative control compound B154 did not induce the activity of caspase 3/7. This experiment indicated the involvement of caspase 3/7-mediated apoptosis in response to PKCδ inhibition. This was further investigated by examining subsequent event characteristic of apoptosis, in the following experiment. In Figure 9, the degree of DNA fragmentation, a hallmark of later events in the sequence of the apoptotic process, in the presence or absence of PKCδ inhibitors was assessed by means of a flow cytometric analysis using propidium iodine staining of DNA. This assay provides information on cellular DNA content in the cell population by dividing the population based on DNA content detected by the amount of propidium iodide incorporated in DNA. The proportion of cells containing a DNA content of less than 2n, that is, fragmented DNA, categorized into the "sub-G1" population and considered to be undergoing the late

apoptotic phase DNA fragmentation, was significantly higher after treatment with rottlerin at 5μM and even higher after treatment with B106 at 0.5μM, whereas B154, a negative control compound for B106 with little PKCδ inhibitory activity, produced the same fraction of fragmented DNA as vehicle control (DMSO), suggesting the effect of B106 on DNA fragmentation was caused by inhibiting PKCδ activity (**Figure 9**). To determine whether activation of caspases by these PKCδ-inhibitory compounds was necessary for the observed apoptosis, the pan-caspase inhibitor Z-VAD-FMK (carbobenzoxy-valyl-alanyl-aspartyl-[Omethyl]-fluoromethylketone) was employed. Z-VAD-FMK irreversibly binds to the catalytic site of caspase proteases and prevents caspases from being cleaved and activated. Pre-treatment of cells with Z-VAD-FMK (50μM) prevented B106-induced caspase 3 cleavage in a preliminary immunoblot analysis (data not shown). B106-induced DNA fragmentation was significantly abrogated when Z-VAD-FMK (100μM) was used in SBcl2 cells (**Figure 9**). Treatment of Z-VAD-FMK alone produced only a similar fraction of sub-G1 cells as did vehicle or B154 treatment. Taken together, these data suggest that PKCδ-inhibition attenuates tumor cell growth by inducing caspase-dependent apoptosis in NRAS-mutated melanoma cells.

B106 in a mouse tumor xenograft model

Based on the potent anti-tumor activity of B106 in the melanoma cell culture systems, I proceeded to test the efficacy of B106 *in vivo* in a mouse xenograft tumor model. Tumor blocks of SBcl2 cells were implanted into 12 mice and dosing was started 8 days after tumor implantation; 6 mice received B106 intraperitoneally at 40 mg/kg and

the other 6 mice were given DMSO, the vehicle solvent of B106, daily for 12 consecutive days. Tumor size was measured daily and tumor growth rate was calculated. Treatment of B106 did not produce any difference in tumor growth compared to the DMSO-treated group (**Figure 10**). There are, however, two concerns remaining at this point regarding pharmacokinetics of B106. First, it is unclear whether the drug entered into the systemic circulation and delivered to the local areas, as B106 is extremely hydrophobic and could not be diluted with hydrophilic solvent. Secondary, there is no information regarding how fast the drug is metabolized at this time. A new generation of compounds with hydrophilic modification of the B106 structure is currently being synthesized (**Figure 11**). When any of these compounds is revealed to be as potent as B106 in the cell culture system, its *in vivo* efficacy and pharmacokinetics will be tested.

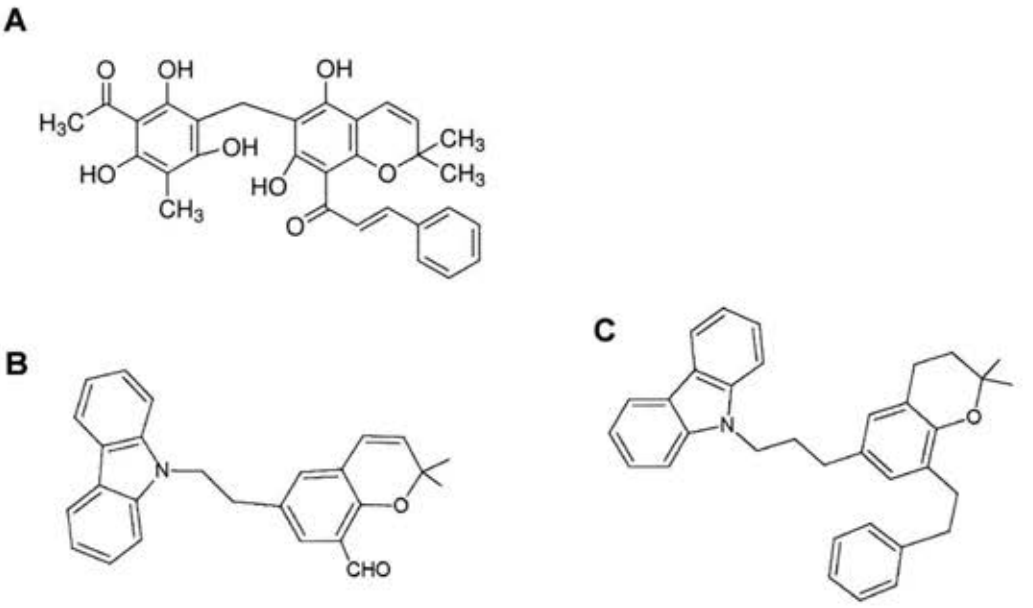

Figure 3: Chemical structures of PKCδ inhibitors. (A) Rottlerin, (B) BJE6-106 [referred as B106], (C) BJE6-154 [referred as B154]. BJE6 compounds were designed based on the structures of pan-PKC inhibitor (for potency) and rottlerin (for isozyme specificity).

Compounds	PKCδ IC_{50}	PKCα IC_{50}	PKCδ/PKCα Selectivity	*In vitro* Ras-specific Cytotoxicity	*In vivo* Ras-specific Cytotoxicity
Rottlerin	3 μM	75 μM	28-fold	3 μM	Yes
B106	0.05 μM	50 μM	1000-fold	0.5 μM	Not active*
B154	>25 μM	>100 μM	-	-	No

Table 1: Comparison of PKCδ inhibitors. *In vitro* kinase assays demonstrated that B106 is more potent as a PKCδ inhibitor and more selective against PKCδ over PKCα than rottlerin. *: not yet optimized for drug-like properties, so *in vitro* activity represents a minimum of the potential activity of a more hydrophilic derivative.

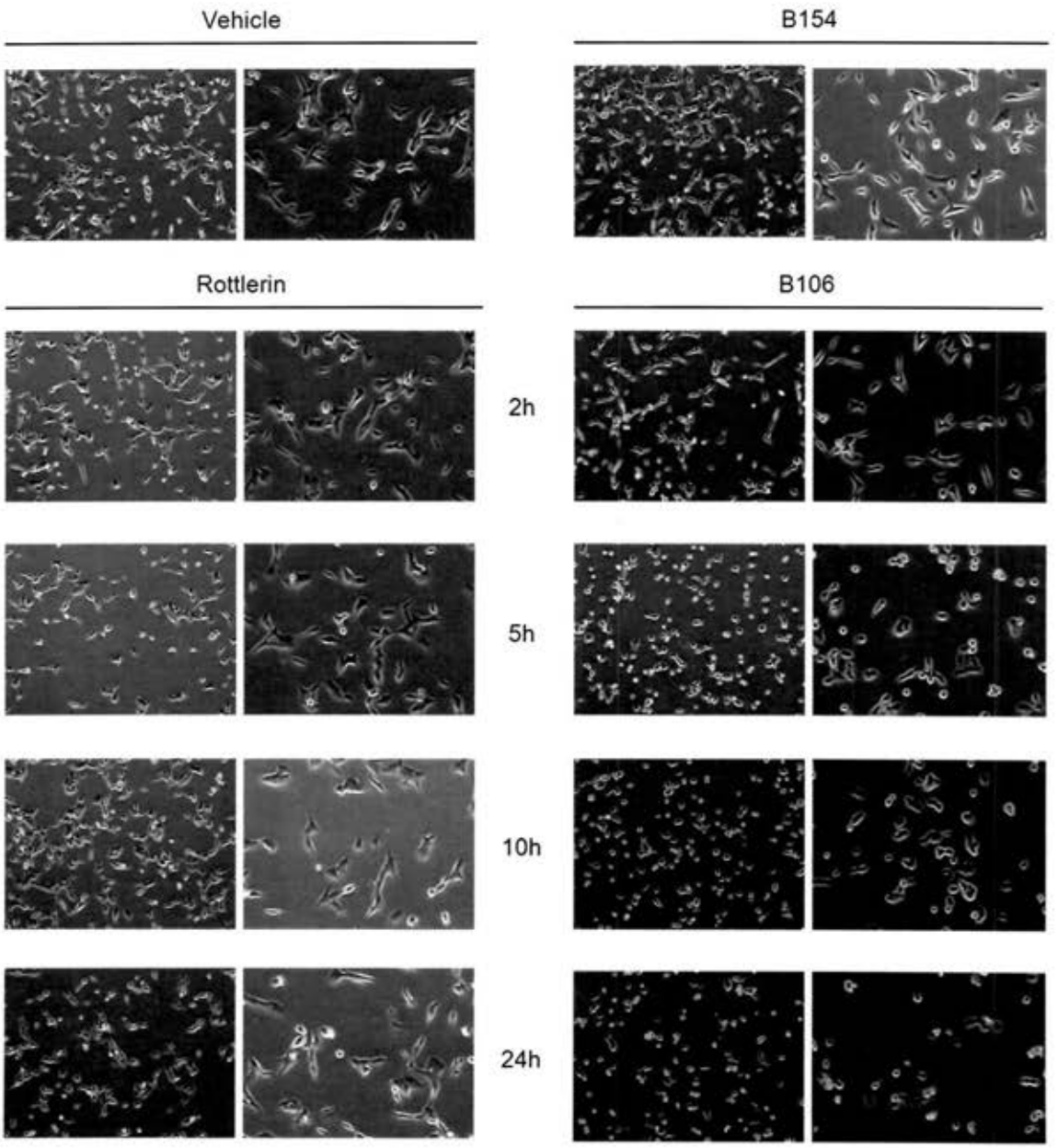

Figure 4: Comparison of morphological changes induced by PKCδ inhibitor treatment in SBcl2 cells. Cells were treated with rottlerin (5μM) or B106 (0.5μM) for the indicated times and microphotographs were taken at a lower (left) and a higher magnification (right). DMSO and B154 (0.5μM) served as a vehicle control and a negative compound control, respectively. Cell morphological changes and induction of floating (dead) cells started as early as 5 hours of B106 treatment. In contrast, rottlerin treatment did not affect the appearance of cells within 24 hours, although the number of the cells per well remained lower in rottlerin-treated cells than that in cells treated with vehicle or B154.

Cell line	Genomic mutation	Amino acid mutation	Allele
SBcl2	C181A	Q61K	Homozygous
FM28	C181A	Q61K	Homozygous
FM6	C181A	Q61K	Heterozygous
WM852	A182G	Q61R	Homozygous
SKMEL2	A182G	Q61R	Heterozygous
WM-1361A	A182G	Q61R	Heterozygous
WM-1366	A182T	Q61L	Heterozygous

Table 2: NRAS Q61 mutations of cell lines used in the project.

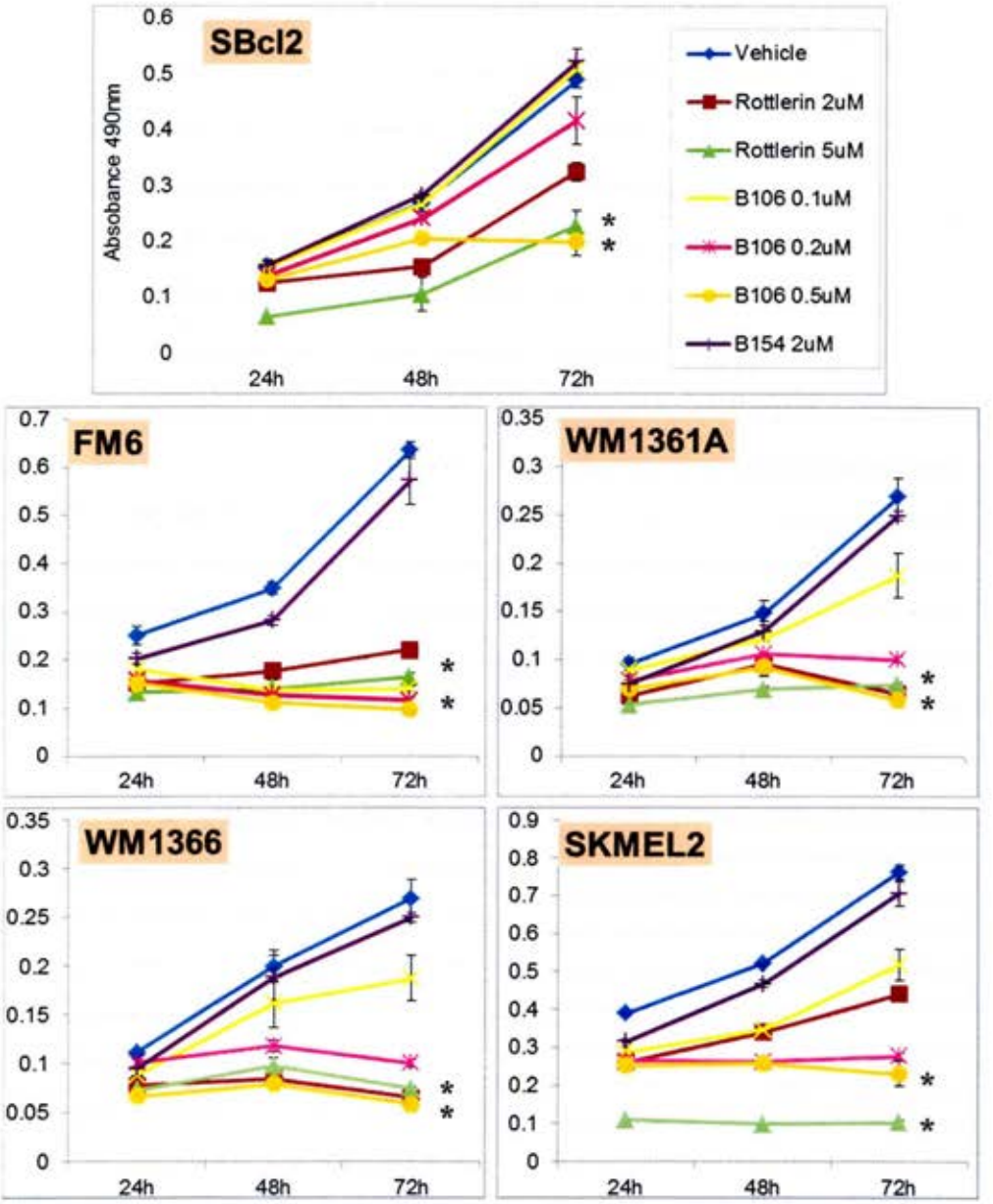

Figure 5: Effect of rottlerin and B106 on cell survival in melanoma cell lines with NRAS mutation. SBcl2, SKMEL2 FM6, WM1361A and WM1366 cells were treated with rottlerin (2 or 5μM) or B106 (0.1, 0.2 or 0.5μM) for 24, 48 or 72 hours. MTS assays were performed at each time point, with the amount of 490nm absorbance being proportional to the number of viable cells. DMSO and B154 (2μM) served as a vehicle control and a negative compound control, respectively. Each point represents the average of triplicates and error bars indicate the standard deviations of triplicates. P values (*) were calculated between DMSO (vehicle control) and rottlerin 5μM, or DMSO and B106 0.5μM in each cell line at 72 hours ($p < 0.0002$). The experiment was repeated at least twice in each cell lines.

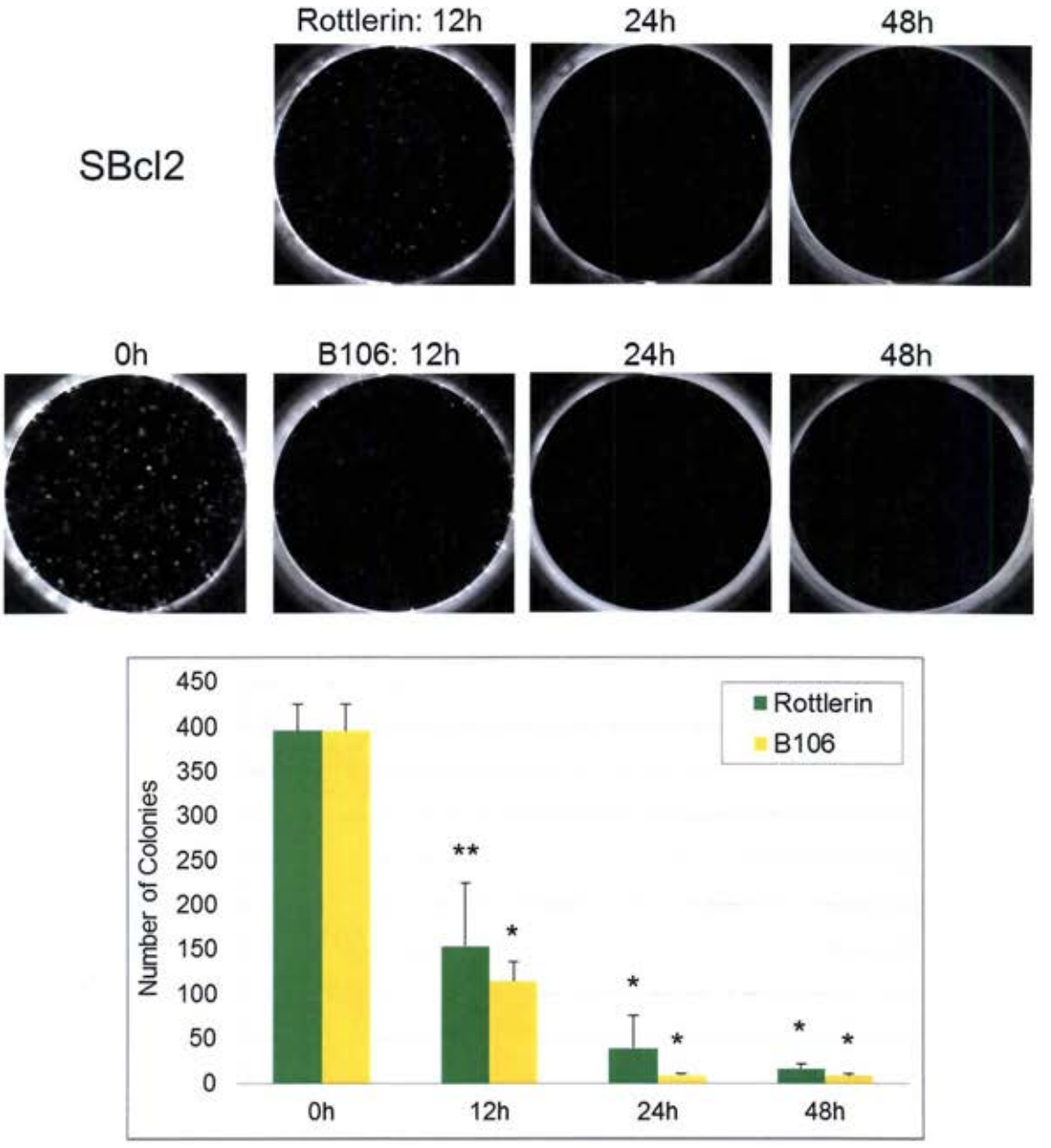

Figure 6: Irreversible effect of rottlerin and B106 on cell growth (clonogenic colony assay) in SBcl2 cells. Cells were treated with rottlerin or B106 at 5μM for 0, 12, 24 or 48 hours. After these treatment time, the same number of viable cells from each treatment was replated at the low cell density and cells cultured in normal medium for 8 days, by which time colony formation was distinctly observed. Cell colonies were stained with ethidium bromide for visualization and counting. Each point represents the average of triplicates and error bars indicate the standard deviations of triplicates. P values: ** $p<0.01$, * $p<0.001$ compared to time 0h. The experiment was repeated twice.

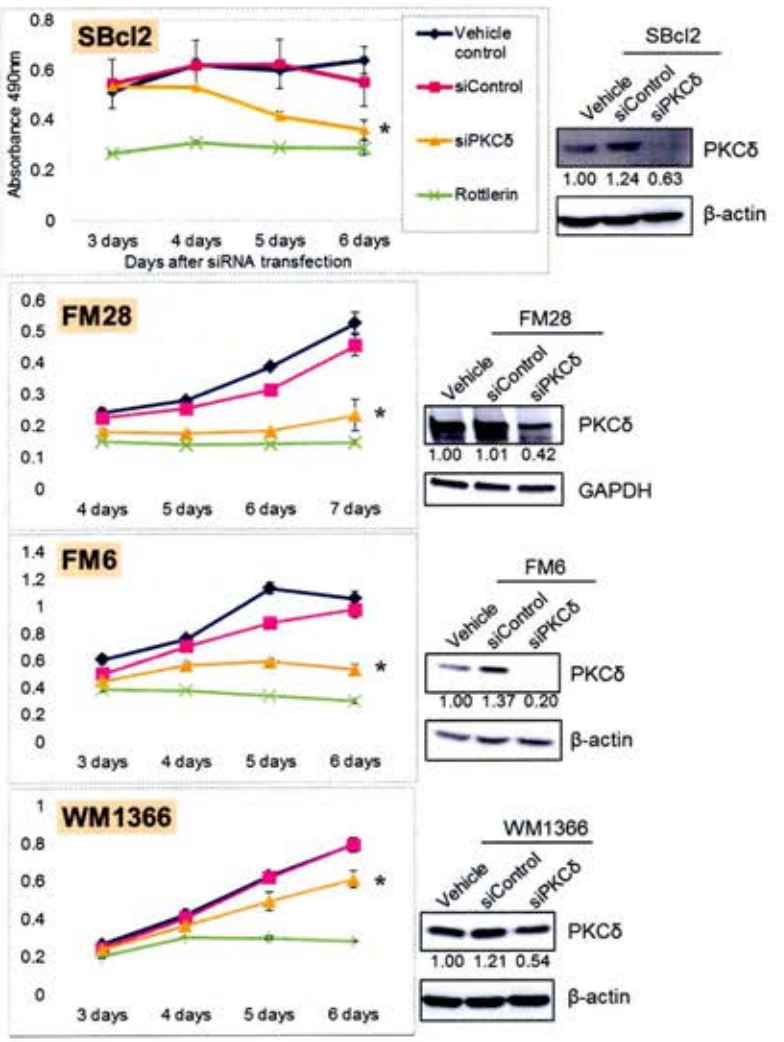

Figure 7: Effect of PKCδ knockdown on cell survival in melanoma cell lines with NRAS mutation. siRNA targeting PKCδ ("siPKCδ") or scrambled siRNA ("siControl") were transfected into SBcl2 and FM28 (50nM), and to FM6 and WM1366 (5nM). Rottlerin (5μM) served as a positive control of cell growth inhibition and "vehicle control" or "vehicle" indicates treatment with transfection reagent alone as another negative control. MTS assays were performed at the indicated days after siRNA transfection to measure the amount of 490nm absorbance being proportional to the number of viable cells. Each point represents the average of triplicates and error bars indicate the standard deviations of triplicates. P values (*) were calculated between vehicle control and siPKCδ on the last MTS-assay-day ($p < 0.006$). Downregulation of PKCδ protein on the first assay-day was assessed by immunoblotting. The relative band intensity of PKCδ was indicated below the image (normalized to loading controls, β-actin or GAPDH). The experiment was repeated at least twice in each cell line.

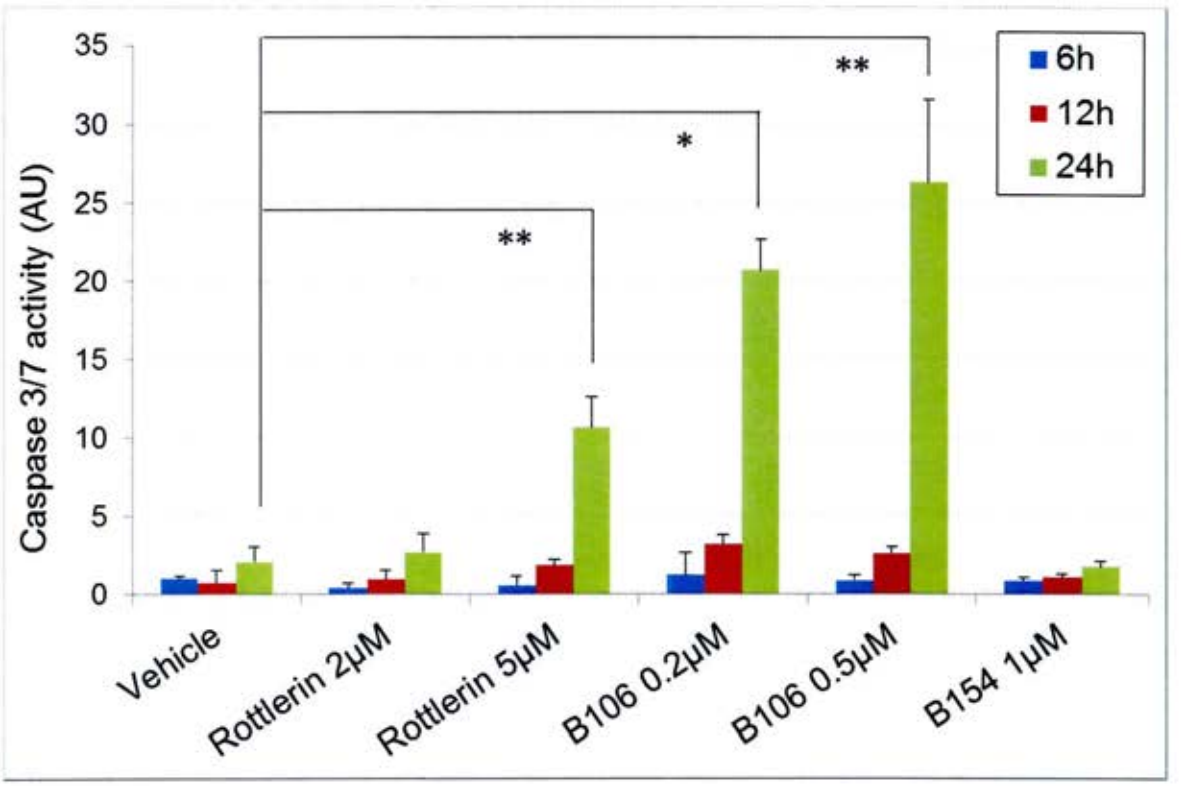

Figure 8: Activation of caspase 3/7 induced by PKCδ inhibitors in SBcl2 cells. Cells were treated with rottlerin (2 or 5μM) or B106 (0.2 or 0.5μM) for 6, 12 or 24 hours and caspase 3/7 activity was measured by luminescense at each time point. DMSO and B154 (1μM) served as a vehicle control and a negative control for PKCδ inhibition, respectively. The assay reagent contains a luminogenic substrate bound to a caspase 3/7 target peptide sequence. The amount of luminescence is proportional to the amount of activated caspase 3/7, which releases the luciferase substrate, making it available for reaction by cleaving it at the target sequence. Values of each treatment and time point were normalized to that of vehicle-treated sample at 6 hours. Error bars indicate the standard deviations of triplicates. P values: ** $p < 0.003$, * $p < 0.0002$. The experiment was repeated twice.

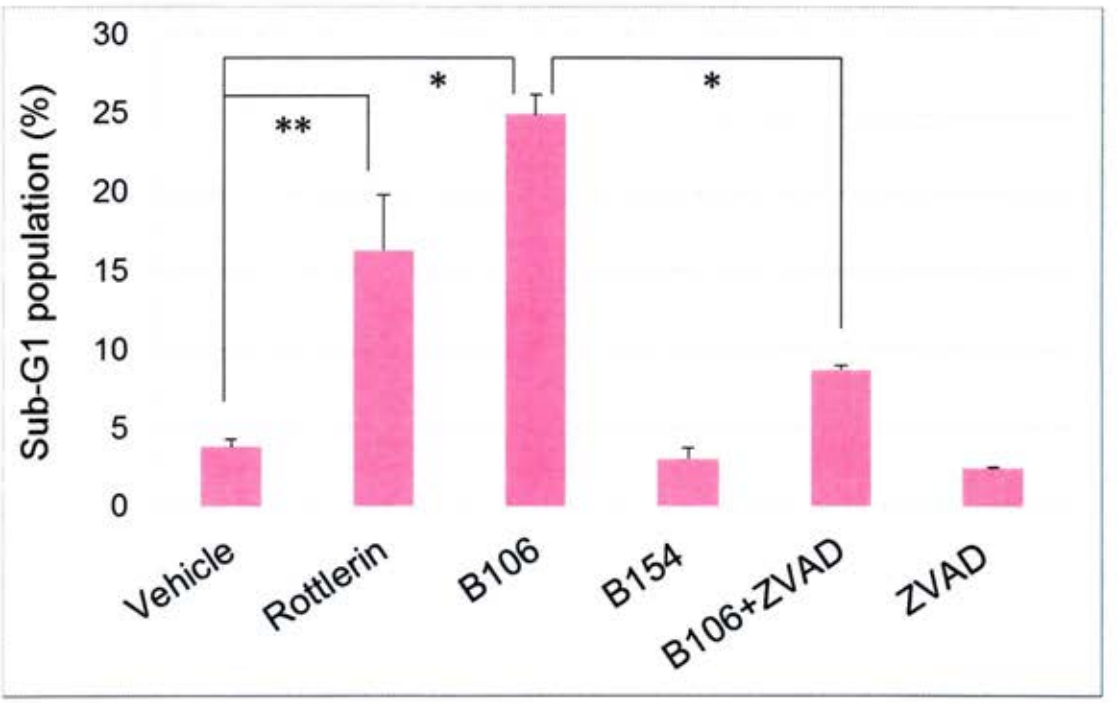

Figure 9: DNA fragmentation induced by PKCδ inhibitors in SBcl2 cells. Cells were treated with rottlerin (5μM), B106 (0.5μM) alone, or B106 (0.5μM) plus the pan-caspase inhibitor Z-VAD-FMK (100μM) together for 24 hours. The proportion of sub-G1 population was measured by flow cytometric analysis using propidium-iodide staining of DNA. DMSO and B154 (0.5μM) served as a vehicle control and a negative control for PKCδ inhibition, respectively. Values represent the average of duplicates and error bars indicate the standard deviations of duplicates. Cells in the sub-G1 population have fragmented DNA, which is a hallmark event of the late apoptotic process. Z-VAD-FMK (carbobenzoxy-valyl-alanyl-aspartyl-[Omethyl]- fluoromethylketone) irreversibly binds to the catalytic site of caspase proteases and prevents caspases from being cleaved and activated. Preliminary immunoblot analysis verified the effect of Z-VAD-FMK at 50μM on prevention of caspase 3 cleavage (data not shown). P values: ** $p < 0.04$, * $p < 0.004$. The experiment was repeated three times.

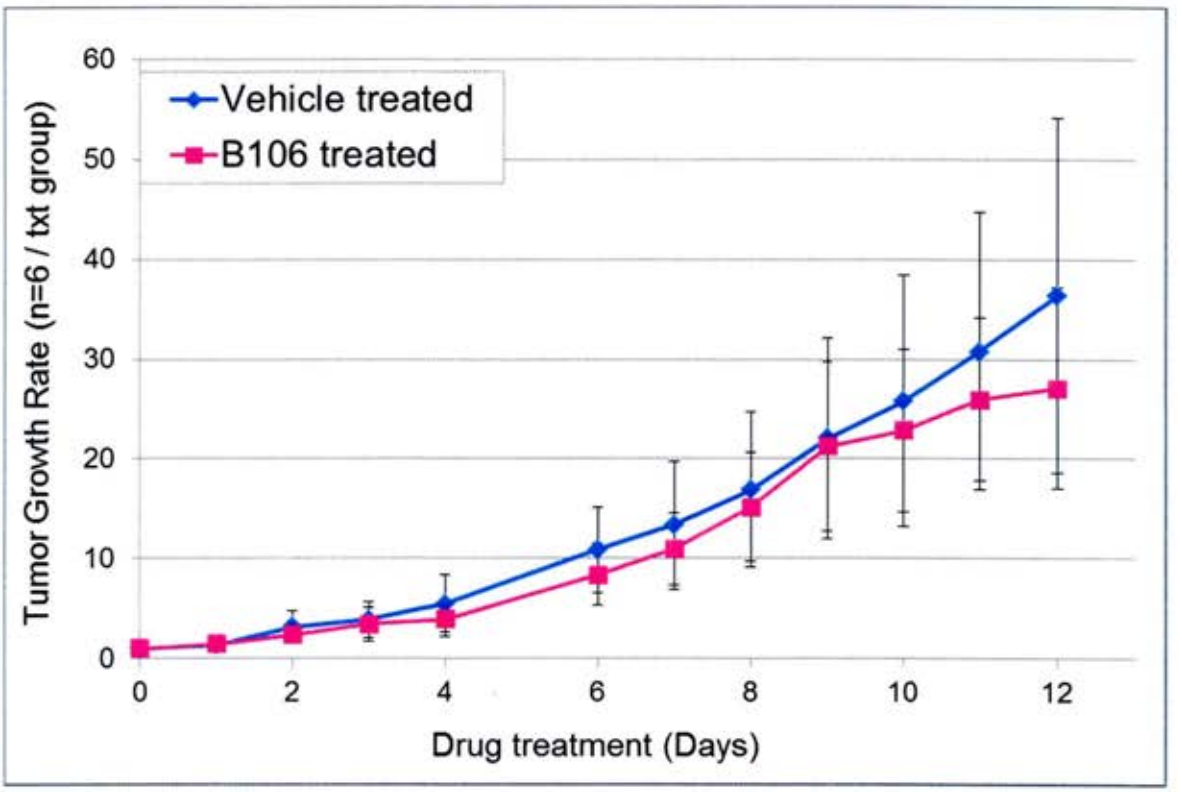

Figure 10: Mouse xenograft model with B106 daily dosing. Donor athymic nude mice were subcutaneously injected with 3 x 10^6 cells of the SBcl2 cell line and tumors were grown. The resulting tumors were harvested, dissected into small blocks (approximately 3 mm^3) and frozen for later use. For the xenograft study, tumor blocks were implanted subcutaneously into 12 mice (1 block / implantation) and 8 days later, when tumor growth was apparent, dosing was initiated. 6 mice were treated with vehicle (DMSO) administered intraperitoneally and the other 6 mice were treated with B106 (40 mg/kg) daily for 12 consecutive days. Tumor size was measured daily using a caliper and tumor growth rate was calculated. Each point represents the average tumor growth rate of 6 mice and error bars indicate the standard deviations.

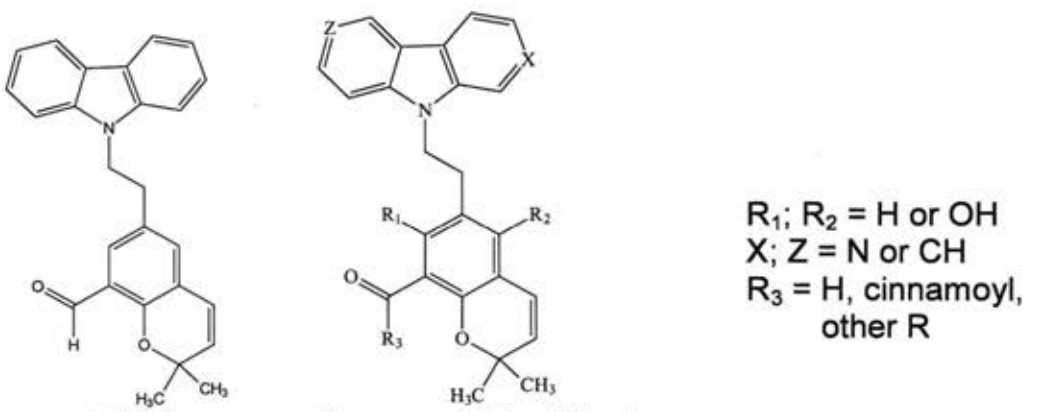

Figure 11: Proposed modifications of B106 to explore Structure-Activity Relationships (SAR) and improve pharmaceutical properties. R1 and R2, which are hydroxyl groups in rottlerin and are hydrogen atoms in B106, will be sequentially substituted with OH groups, which should improve water solubility. In addition, we plan to perform an isosteric replacement of the aromatic CH groups (X and Z) with basic nitrogen atoms which will be protonated at physiological pH providing for additional water solubility and perhaps improved potency.

1-3. Summary

Based on the previous studies that reported its role as essential for survival in RAS-mutated cancer cells while being non-essential for survival of normal cells, PKCδ presented potential as a therapeutic target in melanoma with NRAS mutation. Both of the PKCδ inhibitors rottlerin and B106, which was developed in our lab, inhibited cell growth in melanoma cell lines carrying NRAS mutations, and the specificity of PKCδ inhibition in the cytotoxic effect was verified by specific downregulation using siRNA targeting PKCδ. Promisingly, B106 effectively exerted a cell growth inhibitory effect at nanomolar concentrations throughout the cell lines tested, in comparison to rottlerin which required 10 times higher concentration to induce the same degree of effect. The cell growth inhibition in these cells caused by PKCδ inhibition is likely due to caspase-dependent apoptosis. The *in vivo* efficacy of B106 is still undetermined at this time. When more soluble analogs of B106 are available and their *in vitro* potency is verified, their *in vivo* efficacy as well as pharmacokinetics will be investigated.

Chapter 2: Molecular mechanism by which PKCδ inhibition causes cytotoxicity in melanoma: PKCδ inhibition causes caspase-dependent apoptosis via the JNK/H2AX pathway

2-1. Introduction

Stress-activated protein kinase/c-Jun N-terminal kinase (SAPK/JNK) is activated in response to cellular stresses, including genotoxic stresses (e.g., ionizing radiation (IR), ultraviolet radiation (UV)), chemotherapeutic agents, or reactive oxygen species (ROS) and is involved in a variety of cellular activities, such as cell proliferation, differentiation, inflammatory response, apoptosis, motility, metabolism and DNA repair (63-66).

The JNK pathway comprises one of the three major MAPK pathways. The JNK family is on the MAPK tier and consists of three isozymes: JNK1, JNK2 and JNK3. JNK1 and JNK2 are ubiquitously expressed while JNK3 is restricted to brain, heart and testis (63). Alternative splicing yields multiple splicing variants of all three isozymes: each of JNK1 and 2 genes contributes both a short form (46kDa) and a long form (54kDa) and a minor 52kDa form is believed to derive mostly to JNK3 (63, 67). Upon activation of the JNK pathway, both the 46kDa and 54kDa forms become phosphorylated at Thr183/Tyr185 by two upstream MAPKKs, SEK1/MKK4 and MKK7. MKK4 appears to preferentially phosphorylate Tyr185 and MKK7 favors Thr183 (68). While MKK7 is a JNK-selective MAPKK, MKK4 is capable of activating both JNK and the other MAPK, p38 (69). The most well-studied of the downstream substrates of JNK are components of

activator protein-1 (AP-1), a transcription factor that binds to TRE/AP-1 elements and activates transcription. The AP-1-associated proteins activated by JNK include c-Jun, JunD, and activating transcription factor 2 (ATF2) (68) (**Figure 12**). Other substrates of JNK include a wide range of proteins: Elk1, c-Myc, p53, MLK2, NFATc2, TIF-1A, histone H3, insulin receptor substrate 1 or JIP1 (68). In response to apoptotic signals, JNK activates the pro-apoptotic Bcl-2 family proteins Bax and Bad, possibly in part through regulating BH3-only members of the Bcl-2 family including Bim, Bid or Bif, 14-3-3 or FOXO transcription factor (66) (**Figure 12**).

Recently, H2AX, a histone H2AX variant, was found to be phosphorylated by JNK (70). Phospho-H2AX is known to localize to DNA double-strand breaks (DSBs) on replication foci as part of a repair complex, and is used as an indicator of DSBs in studies of DNA damage response. While previous studies suggested that H2AX phosphorylation is the consequence of a series of apoptotic events (71), a recent study proposed that JNK-mediated H2AX phosphorylation at Ser139 may instead be actively involved in the apoptotic process through induction of DNA fragmentation in UV-damaged cells (70) (**Figure 12**). Subsequently, another report demonstrated that the pan-nuclear distribution of phosphorylated H2AX is a pre-apoptotic signal associated with ATM- and JNK-dependent apoptosis during S-phase, in contrast to replication foci-specific localization at DSBs (72). Interestingly, a series of recent studies supported this model of an active apoptotic role for H2AX, including involvement in apoptosis induced by radiation and chemotherapeutic agents such as enzastaurin and imatinib mesylate (73-76).

PKCδ-mediated regulation of JNK pathway signaling was reported by several groups, especially in association with the pro-apoptotic function of PKCδ (18, 22-24, 27). On the other hand, downregulation of PKCδ using RNAi initiated JNK-mediated apoptosis in prostate cancer cells with Ras activation, suggesting that the anti-apoptotic actions of PKCδ also possibly involve activation of the JNK pathway (47).

In this chapter, the molecular mechanism of PKCδ inhibition which leads to caspase-dependent apoptosis in melanoma cell lines carrying NRAS mutations is examined. Inhibition of PKCδ by B106, or by siRNA, induced the stress-responsive JNK pathway (MKK4/JNK/H2AX) and phospho-H2AX is shown to be essential in B106-induced apoptosis.

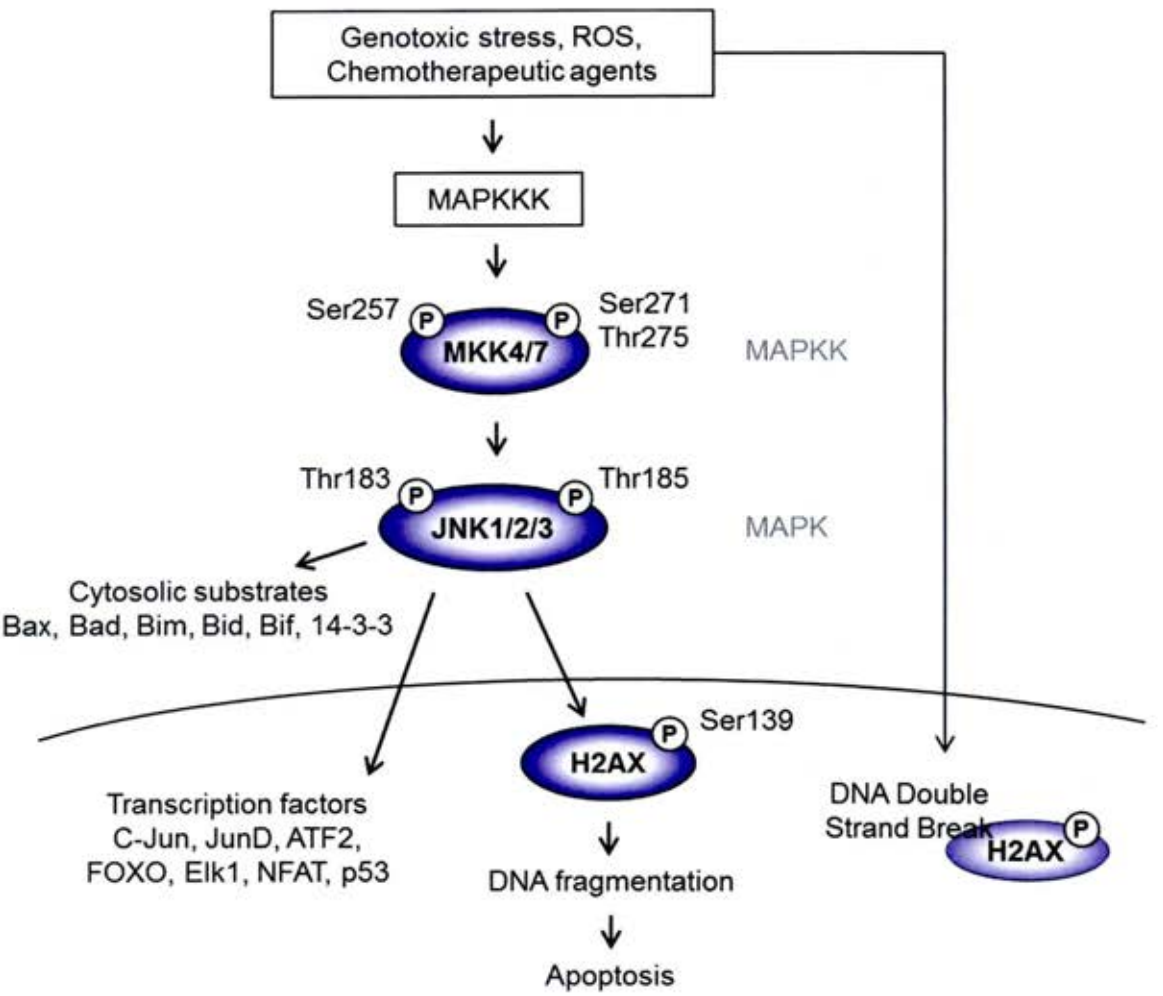

Figure 12: JNK/H2AX pathway. The JNK pathway comprises one of the three major MAPK pathways. Upstream of JNK, MKK4 is phosphorylated at S257 and MKK7 at S271/T275 by MAPKKK resulting in their activation. MKK7 is selective for JNK, while MKK4 phosphorylates JNK as well as p38. Activated JNK exerts a wide range of downstream responses, including activation of transcription factors or pro-apoptotic modulators. Phospho-H2AX is primarily known for its role in DNA repair and localization to DNA double-strand breaks (DSBs) on replication foci, and is used as an indicator of DSBs. A series of recent reports proposed an active role of phospho-H2AX in apoptosis by induction of DNA fragmentation.

2-2. Results

PKCδ inhibition induces the stress-responsive JNK pathway

In order to identify which intracellular signaling pathway PKCδ inhibition employs to induce cytotoxicity, the activation status of reported downstream targets of PKCδ was examined after PKCδ inhibition, including MAPKs (ERK, p38 and JNK), AKT, NFκB pathway, CDK inhibitors, p53, IAPs, GSK3β or c-Abl by immunoblotting of individual proteins. A phospho-protein focused antibody array was also used. These studies revealed that B106 treatment induced phosphorylation of JNK1/2 most strongly after two hours of exposure, with phosphorylation diminishing subsequently, in SBcl2 cells (**Figure 13**). In contrast, activation of the other MAPKs p38 and ERK was not consistently observed (**Figure 13**). Slight increases in phosphorylation of AKT were occasionally seen after rottlerin treatment (**Figure 13**).

The upstream and downstream effectors of the JNK pathway were next examined. The upstream MAPKK, MKK4, was activated by B106 but MKK7 was not. This was somewhat unexpected, as MKK7 activation was anticipated because of its more selective function to activate JNK relative to p38 (**Figure 14**). The activation of the well-described JNK substrate, c-Jun, was also observed, confirming the activation of the JNK pathway by B106 treatment (**Figure 14**). Furthermore, **Figure 14** demonstrated the activation of H2AX at later time points in response to B106 treatment. B106 consistently induces H2AX phosphorylation as early as 10 hours to 24 hours (times later than 24 hours were not studied because significant cytotoxicity is occurring after this time). Phosphorylation

of H2AX was occasionally, but not consistently, observed after rottlerin treatment, in the absence of activation of MKK4/JNK, implying the potential existence of another mechanism that causes H2AX phosphorylation other than the JNK pathway; possibly, mediation by other kinases or secondary consequence of DNA fragmentation in the course of the apoptotic event initiated by rottlerin treatment. To ensure that activation of JNK pathway by B106 is not a cell-type-specific response, the pathway effectors were examined in another NRAS mutant melanoma cell line WM1366. Activation of MKK4, JNK and H2AX was confirmed in these cells (**Figure 15**) as well as other NRAS-mutated melanoma cell lines, WM852 and FM28 (data not shown).

Collectively, these data suggest that B106 treatment activates MKK4, directly or indirectly, which turns into the activation of JNK1/2 and eventually H2AX.

Selective downregulation of PKCδ verifies the effect of PKCδ inhibitors on JNK/H2AX activation

As discussed in Chapter 1, the target specificity of PKCδ inhibitors resulting JNK-pathway activation needed to be confirmed by more selective downregulation of PKCδ using siRNA, especially because rottlerin and B106 produced differences in the activation of the JNK pathway. Consistent with the observations following B106 treatment described above, selective downregulation of PKCδ by PKCδ-specific siRNA transfection induced phosphorylation of JNK1/2 at 24 hours (when effects of siRNA on PKCδ levels are first observed), in contrast to transfection with negative control scrambled siRNA. No difference between PKCδ and negative control siRNA

transfectants was observed on the phosphorylation levels of ERK or p38 (**Figure 16A**). Phosphorylation of H2AX was observed at 72 hours after PKCδ siRNA transfection compared to the cells transfected with negative control siRNA. This was consistent with my observation of H2AX phosphorylation subsequent to the initiation of the MKK4/JNK cascade activation seen with PKCδ inhibitor treatment (**Figure 16B**). These results verified that the selective inhibition of PKCδ induces activation of the JNK/H2AX signaling in NRAS mutant melanoma cells, and supported my hypothesis that the effect of B106 on JNK/H2AX pathway is likely to be causally related to PKCδ inhibition.

B106-induced phosphorylation of H2AX is mediated via JNK

Because JNK affects diverse downstream effectors, I then investigated whether JNK activation caused by PKCδ inhibition is directly linked to B106-induced H2AX activation. Cells were transfected with either negative control siRNA or JNK1/2 siRNA for 72 hours and then treated with vehicle or B106 for another 24 hours. Knockdown of JNK1/2 itself slightly reduced basal phospho-H2AX expression, indicating that basal phosphorylation of H2AX is indeed regulated by JNK (Lane 2, **Figure 17**). B106 treatment robustly induced phosphorylation of H2AX (pH2AX) in control siRNA-treated cells (Lane 3, **Figure 17)** as expected; in comparison, prior downregulation of JNK1/2 protein greatly suppressed B106-induced H2AX phosphorylation (Lane 4, **Figure 17**). This experiment confirmed that JNK lies upstream of H2AX, and H2AX is not activated in the absence of JNK in response to PKCδ inhibition, supporting the model in which inhibition of PKCδ by B106 causes JNK/H2AX pathway signaling.

Caspase-dependent apoptosis initiated by B106 treatment is mediated via JNK/H2AX pathway

Although phosphorylation of H2AX has been primarily considered to be a consequence of/response to DSBs in the DNA damage response, a recent study reported that phosphorylation of H2AX resulting from JNK activation actively mediates the induction of apoptosis (70) (**Figure 12**). This report, together with the above observations of B106-induced activation of the JNK/H2AX pathway and caspase-dependent apoptosis (Chapter 1), led me to hypothesize that inhibition of PKCδ activity by B106 causes caspase-dependent apoptosis through activation of the JNK/H2AX pathway. Accordingly, the effect of inhibition of the JNK pathway during B106 treatment was explored. In Figure 18, cells were transfected with siRNA specific for JNK1 or 2 alone, or co-transfected with JNK1 and 2 siRNA together for 72 hours and then treated with B106 for 6, 12 or 24 hours, followed by measurement of caspase activity. Analysis at 24 hours after B106 treatment showed that knockdown of JNK2, and co-knockdown of JNK1 and 2, mitigated B106-induced caspase 3/7 activation in rough proportion to the knockdown efficiency of JNK1/2 proteins, as confirmed by immunoblotting (**Figure18**). Similarly, as expected from the observed causal link from JNK activation to H2AX phosphorylation after PKCδ inhibition (Figure 17), downregulation of H2AX prior to B106 treatment greatly decreased the level of caspase 3/7 activation at 24 hours after B106 treatment compared to the cells pre-treated with control siRNA (**Figure 19**). These

experiments suggested that JNK activation/phosphorylation of H2AX is required for the activation of caspases, the ultimate executers of apoptosis, during PKCδ inhibition.

Subsequently, in order to explore the more direct link of H2AX in the execution of apoptosis, PKCδ inhibition-induced DNA fragmentation, a hallmark of the late apoptotic process which is seen in cells destined for apoptosis, was examined in the presence or absence of H2AX. Similar to the results shown in Figure 19, SBcl2 cells were transfected with either negative control siRNA or siRNA targeting H2AX for 72 hours, and then subjected to PKCδ inhibition by B106 treatment for the next 24 hours. DNA fragmentation was assessed by flow cytometric analysis using propidium iodide staining of DNA. PKCδ inhibition by B106 treatment increased DNA fragmentation 8.5-fold in the cells transfected with negative control siRNA (**Figure 20**). In contrast, PKCδ inhibition by B106 treatment failed to induce DNA fragmentation in the absence of H2AX induced by transfection of siRNA against H2AX (**Figure 20**). B106-induced DNA fragmentation in the cells with H2AX downregulation was significantly reduced compared to that in the cells with H2AX expression, indicating that H2AX is necessary for B106-induced apoptosis (**Figure 20**). Collectively, these results suggest that inhibition of PKCδ by B106 treatment triggers caspase-dependent apoptosis through activation of the JNK-H2AX stress-responsive signaling pathway.

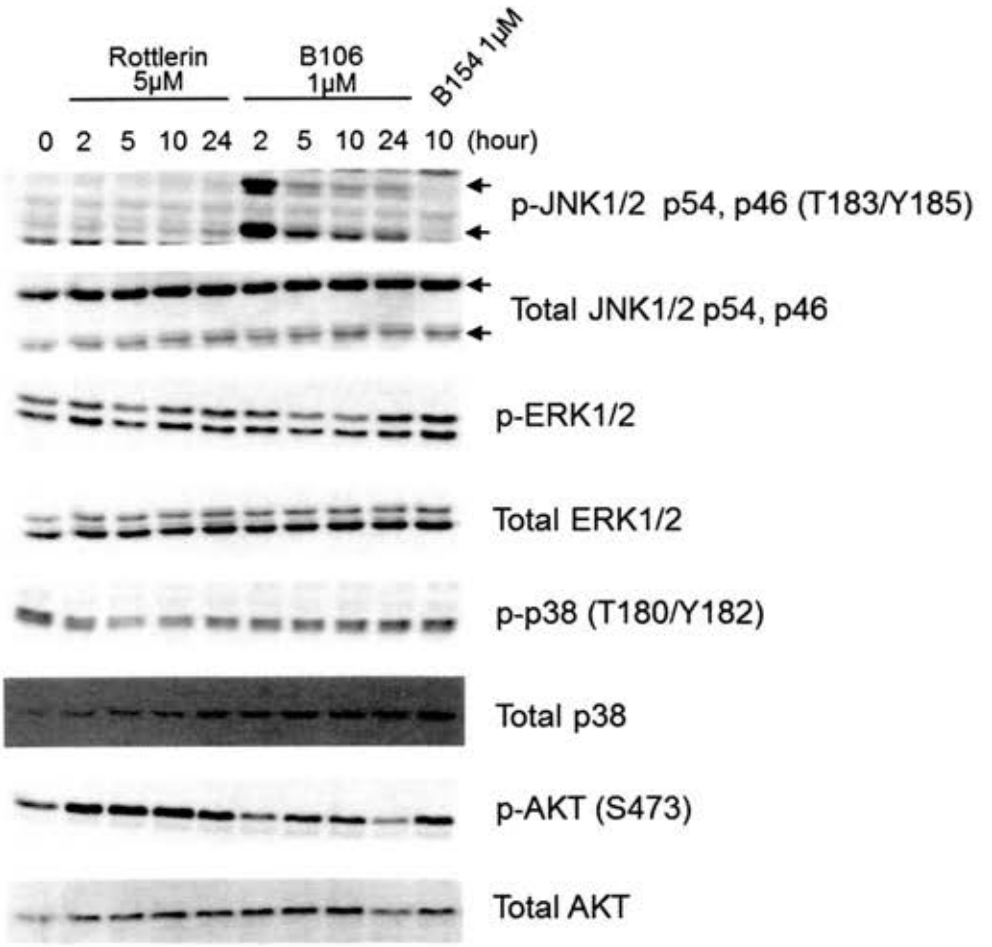

Figure 13: JNK activation by B106 in SBcl2 cells. Cells were treated with rottlerin (5μM) or B106 (1μM) for the indicated times. B154 (1μM) served as a negative compound control for B106. Protein lysates were subjected to immunoblotting for phosphorylation or total expression level of MAP kinase proteins. Note: each of JNK1 and 2 genes contributes both a short form (46kDa: lower arrow) and a long form (54kDa: upper arrow) of the protein, as a result of differential splicing. The experiment was repeated at least three times.

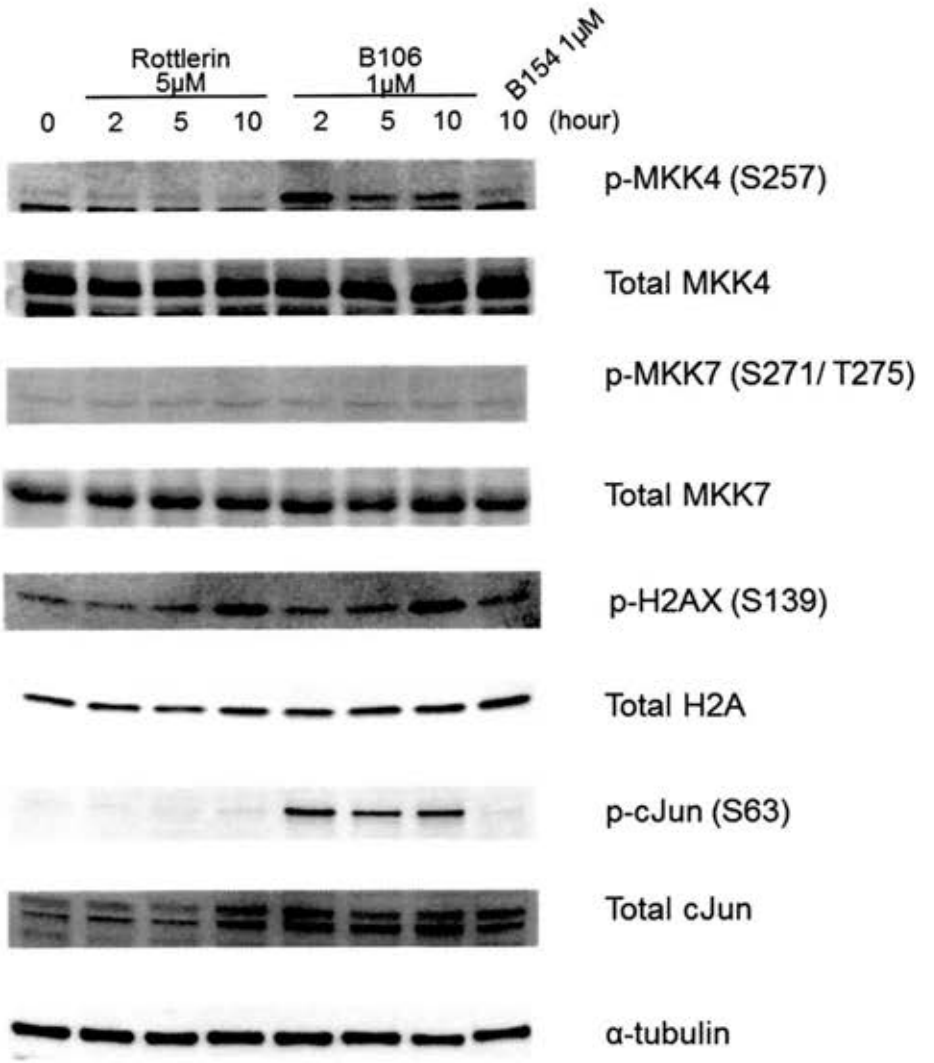

Figure 14: Activation of upstream and downstream components of the JNK pathway by B106 in SBcl2 cells. Cells were treated with rottlerin (5μM) or B106 (1μM) for the indicated times. B154 (1μM) served as a negative compound control for B106. Protein lysates were subjected to immunoblotting for phosphorylation or total expression levels of proteins. Activation of MKK4 (activator of JNK), H2AX and c-Jun (target of JNK) was observed; however, activation of MKK7, the alternate MAPKK for JNK, could not be detected. Levels of α-tubulin served as a loading control. The experiment was repeated at least three times.

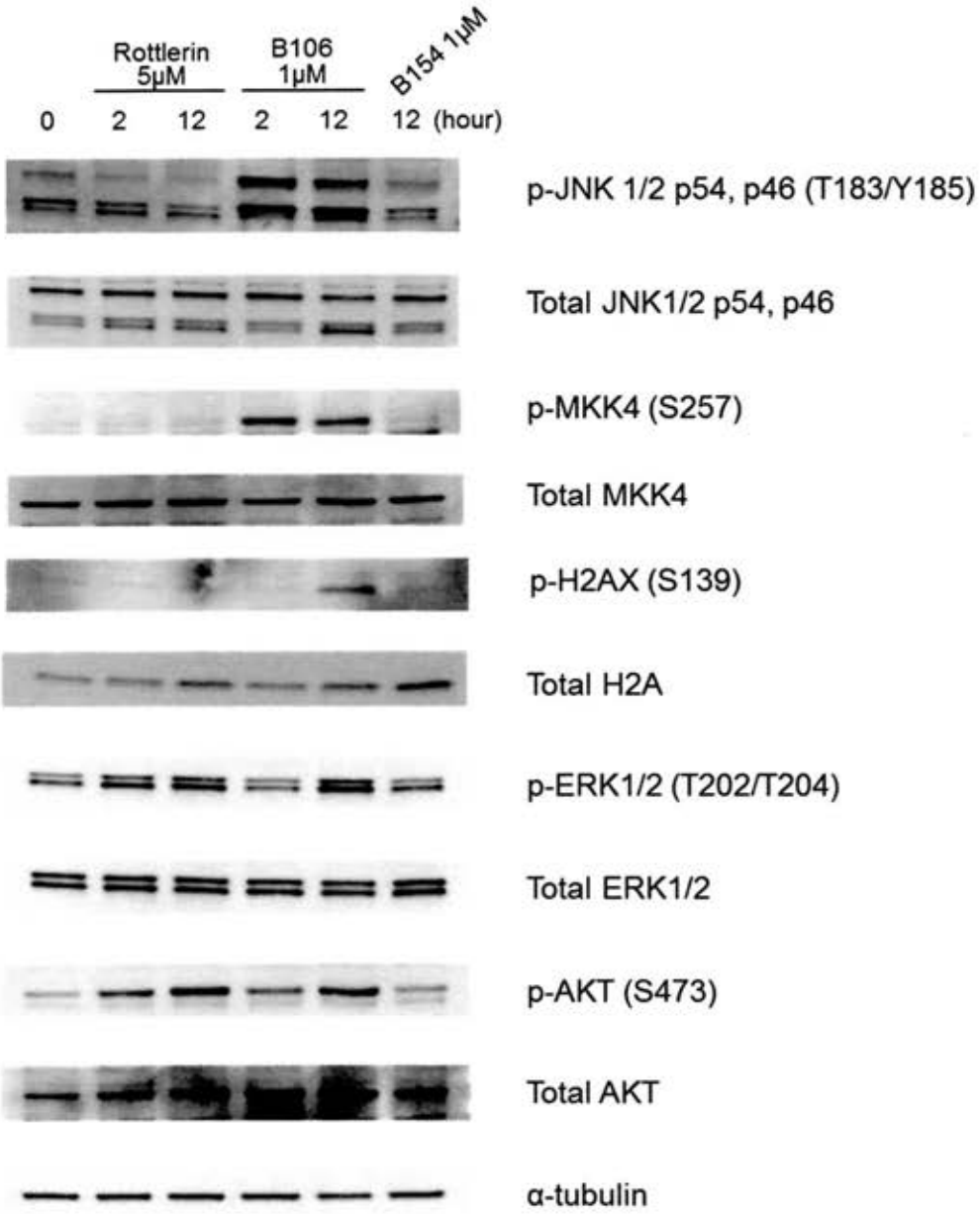

Figure 15: Activation of upstream and downstream components of the JNK pathway by B106 in WM1366 cells. In order to verify that the preceding observation of the activation of the JNK pathway in SBcl2 cells is not specific to the cell type, WM1366 cells (NRAS mutant melanoma cell line) were treated with rottlerin (5μM) or B106 (1μM) for the indicated times. B154 (1μM) served as a negative control for PKCδ inhibition. Protein lysates were subjected to immunoblotting for phosphorylation or total expression levels of proteins. Levels of α-tubulin served as a loading control. The experiment was repeated at least two times.

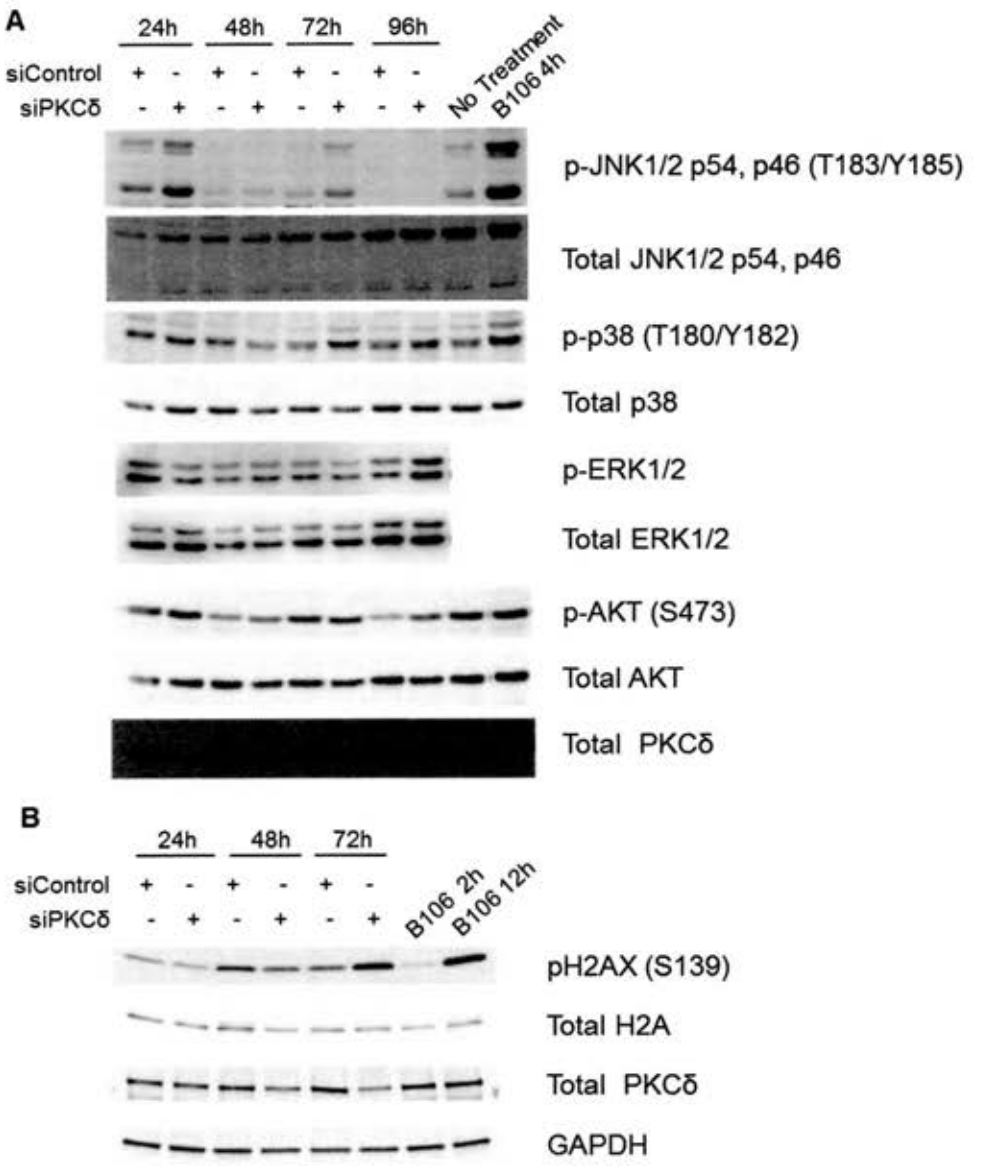

Figure 16: Knockdown of PKCδ induces phosphorylation of JNK and H2AX in SBcl2 cells. (A) Cells were transfected with scrambled negative control ("siControl") or PKCδ siRNA ("siPKCδ") at 5nM for the indicated times. B106 treatment (1μM) serves as a positive control of JNK activation. Protein lysates were subjected to immunoblotting for phosphorylation and total expression levels of MAPK proteins. The experiment was repeated at least two times. (B) Cells were transfected with scrambled negative control ("siControl") or PKCδ siRNA ("siPKCδ") at 50nM for the indicated times. B106 treatment at 0.5μM served as a positive control of H2AX activation. Protein lysates were subjected to immunoblotting for phosphorylation and total expression levels of H2AX protein. Levels of GAPDH served as a loading control. The experiment was repeated three times.

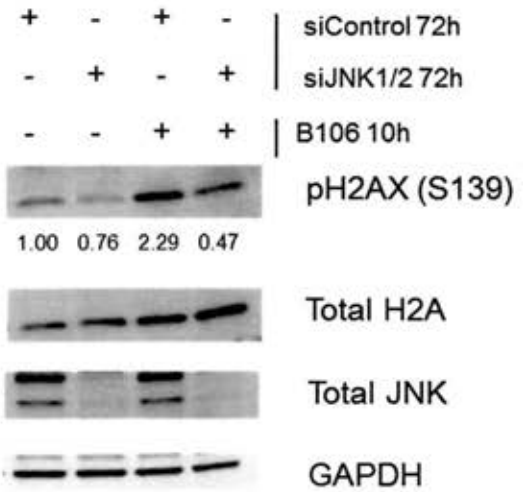

Figure 17: Prior downregulation of JNK prevents B106-induced H2AX activation in SBcl2 cells. SBcl2 cells were co-transfected with siRNA against JNK1 and JNK2 (5nM each) or scramble siRNA (10nM) for 72 hours and subsequently with B106 (0.5μM) or vehicle for 10 hours. Protein lysates were subjected to immunoblotting for phosphorylation and total expression levels of proteins. The relative band intensity of phospho-H2AX was indicated below the image (normalized to total H2A). Levels of GAPDH served as a loading control. The experiment was performed once.

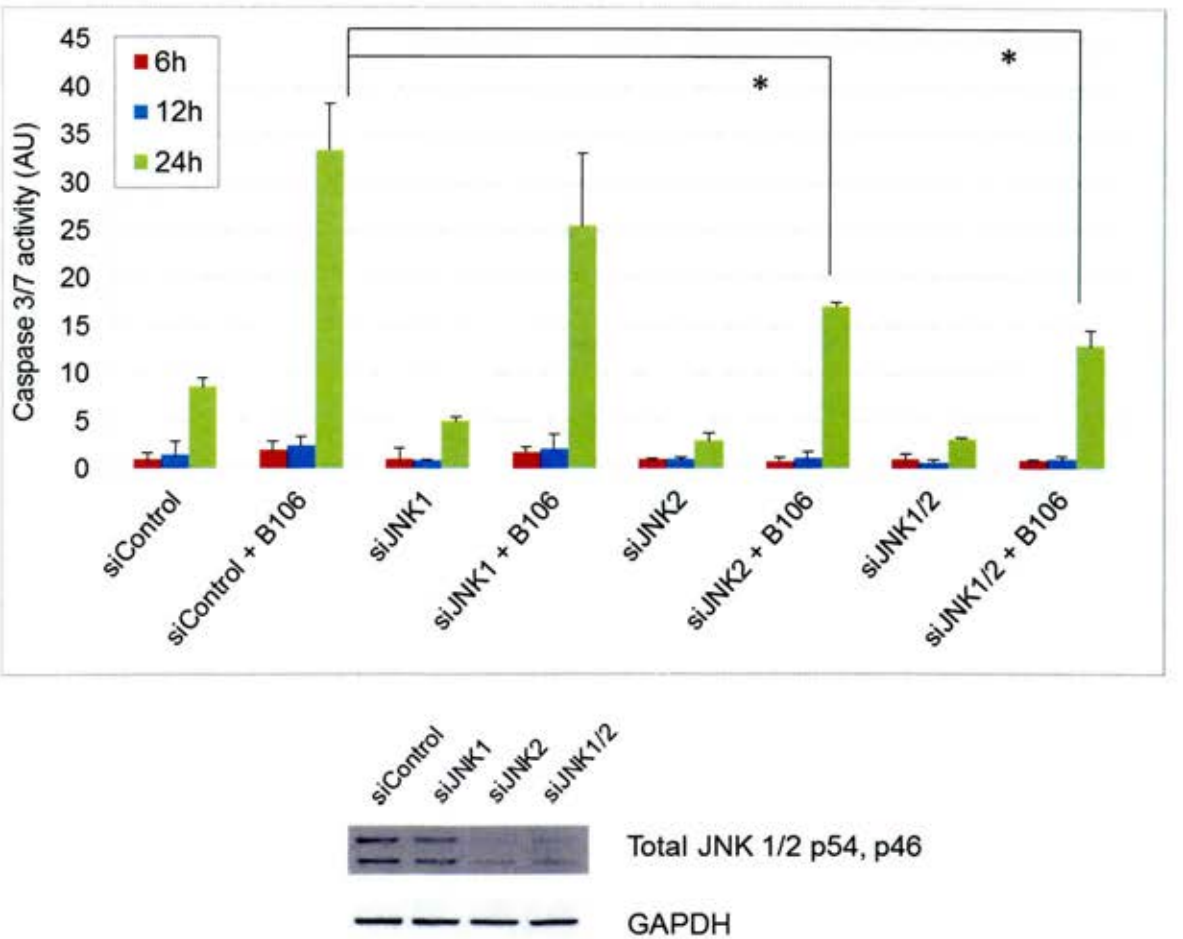

Figure 18: Activation of caspase 3/7 is mitigated by knockdown of JNK prior to B106 treatment in SBcl2 cells. (Top) SBcl2 cells were transfected with negative control siRNA (10nM), siRNA against JNK1 or JNK2 alone (5nM), or the combination of JNK1 and JNK2 (5nM each) for 72 hours, and subsequently treated with B106 (0.5μM) or vehicle for 6, 12 and 24 hours. Activity of caspase 3/7 was measured by luminescence at each time point. The average values of triplicates were normalized to that of the vehicle-treated sample at 6 hours between the pairs of the same siRNA with or without B106 treatment. Error bars indicate the standard deviations of triplicates. P values: * $p < 0.005$. (Bottom) Downregulation of JNK1/2 proteins were confirmed by immunoblotting. Cells were lysed after 72 hours of siRNA transfection. Each of the two bands detected in immunoblotting with JNK1/2 antibodies represent assembly of different splicing variants from both JNK1 and 2 isoforms. Levels of GAPDH served as a loading control. The experiment was repeated twice.

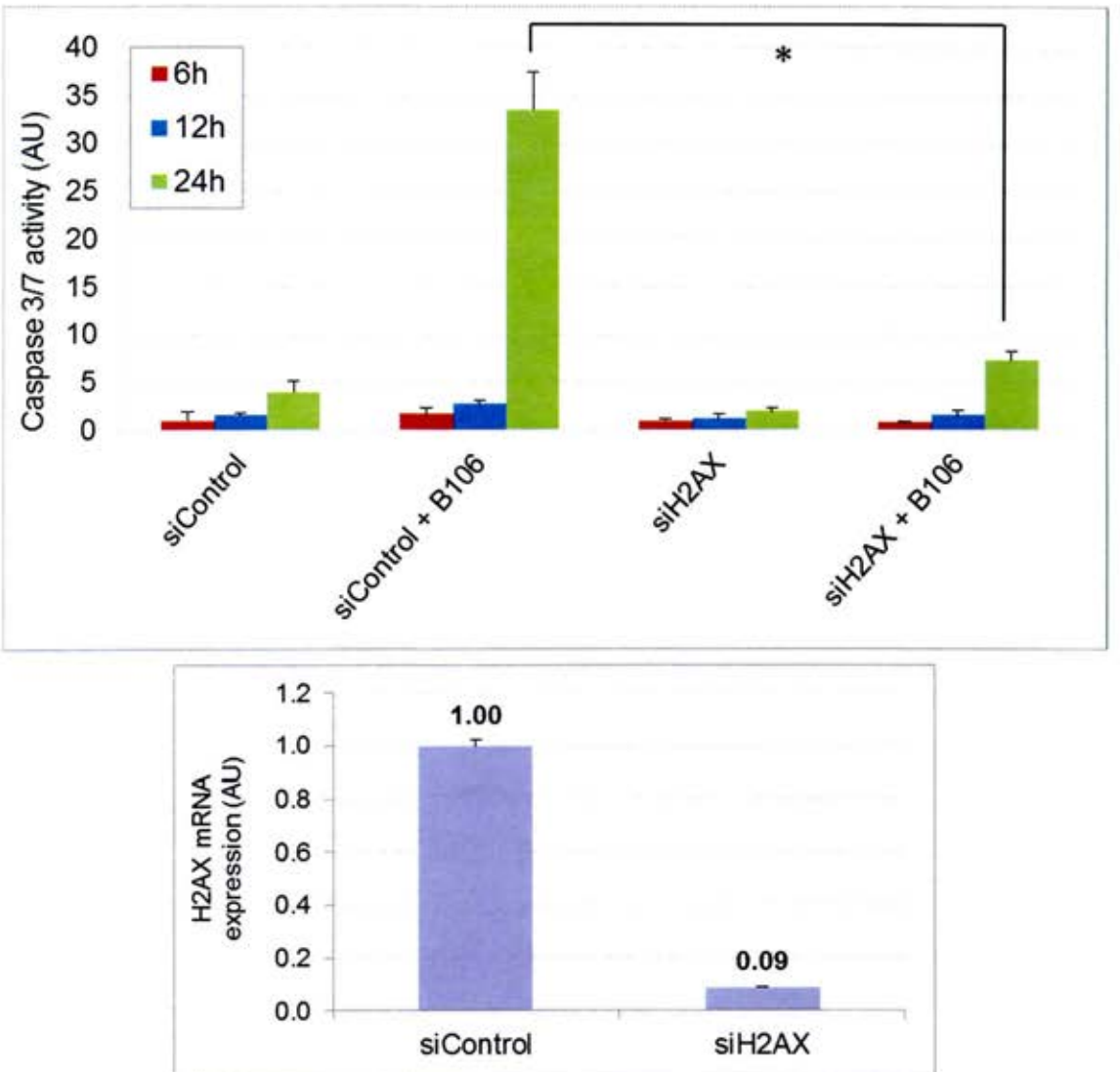

Figure 19: Activation of caspase 3/7 is mitigated by knockdown of H2AX prior to B106 treatment in SBcl2 cells. (Top) Cells were transfected with negative control siRNA (5nM) or siRNA against H2AX (5nM) for 72 hours, and subsequently treated with B106 (0.5μM) or vehicle for 6, 12 and 24 hours. Activity of caspase 3/7 was measured by luminescence at each time point. The average values of triplicates were normalized to that of the vehicle-treated sample at 6 hours between the pairs of the same siRNA with or without B106 treatment. Error bars indicate the standard deviations of triplicates. P value: * $p < 0.002$. (Bottom) Downregulation of H2AX mRNA was confirmed by real-time PCR. mRNA was collected 72 hours after siRNA transfection (5nM), from which cDNA was synthesized. Relative amount of H2AX mRNA was calculated by normalizing Ct value of H2AX to that of β-actin (internal control) obtained from real-time PCR. The experiment was repeated twice.

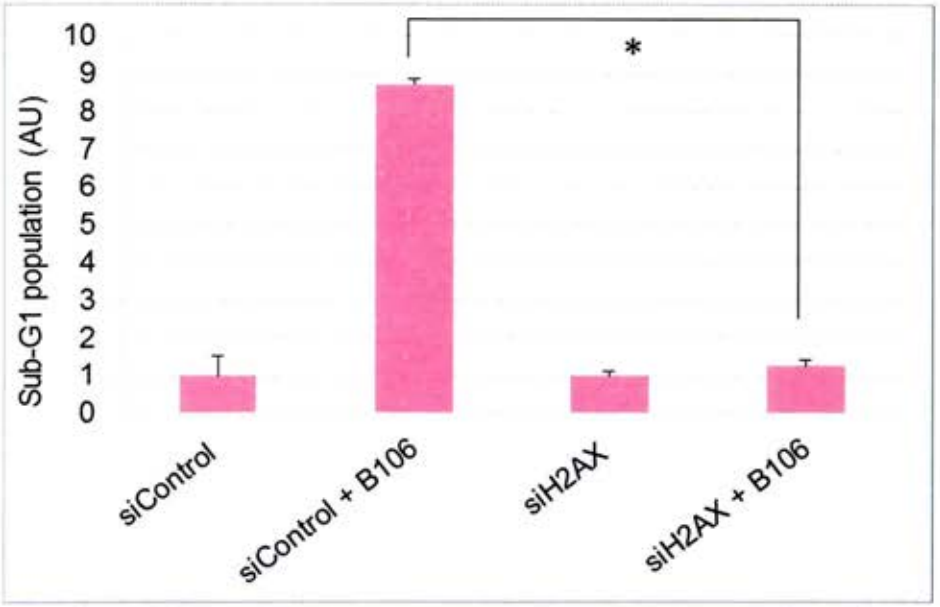

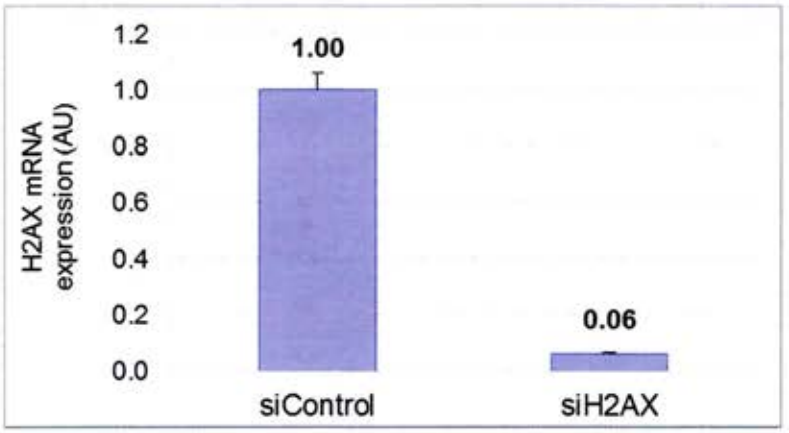

Figure 20: Induction of DNA fragmentation is mitigated by knockdown of H2AX prior to B106 treatment in SBcl2 cells. (Top) Cells were transfected with negative control siRNA (5nM) or siRNA against H2AX (5nM) for 72 hours, and subsequently treated with B106 (0.5μM) or vehicle for 24 hours. The proportion of sub-G1 population was measured by flow cytometric analysis using propidium-iodine staining. The average values of duplicate were normalized to that of the vehicle-treated sample between the pairs of the same siRNA with or without B106 treatment. Error bars indicate the standard deviations of duplicates. P value: * $p < 0.0004$. (Bottom) Downregulation of H2AX mRNA was confirmed by real time PCR. mRNA was collected 72 hours after siRNA transfection (5nM), from which cDNA was synthesized. Relative amount of H2AX mRNA was calculated by normalizing the Ct value of H2AX to that of β-actin (internal control) obtained from real-time PCR. The experiment was repeated three times.

2-3. Summary

To better understand the molecular mechanism of action of the PKCδ inhibitor B106 as well as the effect of PKCδ inhibition itself, the signaling pathway that PKCδ inhibition employs to initiate caspase-dependent apoptosis was sought in this chapter. Among the reported downstream targets of PKCδ, B106 treatment and PKCδ knockdown was shown to induce activation of the JNK cascade, a stress responsive MAPK pathway. A series of focused analyses of the signaling pathway identified that the MKK4/JNK/H2AX cascade is induced by treatment with B106 in four melanoma cell lines with NRAS mutations. Selective downregulation of PKCδ using siRNA verified the activation of JNK and H2AX subsequent to PKCδ inhibition. JNK was essential for B106-induced H2AX activation, and the phosphorylation of H2AX by B106 treatment was abrogated in the absence of JNK expression. Consistent with a necessary role for JNK and H2AX in this apoptotic signaling cascade, caspase activation was suppressed when either JNK or H2AX was downregulated prior to B106 exposure, and more importantly, DNA fragmentation initiated by B106 treatment was prevented by prior knockdown of H2AX. These results suggest that PKCδ inhibition, either by B106 treatment or by siRNA transfection, initiates caspase-dependent apoptosis through activation of the stress-responsive kinase cascade MKK4-JNK-H2AX.

Phosphorylation of H2AX has long been identified as a cellular response to DNA double strand breaks; however, a series of recent reports proposed an active role for H2AX phosphorylation in apoptosis. My finding of H2AX as an apoptotic mediator in

apoptosis induced by PKCδ inhibition in cells with aberrant Ras signaling not only supports this model but also demonstrates a necessary role for phospho-H2AX, in that the absence of H2AX suppresses the initiation of apoptosis.

Chapter 3: PKCδ inhibition induces growth inhibition in B-Raf inhibitor-resistant melanoma cells

3-1. Introduction

In the search for potential therapeutics to block aberrant activation of the Raf/MEK/ERK pathway in cancer cells, pharmacological inhibitors of Raf kinases and MEK kinases have been intensively pursued. Among three Raf isozymes, the discovery of frequent BRAF mutations in a wide range of cancers attracted attention to B-Raf as a druggable target (77). Theoretically, specifically targeting mutant B-Raf, the expression of which is confined to cancer cells, would enable tumor-selective drug activity, while sparing normal cells that carry wild-type B-Raf. Most investigational drugs currently in clinical trials are selective for the BRAF-V600E mutant, which is particularly common in melanoma. The recently FDA-approved agent vemurafenib (also known as PLX4032) preferentially inhibits the V600E mutant form of B-Raf over wild-type (78). Inhibition of ERK phosphorylation, induction of cell cycle arrest, and apoptosis induced by PLX4032 are exclusively observed in BRAF-V600E-positive cells (78). A phase II trial in previously-treated melanoma patients with mutant B-Raf achieved a remarkable response rate of 53% and a median duration of response of 6.7 months (79). A phase III trial which compared the efficacy of vemurafenib to that of dacarbazine in patients with previously-untreated BRAF-V600E-positive melanomas verified the higher response rate and improved rates of overall survival and progression free survival (PFS) over the standard

treatment group (7). Vemurafenib was approved by FDA in 2011 for the treatment of patients with previously untreated metastatic or unresectable melanoma with the BRAF-V600E mutation, with concurrent approval of a BRAF-V600E mutation assay (companion diagnostic). Among the investigational drugs in this class, the most advanced at this time is dabrafenib, which has higher specificity against mutant B-Raf and a similar preclinical profile to vemurafenib (80). Encouraged by a phase II trial that confirmed a 59% response rate to dabrafenib in melanoma, several phase III trials are currently ongoing. Preliminary result from a randomized monotherapy trial reported improved median PFS over dacarbazine treatment (80).

While these mutant B-Raf inhibitors produce improved overall survival in the patients with BRAF mutations compared to standard treatment options, a major challenge remains: essentially all patients treated with these drugs relapse due to the development of drug resistance, with the median time to progression (TTP) of 7 months for vemurafenib and 5 months for dabrafenib (79, 80). Several models for resistance have been proposed: 1) reactivation of the MEK/ERK pathway, bypassing mutated BRAF (*e.g.*, secondary mutation in NRAS, hyperactivation/overexpression of C-Raf, or activation of another MAPKK COT); or, 2) adaptive dependency upon alternative pathways (hyperactivation/overexpression of RTKs, such as PDGFRβ or IGF1R, or the AKT pathway) (**Figure 21**) (8, 81-83).

Another issue that needs to be addressed regarding B-Raf inhibitors is the potential risks of their use in RAS-mutant melanoma. Interestingly, B-Raf mutant-selective inhibitors were reported to paradoxically activate the MEK-ERK pathway via

C-Raf in a Ras activity-dependent manner in RAS-mutant cells, leading to accelerated cell proliferation (84-87). Moreover, RAS mutations (predominantly HRAS) were detected in 60% of tumor samples taken from patients who developed secondary tumors (cutaneous squamous-cell carcinomas and keratoacanthomas) after treatment with B-Raf inhibitors (88). In this report, HRAS mutation was demonstrated to be associated with accelerated cell proliferation due to increased MAPK pathway activity both *in vitro* and *in vivo* in response to exposure to B-Raf inhibitors. Recently, acceleration of an acute myelogenous leukemia with mutant Ras was reported as a result of vemurafenib therapy for melanoma (89). While the sequence of the event between the evolution of RAS mutations and the development of secondary tumors is still unclear, these reports suggest that the mutational status of the RAS genes should be carefully monitored in patients who are treated with a mutant specific B-Raf inhibitor over the course of the treatment. Furthermore, they also highlight the urgent need to develop therapies selectively targeting RAS-mutated melanomas. As described in Chapter 1, targeting Ras protein themselves was discovered to be extremely difficult, underlining the need for alternative strategies in these types of melanomas, such as the synthetic lethal approach introduced in Chapter 1.

In this chapter, the efficacy of B106 in BRAF-mutated melanoma cell lines that have developed resistance to vemurafenib (called by its alternative name PLX4032 in the following section), the mechanism of drug resistance, and its potential relation to NRAS-mutated cells are studied. The differential response to B106 between PLX4032-resistant cells and their parental cells provides an insight towards the potential clinical application of PKCδ inhibitors in the future.

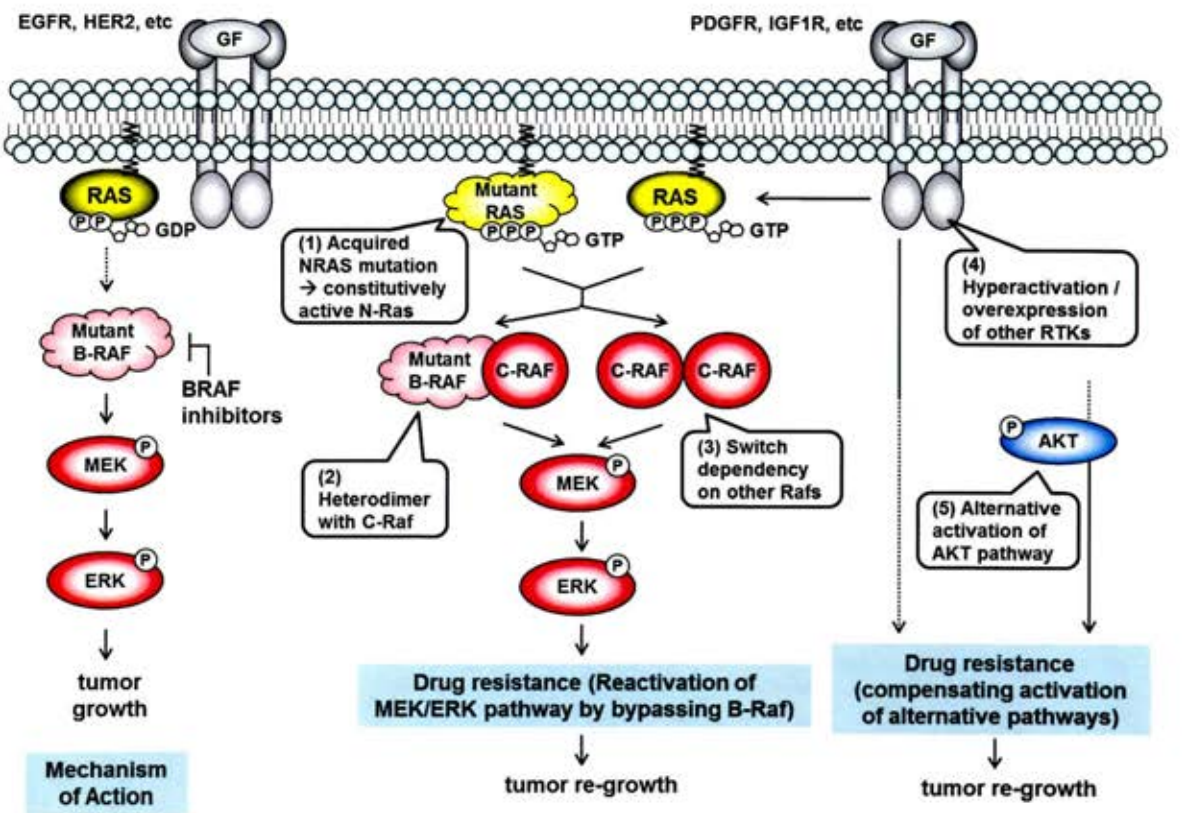

Figure 21: Mechanism of action and resistance to B-Raf inhibitors. (Left) **Mechanism of action**: B-Raf inhibitors prevent transmission of the MEK/ERK pathway specifically in tumorigenic cells carrying mutant B-Raf which have low Ras activity. (Middle) **Mechanism of resistance (reactivation of MEK/ERK pathway)**: Secondary mutation in NRAS converts normal N-Ras protein that is activated only on GTP-bound state into oncogenic Ras protein that is constitutively activated (1). High Ras activity induces heterodimerization of mutant B-Raf with C-Raf (2) or increases dependency on other Raf family members (3) in accordance with hyperactivation or overexpression of C-Raf. These events reactivate MEK/ERK pathway by bypassing B-Raf inhibition by the inhibitors. (Right) **Mechanism of resistance (activation of alternative pathways)**: constant inhibition of B-Raf increases the activity or expression of other RTKs, such as PDGFR or IGF1R (4) or the activity of AKT pathway (5). Cells adapt to the condition of suppression of mB-Raf/MEK/ERK signaling by switching survival signaling to dependency on alternative pathways.

3-2. Results

Establishment of PLX4032-resistant BRAF mutant melanoma cell sub-lines and their susceptibility to cell growth inhibition initiated by PKCδ inhibition

Although the B-Raf inhibitor PLX4032 (vemurafenib) was a great advance in melanoma therapy, development of resistance to the drug in most patients has been an ongoing challenge. Because one of the proposed models of PLX4032 resistance involves the secondary mutation of NRAS and because my initial studies revealed the effectiveness of PKCδ inhibitors in NRAS mutant cells, I next tested whether B106 could be effective in those BRAF mutant melanoma cells that have become refractory to PLX4032. I established the BRAF V600E mutant melanoma cell sub-lines resistant to PLX4032 by continuously exposing A375 and SKMEL5 cells to PLX4032, with the concentrations gradually increased over weeks. The morphology of PLX-4032 resistant cells (referred as "PLX-R") was flatter, and more enlarged and spindle-looking compared to their parental cells in both the A375-PLX-Rs and SKMEL5-PLX-Rs derivatives (**Figure 22**). Resistance of PLX-Rs to PLX4032 was verified by comparing their sensitivity to the drug with that of their parental cells (**Figure 23**). PLX-R derivative lines from both A375 and SKMEL5 grow in the presence of concentrations of PLX4032 which were cytotoxic to the parental cells, as assessed by MTS assay.

B106 effectively inhibited cell growth of both A375-PLX-Rs and SKMEL5-PLX-Rs, verifying the potency of B106 in B-Raf inhibitor-resistant melanoma cells with BRAF mutation in addition to melanoma cells with NRAS mutations (**Figure 23**). The

specificity of this growth inhibitory effect on cell survival produced by PKCδ inhibition was confirmed by lack of the same effect by negative control compound B154 (**Figure 23**). In addition, proliferation of melanoma cells carrying BRAF mutations (the parental cells of the PLX-Rs) was also prevented by B106 (**Figure 23**). As discussed below, parental cells and PLX-R cells show differential behaviors in response to B106 treatment. Although B106 abrogates proliferation of both parental cells and PLX-R cells, it is possible that they undergo growth inhibition via distinct molecular mechanisms. Alternatively, our previous studies had shown that oncogenic mutation of CRAF makes non-transformed cells susceptible to PKCδ inhibition (10). It is also possible that the V600E BRAF mutation may be similarly sensitizing the cells to growth inhibition by PKCδ inhibitors.

Mechanism of resistance to a B-Raf inhibitor

As a part of the scheme approach to better understand the actions of B106, the mechanism of resistance of PLX-R cells was studied. Genomic DNA was sequenced in the region flanking frequently mutated codon 61 of NRAS in order to examine whether development of resistance is the consequence of secondary NRAS mutations, as one of the proposed models of resistance has suggested. SBcl2 cells were found to possess Q61K mutations homozygously as predicted, validating the assay. The sequencing analysis demonstrated that neither of the A375-PLX-Rs or the SKMEL5-PLX-Rs had acquired a mutation in NRAS residue 61 (**Table 3**).

Subsequently, the activity of the endogenous Ras proteins was assayed to explore the possibility that aberrant Ras activity other than NRAS mutation was responsible for the acquired PLX4032 resistance, because aberrant activation of Ras proteins can result from a number of events other than genetic mutations in the RAS genes. Under physiological conditions, Ras proteins, when activated by extracellular signals and GTP bound, bind to the Ras-binding domain (RBD) in the Ras effector proteins. In this assay, activated Ras proteins were pulled down with an agarose-conjugated RBD peptide and detected by immunoblot analysis with antibodies against N-Ras or pan-Ras. As predicted, NRAS mutant SBcl2 melanoma cells and NIH-3T3 cells that were stably-transfected with NRAS-Q61K mutant (called "NIH-NRAS" below) showed high N-Ras activity, serving as positive controls for the assay system (Right panel at Row 1, **Figure 24**). The left panel in Row 1 showed slightly higher activity levels of N-Ras in A375-PLX-R lines compared to A375 parent cells (**Figure 24**). Row 2 panels were blotted for pan-Ras activity (K-Ras, H-Ras and N-Ras) and the left panel also suggests slightly elevated activation of Ras proteins in A375-PLX-Rs (**Figure 24**); however, further data is needed to confirm elevated Ras activity in these sub lines.

Immunoblot analyses were next conducted under two conditions of PLX4032 exposure treatment to determine a pathway or molecules whose basal activity are altered in PLX-R cells and contribute to build resistance to PLX4032. PLX4032 was withdrawn from PLX-R cells for 48 or 72 hours in the first set in order to determine basal levels of activity or expression of the molecules in PLX-R cells that have previously been reported to be involved in mechanisms of resistance (left half in each cell series in Figure 25). The

second treatment condition compared the basal activity or expression levels of PLX-R cells in the presence of the inhibitor to the response of parent cells to the drug (right half in each cell series in Figure 25). The parent cells were exposed to the drug for only 6 hours to decrease cytotoxic effects which might confound interpretation. C-Raf was expressed at high levels in SKMEL5-PLX-Rs, whereas hyperactivation of C-Raf, as evidenced by phosphorylation, was observed in A375-PLX-Rs (**Figure 25**). Differences in AKT or B-Raf activation between parental cells and PLX-R cells were not observed. In addition, **Figure 25** demonstrated that both SKMEL5-PLX-Rs remain responsive to ERK-MAPK pathway inhibition by PLX4032, and yet are capable of surviving under the drug-treatment conditions, indicating that these cells employ an alternative pathway for survival to compensate for mutant B-Raf/ERK inhibition by the drug. Conversely, A375-PLX-Rs exhibited higher phosphorylation levels of ERK regardless of the presence or absence of PLX4032 compared to parent A375 cells (**Figure 25**). Combined with the observation of hyperactivation of C-Raf, the results imply that A375-PLX-R cells have overcome drug-induced inhibition of aberrant B-Raf activity after prolonged exposure to the drug and maintain their survival by bypassing B-Raf inhibition and switching over to C-Raf-mediated ERK signaling reactivation.

As described in the chapter introduction, B-Raf selective inhibitors were reported to paradoxically activate the MEK/ERK pathway via C-Raf in RAS-mutant cells, leading to accelerated cell proliferation. This model was, indeed, confirmed in my NIH-NRAS cells as well: exposure of NIH-NRAS cells to PLX4032 increased the phosphorylation level of ERK. In contrast, exposure to the MEK inhibitor U0126 resulted in attenuated

ERK phosphorylation, compared to the vehicle-treated cells (**Figure 26**). U0126 treatment decreased ERK phosphorylation in parental NIH-3T3 cells as well as NIH-3T3 cells that were stably-transfected with BRAF-V600E mutant ("NIH-BRAF"), whereas only NIH-BRAF cells, but not parental cells which do not express oncogenic B-Raf decreased phospho-ERK level in response to U0126 (**Figure 26**). Indication of elevated Ras activity (Figure 24) and switched dependency from B-Raf to C-Raf for ERK signaling (Figure 25) in A375-PLX-R cells might provide a basis for a Ras/C-Raf-mediated mechanism of resistance, at least in A375-PLX-R cells.

Resistance to PLX4032 transforms the response of BRAF-mutated cells to resemble that of NRAS-mutant type with respect to H2AX activity

As the JNK-H2AX cascade was shown to play an important role in B106-induced apoptosis in NRAS mutant melanoma cells (Chapter 2), the activation of JNK and H2AX was studied in PLX-R cells and their parental cells in response to B106 treatment. A375 parental and A375-PLX-R5 cells, and SKMEL5 parental and SKMEL5-PLX-R4 cells, were treated with B106 at two different concentrations (0.5 or 2μM) for two different durations (2 or 10 hours).

An immunoblot analysis demonstrated that the basal level of H2AX phosphorylation was elevated in both A375-PLX-R5 and SKMEL5-PLX-R4 cells (**Figure 27**). Furthermore, B106 treatment consistently induced more robust activation of H2AX in these cells, in comparison to parental cells, in which H2AX activation following B106 treatment was not observed (A375 cells), or only slightly induced

(SKMEL5 cells) (**Figure 27**). These results from PLX-R lines derived from two independent BRAF mutant cell lines suggest that acquired resistance to PLX4032 may change the sensitivity of the cells to B106-induced H2AX phosphorylation, making their response more similar to the response of NRAS mutant melanoma cell lines. Considering that cell growth inhibition is induced in BRAF mutant melanoma cells as effectively as in NRAS mutant cells by PKCδ inhibition (Figure 23), this might suggest that inhibition of PKCδ causes cell growth inhibition through different molecular mechanisms in BRAF mutant cells and NRAS mutant cells, and acquired drug resistance in BRAF mutant cells might introduce the NRAS-mutant type mechanism to BRAF mutant cells.

Interestingly, basal JNK activity was higher in A375-PLX-R5 cells than in A375 parental cells, while SKMEL5 parental cells displayed more basal JNK activity than SKMEL5-PLX-R4 cells (**Figure 27**). This observation together with other published studies raises a hypothesis about a crosstalk between ERK and JNK, although it is beyond the scope of this dissertation project. This crosstalk is to be addressed in more detail in the discussion section below.

PLX4032 and B106 together additively inhibit cell growth in melanoma cells with BRAF mutation

Fundamentally, cancer recurrence resulting from drug resistance occurs because a small number of cells develop resistance to the therapy and survive the regimen to gradually proliferate into a recurrent cancer. Therefore, ideally, recurrence can be preventable if the first regimen could eliminate all the cancerous cells. Generally, the

dose of any drug required to do so might be far above the therapeutic window and produce serious adverse effects to normal cells, and ultimately, the entire body. In this sense, a combination therapy of multiple drugs could provide a more reasonable strategy if those drugs, at the doses within their therapeutic windows, together generate a greater anti-cancer effect with manageable adverse events.

Based on this principle, therefore, the potential combinatorial application of B106 with PLX4032 in a regimen in melanomas with a BRAF mutation was explored. A375 and SKMEL5 cells were plated at low cell density and treated with B106 or PLX4032 alone or together for 8 days. Then, cell colonies, each of which was formed from an individual viable cell, were stained and quantified. Combinational use of B106 and PLX4032 reduced the number of colonies from both A375 and SKMEL5 cells to a greater effect than B106 or PLX4032 alone, exhibiting a more extensive effect on irreversible cell growth inhibition (**Figure 28**). This experiment suggests the potential benefit of B106 in combination with PLX4032 in melanomas with BRAF mutations, by further lowering the number of cells that survive the drug treatment and might eventually develop resistance to PLX4032.

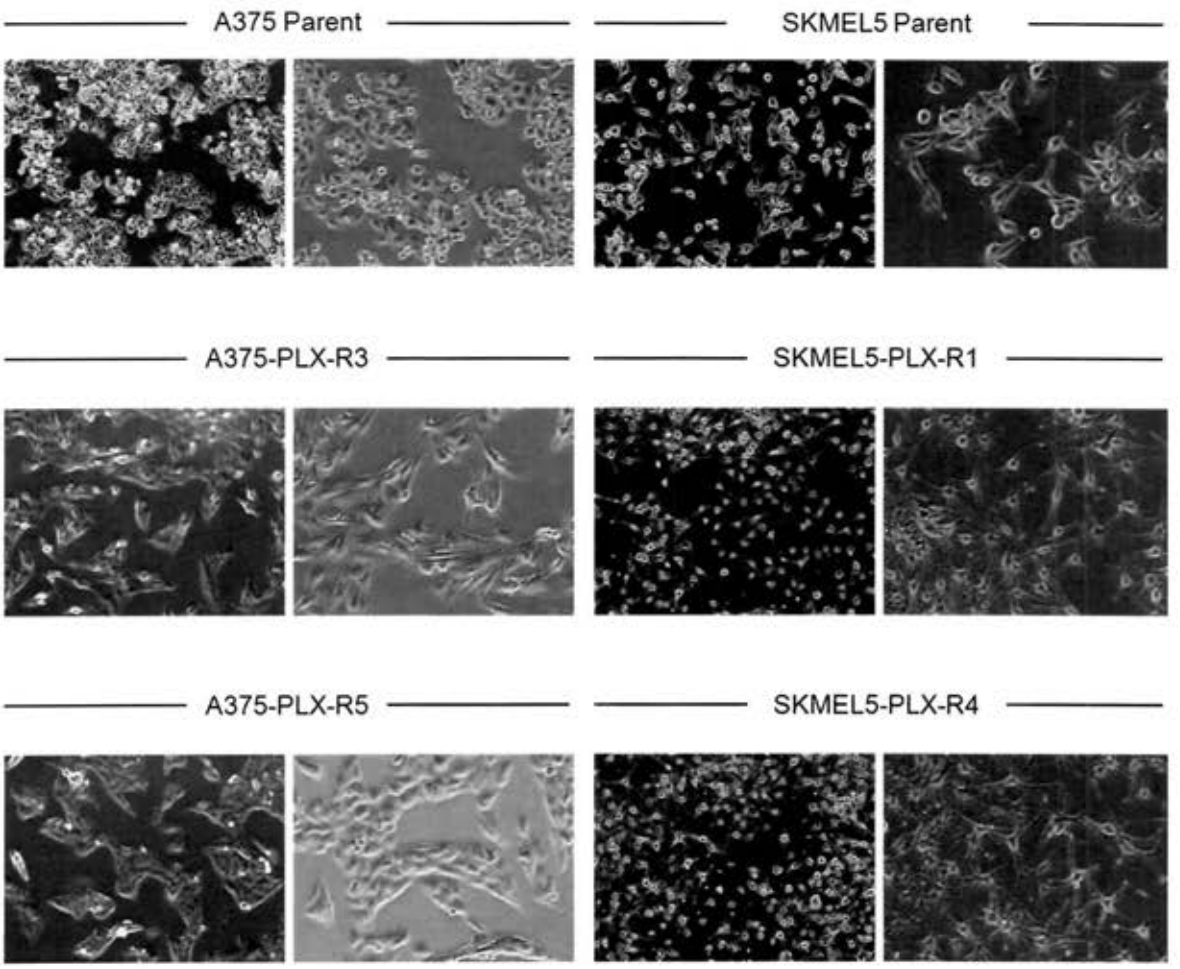

Figure 22: Establishment of PLX4032-resistant BRAF mutant melanoma cell sub-lines and morphological comparison between parent and PLX4032-resistant cells. To derive PLX4032-resistant sub-lines (referred as "PLX-R"), A375 and SKMEL5 cells were plated at low cell density and treated with PLX4032 at 1μM or 0.5μM, respectively. Over the course of a 3-4 week period, the concentration of PLX4032 was gradually increased up to 4μM (A375) or 2μM (SKMEL5) and clonal colonies were picked. Derived cells have been maintained in PLX4032-containing medium (1μM: A375-PLX-Rs, 0.5μM: SKMEL5-PLX-Rs). Photographs were taken at the lower (left) and higher magnifications (right).

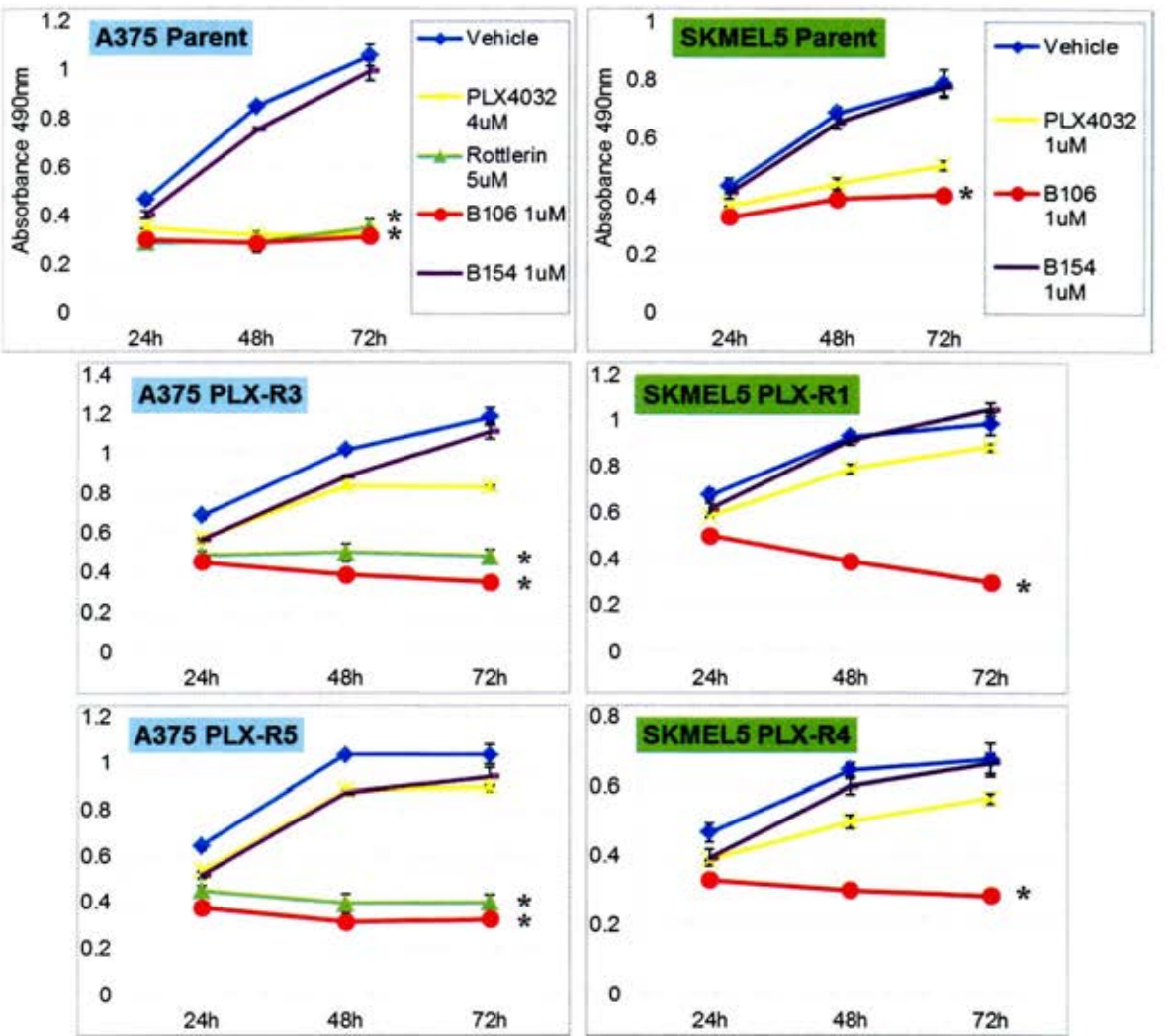

Figure 23: Resistance of A375-PLX-R and SKMEL5-PLX-R cells to PLX4032 and effect of PKCδ inhibitors on cell survival. (Left) A375 parental and two A375-derived PLX4032-resistant cell lines, R3 and R5, (Right) SKMEL5 parental and two SKMEL5-derived PLX4032-resistant cell lines, R1 and R4. To confirm resistance to PLX4032, the viability of PLX4032-resistant cells and their parental cells was measured by MTS assay during treatment with PLX4032 (4μM: A375 and its derivatives, 1μM: SKMEL5 and its derivatives). To assess the effect of PKCδ inhibition, cells were treated with rottlerin (5μM) or B106 (1μM) at the indicated times, and MTS assays were performed. DMSO and B154 (2μM) served as a vehicle control and a compound negative control for B106, respectively. Each point represents the average of triplicate and error bars indicate the standard deviations of triplicates. P values (*) were calculated between DMSO (vehicle control) and rottlerin or DMSO and B106 in each cell line at 72 hours ($p < 0.0002$). The experiment was repeated at least twice in each cell series.

	NRAS			BRAF		
Cell line	Genomic mutation	A.A. mutation	Allele	Genomic mutation	A.A. mutation	Allele
A375 Parent	-	-	-	T1799A	V600E	Homo
A375 PLX-R3	-	-	-	T1799A	V600E	Homo
A375 PLX-R5	-	-	-	T1799A	V600E	Homo
SKMEL5 Parent	-	-	-	T1799A	V600E	Hetero
SKMEL5 PLX-R1	-	-	-	T1799A	V600E	Hetero
SKMEL5 PLX-R4	-	-	-	T1799A	V600E	Hetero
SBcl2	C181A	Q61K	Homo	-	-	-

Table 3: Analysis of genomic NRAS mutations of A375-PLX-R and SKMEL5-PLX-R cells. Genomic DNA of A375 and SKMEL5 cells, and their derivative PLX4032-resistant (PLX-R) sub lines were sequenced around the commonly mutated codon 61 in NRAS and codon 600 in BRAF. Resistant cell lines did not acquire secondary mutations at codon 61 in NRAS. The presence of BRAF V600E mutation was also confirmed in these cell lines.

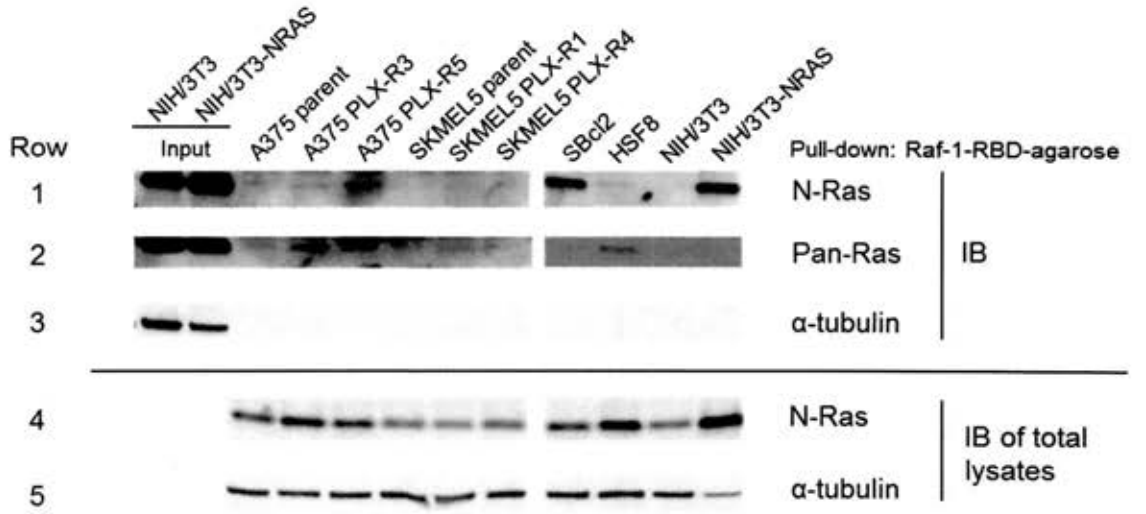

Figure 24: Analysis of Ras protein activity of A375-PLX-R and SKMEL5-PLX-R cells. (Top) Activated Ras protein (GTP-bound) was pulled down from whole cell lysates with agarose-conjugated Ras-binding domain (RBD) peptide, and detected by immunoblot analysis with N-Ras specific antibody (Row 1) or pan-Ras antibody (Row 2). Levels of α-tubulin served as a loading control for input (Row 3). (Bottom) Immunoblotting of total lysates was performed to confirm the basal level of N-Ras expression. Levels of α-tubulin served as a loading control. This experiment was performed once.

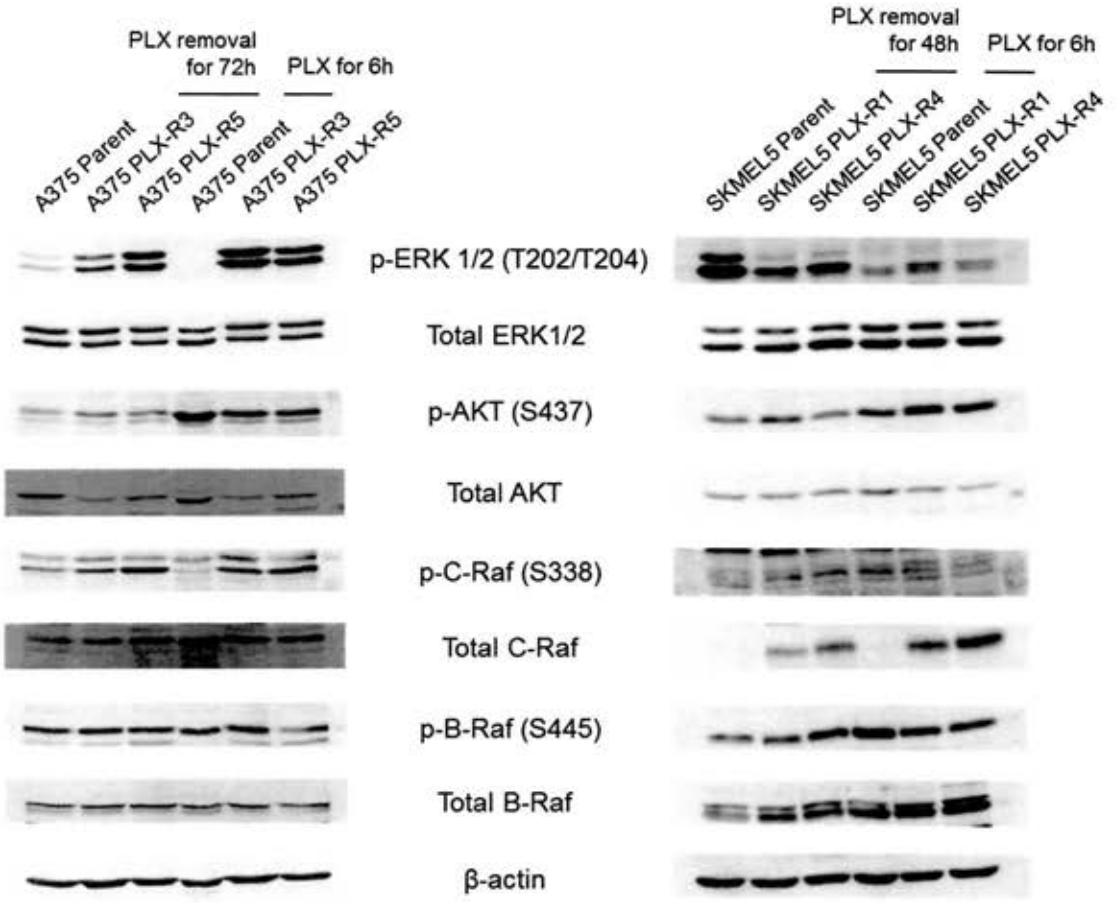

Figure 25: Mechanism of PLX4032 resistance. In the left three lanes of A375 and SKMEL5 samples, parental cells were maintained in normal medium (no PLX4032) for the entire period of experiment, whereas PLX4032 had been washed out of the medium for at least 48 hours in the A375-PLX-Rs and SKMEL5-PLX-Rs lines prior to lysis. In the right three lanes of the A375 and SKMEL5 samples, fresh PLX4032-containing medium (4μM: A375, 2μM: SKMEL5) was replaced with normal medium (no PLX4032) in parental cell plates and with PLX4032-containing medium in PLX-R cell plates 6 hours before lysing. Protein lysates were subjected to immunoblotting for phosphorylation or total expression levels of the indicated proteins. Levels of β-actin served as a loading control. This experiment was performed once.

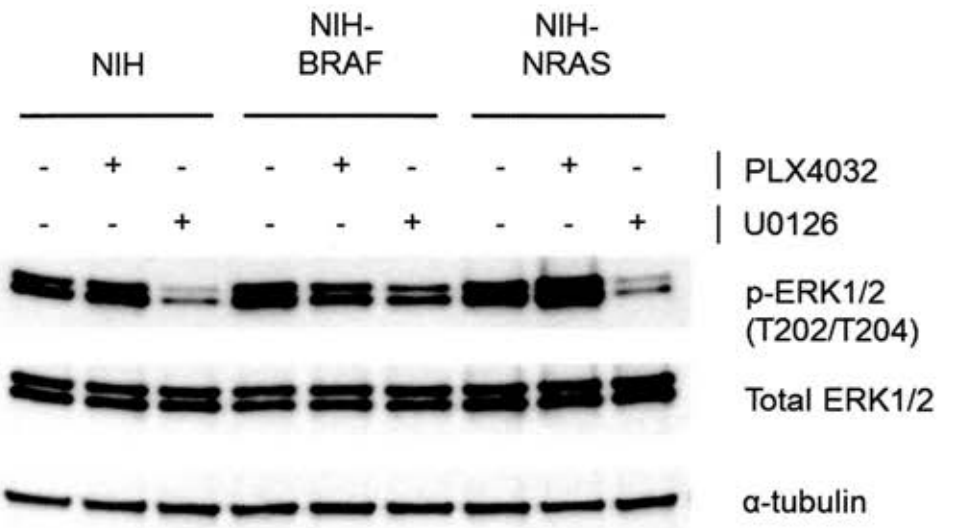

Figure 26: Paradoxical activation of ERK by PLX4032 treatment in NIH-NRAS cells. NIH-BRAF and NIH-NRAS cells stably express mutant form of B-Raf V600E or N-Ras Q61K. These cells were established by stably-transfecting NIH/3T3 cells with BRAF V600E mutant or NRAS Q61K mutant expressing plasmid and selected by puromycin treatment (2.5μg/ml). The cells were treated with PLX4032 (2μM), U0126 (5μM) or vehicle for 24 hours. Protein lysates were subjected to immunoblotting for phosphorylation or total expression levels of the indicated proteins. Levels of α-tubulin served as a loading control. PLX4032 preferentially inhibits the V600E mutant form of B-Raf. ERK phosphorylation was attenuated by PLX4032 treatment in NIH-BRAF cells, while NIH/3T3 parental cells which do not carry mutant B-Raf were not susceptible to PLX4032. On the other hand, PLX4032 paradoxically increased the level of ERK phosphorylation in NIH-NRAS cells, consistent with previous reports. The MEK inhibitor U0126 reduced the level of ERK phosphorylation in all three cell lines. This experiment was performed once.

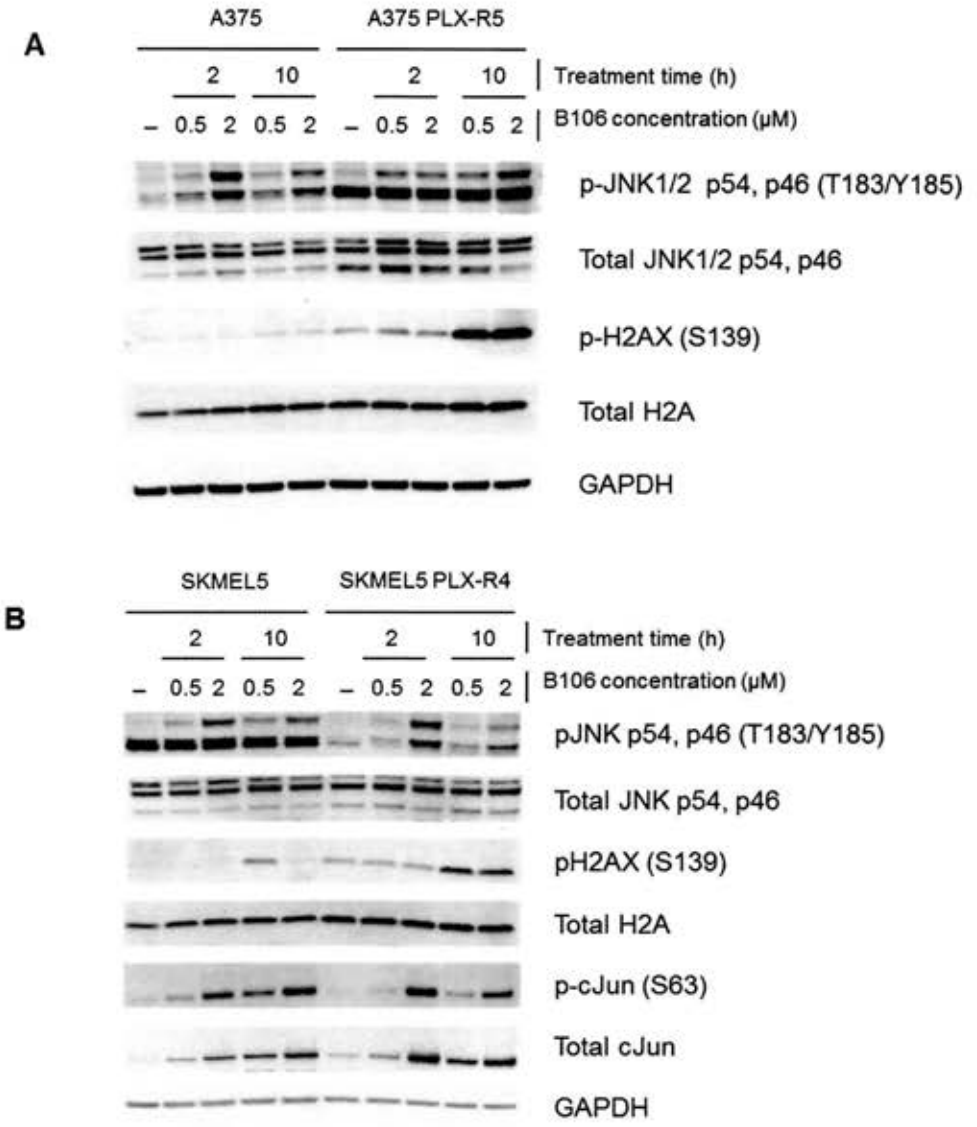

Figure 27: Activation of H2AX by B106 treatment in A375-PLX-R5 and SKMEL5-PLX-R1 cells compared to parental cells. Cells were treated with B106 at the indicated concentrations for the indicated times. A375-PLX-R5 and SKMEL5-PLX-R4 cells were treated with B106 in the presence of PLX4032 (4μM for A375 and its derivative, 2μM for SKMEL5 and its derivative). Protein lysates were subjected to immunoblotting for phosphorylation or total expression levels of the indicated proteins. Levels of GAPDH served as a loading control. Both A375 PLX-R5 and SKMEL5 PLX-R4 cells had higher basal phosphorylation levels of H2AX compared to parental lines, and B106 treatment induced more robust activation of H2AX in both PLX-R cell lines than in parental cells. The experiment was repeated twice using A375 and A375-PLX-R5 and performed once using SKMEL5 and SKMEL5-PLX-R4. The same experiment was performed in SKMEL5 and SKMEL5-PLX-R1 as well, with the same results.

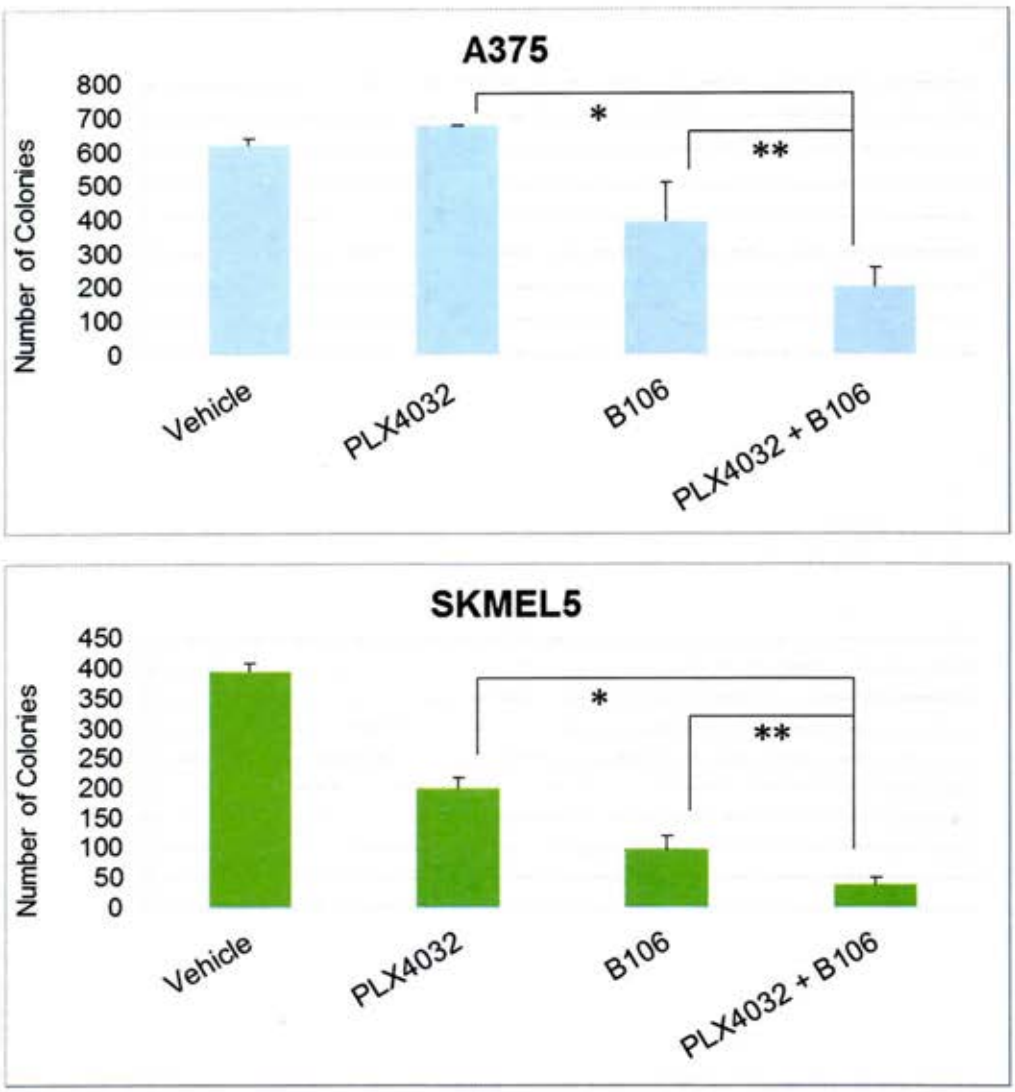

Figure 28: Additive irreversible effect of PLX4032 and B106 on cell viability in BRAF mutant cells. The same numbers of A375 and SKMEL5 cells were plated at low cell density and treated with PLX4032 (4μM: A375, 0.5μM: SKMEL5) or B106 (0.1μM) alone or together for 8 days. DMSO served as a vehicle control. Cell colonies were stained with ethidium bromide for visualization and counting. Each point represents the average of duplicate and error bars indicate the standard deviations of duplicate. P values: ** $p \leq 0.05$, * $p < 0.002$. Combination treatment of PLX4032 and B106 had an additive inhibitory effecte on the colony formation ability of the cells compared to treatment with PLX4032 or B106 alone. This experiment was repeated more than five times.

3-3. Summary

In spite of the high response rate and initial tumor regression, PLX4032, a potent B-Raf inhibitor approved for melanomas carrying oncogenic BRAF-V600E mutations, challenges remain: most patients relapse due to resistance to this drug and the drug is ineffective in the 40-50% of patients with melanomas lacking the mutation. In this chapter, the possibility of the potential application of PKCδ inhibition in PLX4032-resistant melanomas, in addition to melanomas with NRAS mutation as studied in Chapter 1, was explored. First, PLX4032-resistant sub-cell lines of BRAF-mutated cells A375 and SKMEL5 (termed as "PLX-Rs") were established by constantly exposing those cells to the drug. Proliferation of PLX-R cells of both A375 and SKMEL5 was inhibited in the presence of B106, indicating PKCδ can potentially be a therapeutic target in B-Raf inhibitor resistant melanomas as well as in melanomas with NRAS mutations. Among the proposed mechanisms of resistance to B-Raf inhibitors, C-Raf hyperactivation appears to be the mechanism at least in A375-PLX-Rs possibly in the association with elevated Ras activity. Both A375-PLX-Rs and SKMEL5-PLX-Rs possess higher levels of basal H2AX activity, and induced more robust activation of H2AX in response to B106 than their parental cell lines. This observation raises the hypothesis that acquiring B-Raf inhibitor resistance results in BRAF-mutated melanoma cells responding more similarly to NRAS-mutated type cells in terms of their response to B106 treatment.

Furthermore, combinatorial treatment of B106 and PLX4032 produced a greater effect on cell growth inhibition in melanoma cells with BRAF mutations, which suggests

that this combination therapy may have clinical benefit in delivering superior anti-proliferation activity.

Discussion and Future Directions

Overview of melanoma and current obstacles to effective therapy

2011 was an exciting year in the history of melanoma treatment: the FDA approved the first two targeted therapies for metastatic melanoma, in which conventional treatment options have not made a significant improvement in patients' overall survival for decades. In particular, the impressively high response rates of over 50% produced by vemurafenib treatment appeared revolutionary. However, almost all responders who have experienced significant tumor regression from vemurafenib treatment relapse due to acquired drug resistance to the drug (7). Although B-Raf mutant tumors, one form of which (V600E) is exclusively the target of vemurafenib, account for 50-70% of melanoma cases (4), B-Raf inhibitors alone do not represent the ultimate treatment for metastatic melanomas due to this issue of drug resistance. On the other hand, there has not to date been a targeted therapy for melanomas harboring NRAS mutations, the second most frequent genotype after BRAF, and MEK inhibitors currently in clinical trials are not likely to become an important option in NRAS-mutated melanomas due to their preferential activity against BRAF-mutated melanomas (even though they should theoretically be as effective in NRAS-mutated melanomas as BRAF-mutated melanomas) (3). This reality means that melanomas remain among the cancers that still await potent treatment options. In particular, melanomas with NRAS mutations and melanomas previously treated with B-Raf inhibitors represent an unmet medical need, as they constitute a large proportion of the melanoma cases.

B-Raf inhibitor resistance and its mechanisms

B-Raf inhibitor PLX4032 (vemurafenib), one of the first two targeted therapy in melanoma, was a major advance in melanoma therapy. Although it achieves a remarkably high response rate and tumor regression in responders initially in treatment, tumors eventually and inevitably relapse due to the development of resistance to this drug. Several models have been proposed as to how cells acquire resistance to PLX4032: 1) reactivating MEK/ERK pathway through bypassing BRAF (via secondary mutation in NRAS, hyperactivation/overexpression of C-Raf, or activation of another MAPKK COT), or 2) adapting dependency on alternative pathways (hyperactivation or overexpression of receptor tyrosine kinases, such as PDGFRβ or IGF1R). Ironically, the complexity and redundancy of Ras signaling pathways that allow the cells to adjust the change in the surrounding environment with flexibility provide the tumor cells many opportunities for drug resistance. While not diminishing the importance of PLX4032 as a breakthrough drug, development of strategies to conquer or bypass the resistance has now become the next urgent task in the field, as has the development of therapies for category of melanomas that remain unaddressed: NRAS-mutated melanomas. Moreover, the potential risks of the use of B-Raf inhibitor in RAS-mutated melanomas (84-87), and their potential to cause secondary tumors with RAS mutations (88, 89) further highlight the necessity to explore the mechanisms of action, resistance or influence of B-Raf inhibitors.

To explore the potential of a PKCδ-targeted inhibition therapeutic strategy, PLX4032-resistant cell lines were established from two individual BRAF-mutated melanoma cell lines. These sub lines can survive in the presence of PLX4032 at

concentrations that effectively inhibit the growth of the parental lines (Figure 23). None of the PLX4032-resistant cell lines tested harbors a secondary genomic mutation in NRAS codon 61 (Table 3), but some sub lines showed the potential evidence of elevated activity of the endogenous Ras proteins (Figure 24). Furthermore, PLX4032-resistant cell lines demonstrated hyperactivation/overexpression of C-Raf, another isozyme in the Raf family (Figure 25). Previously, C-Raf was demonstrated to mediate the activity of the ERK-MEPK pathway in RAS mutated cells, resulting in accelerated tumor cell growth (84-87). Considered together, the mechanism of resistance in the PLX4032-resistant cell lines established in this study might be the result of the hyperactivation/overexpression of C-Raf, in possible association with elevated Ras activity, at least in derivatives from one of the two cell resistant cell types.

Apoptosis and chemotherapy

Apoptosis or programmed cell death plays a critical role in the action of many anti-cancer drugs. Because apoptosis induces ordered disruption of the cell without leakage of cellular components and induction of inflammation, it is fundamental for development and regulation of tissue homeostasis whose alteration has serious consequences. For an anti-cancer therapy that aims selective toxicity to only tumorigenic cells without damaging neighboring normal cells, apoptosis is an ideal ultimate mechanism of action. There are two major forms of apoptosis. Extrinsic apoptosis is induced by extracellular signals/ligands bound to the death receptors that belong to the TNF/NGF family, while the intrinsic pathway is activated in response to stress conditions

including DNA damage or oxidative stress (61). In spite of the differences in initiation processes, apoptosis is executed in a complicated multistep cascade regulated by the balance between pro-apoptotic and anti-apoptotic effectors to ensure it happens only when needed to maintain the homeostasis with the surrounding environment. Caspases are at the center of apoptosis regulation. Early in the apoptotic sequence, initiator caspases (caspases 8 or 9) are activated following the initiation of apoptosis, which in turn cleave and mature the downstream caspases, called effector caspases, such as caspases 3, 6 or 7, which then regulate further downstream apoptotic modulators (61). The most well-known apoptotic regulators, the Bcl2 family proteins, are divided into pro-apoptotic members and anti-apoptotic members. Pro-apoptotic members mediate apoptosis by disrupting mitochondrial membrane integrity, either directly forming pores or indirectly by binding to mitochondrial channel proteins, while anti-apoptotic members prevent apoptosis by interfering with pro-apoptotic members (61). The Bcl2 family as well as IAPs also regulate the activity of caspases. Apoptotic cells undergo a series of morphological events: DNA fragmentation, nuclear and cytoplasmic condensation and formation of apoptotic bodies, small membrane-enclosed particles containing cellular components which are eliminated by neighboring cells or phagocyte.

PKCδ as a therapeutic target in melanoma with NRAS mutations and B-Raf inhibitor resistance

The rationale for a potential PKCδ-targeted therapy against tumors with aberrant Ras signaling is based on prior reports. Firstly, PKCδ was demonstrated to be non-essential for the survival and proliferation of normal cells and PKCδ-null animals develop normally and are fertile (11), providing a postulate that a therapeutic approach targeting PKCδ would likely spare normal cells, but inhibit proliferation of cancerous cells whose survival depend on PKCδ activity. Thus, this approach would provide a tumor-specific therapy. In contrast, PKCα and λ are required for normal development (60). In this respect, selectivity of PKCδ inhibitors against PKCδ over other PKC isozymes is critical in the development of PKCδ inhibitors.

Second, inhibition of PKCδ preferentially inhibited growth of cancer cell lines with genomic mutations in the RAS genes, oncogenic activation of Ras proteins, or aberrant activation of Ras signaling pathways (10, 58). The incidence of urethane-induced lung tumors was 69% lower in PKCδ-knockout mice compared with wild-type mice (90). All of these wild type mice that developed tumors had activating mutations in KRAS, while only 69% of PKCδ-knockout tumors had KRAS mutations (90). These studies proposed the possible correlation between PKCδ inhibition and aberrant Ras activation in cancers. Oncogenic mutations of RAS are prominent in many types of cancers with particularly high prevalence and mortality rates and approximately 30% of human cancers are estimated to harbor activating mutations in one of the three Ras isoforms (KRAS, NRAS and HRAS) (91). Taken together, these reports above underline the potential of PKCδ-targeted therapy as a cancer-specific therapy targeting tumors with RAS mutations or aberrant Ras activity, those types of tumors which are particularly

difficult to treat, such as pancreatic cancers, lung cancers, colorectal cancers and melanomas. One of the proposed mechanisms of B-Raf inhibitor-resistance is the evolution of secondary mutations in NRAS, suggesting a potential link between B-Raf resistant melanoma and RAS mutations.

Motivated by this background on PKCδ and Ras, this dissertation project was aimed to assess the potential of PKCδ as a therapeutic target in NRAS-mutant melanomas and B-Raf inhibitor-resistant melanoma potentially with secondary NRAS mutations, which remain insensitive to the currently available treatment options. The goals of the project were: 1) to examine the effect of PKCδ inhibition on the suppression of tumor cell growth in melanomas with NRAS mutations and B-Raf inhibitor-resistant melanomas; 2) to identify the molecular mechanism of tumor cell growth inhibition initiated by PKCδ inhibition; and 3) to evaluate the efficacy of a novel PKCδ inhibitor BJE6-106 (B106), which has been developed in our lab, against these cancers (Figure 3, Table 1).

The dissertation work supports the potential of PKCδ as a therapeutic target in melanomas. Cell proliferation assays demonstrated that inhibition of PKCδ suppressed cell growth in multiple melanoma cell lines with NRAS mutations (Figure 5). PKCδ inhibitors were also demonstrated to be effective in PLX4032-resistant cell lines (Figure 23). The cell lines tested included different types of amino acid substitution of NRAS codon 61, the most frequently mutated codon at NRAS (Table 2), suggesting the effect of PKCδ inhibitors does not depend on a specific NRAS mutation for their activity (unlike B-Raf inhibitors, some of which are selective to only the most common mutation, V600E). B106, which showed 1000-fold selectivity against PKCδ over PKCα in

preliminary *in vitro* kinase assay, was active at nano molar concentrations, ten times lower than for rottlerin (Figure 5). The suppression of tumor cell growth was shown to be induced through caspase-dependent apoptosis (Figures 8 and 9). These results in the cell culture system exhibited a great potential of PKCδ inhibitors as targeted agents, although the *in vivo* efficacy of B106 is yet to be determined.

JNK signaling in apoptosis and PKCδ inhibition

Comprising one of the three MAPK pathways, the JNK pathway is involved in a wide variety of critical cellular activities, including apoptosis and the DNA-damage response. The JNK pathway, initially discovered as a UV radiation-responsive signal (92, 93), induces apoptosis in part through regulating the Bcl2 family members mentioned above. JNK activates pro-apoptotic BAD by phosphorylation at Ser 128, which keeps scaffold protein 14-3-3 from sequestering BAD (94, 95). Activated BAD binds the anti-apoptotic Bcl2 members and prevents them from being activated (96). Direct phosphorylation of anti-apoptotic Bcl2 by JNK was shown to inhibit its activity (97, 98). JNK also regulates translocation of pro-apoptotic Bax to mitochondria for activation through phosphorylating 14-3-3, which prevents 14-3-3 from sequestering Bax. JNK-induced cleavage of pro-apoptotic Bid prevents activation of Bax (99-101). Alternatively, JNK also activates transcription of genes that regulate apoptosis. JNK phosphorylates components of activator protein 1 (AP-1), a transcription factor complex, including c-Jun, JunD or ATF2, which activate transcription of pro-apoptotic facilitators, such as TNFα or Fas-L (death receptor ligands) or Bak (a pro-apoptotic Bcl2 member) (102, 103).

Furthermore, a series of recent reports proposed a role for phospho-H2AX in apoptosis downstream of JNK, as discussed below. Supporting the critical role of JNK in apoptosis, mouse embryonic fibroblasts with JNK1/2 knocked-down were resistant to apoptosis induced by various apoptotic stimuli (104). Many chemotherapeutic agents employ the JNK pathway for their anti-cancer activity, such agents including paclitaxel, cisplatin or doxorubicin (105, 106).

In this dissertation project, activation of the JNK pathway was found to mediate caspase-dependent apoptosis induced by PKCδ inhibition. Among the previously-reported substrates of PKCδ, activation of JNK was consistently induced by B106 treatment, but other molecules, including the closely-related MAPKs p38 or ERK, were not activated (Figure 13). The effect of PKCδ inhibition specifically on JNK was further confirmed by selective downregulation of PKCδ protein using PKCδ-specific siRNA (Figure 16). Detailed pathway analysis demonstrated the cascade of MKK4-JNK1/2-H2AX is activated by B106 treatment (Figure 14). Furthermore, absence of JNK1/2 expression in the cells significantly mitigated caspase activity induced by PKCδ inhibition (Figure 18). These results imply the functional importance and necessity of the activation of this pathway in PKCδ inhibition-induced caspase-dependent apoptosis in NRAS mutant melanoma cells.

While almost all studies that link PKCδ and JNK were reported in the context of the pro-apoptotic function of PKCδ, one recent report demonstrated that knockdown of PKCδ induced apoptosis with increased phosphorylation of JNK in NIH-3T3 cells stably transfected with HRAS, consistent with my findings (47). In this report, knockdown of

PKCδ increased expression of PKCα and β, which subsequently interacted with Rack1 (an adaptor protein) to recruit JNK to the complex, which induced an apoptotic response. Although it is encouraging to find this similar observation produced in independent systems, it should be noted that the assays employed in that report were entirely performed using siRNA. While RNAi-based studies have an advantage in elucidating molecule-specific functions in the cells; the biological consequences of down-regulating a protein target by RNAi do not necessarily mimic the effects of a small molecule inhibitor bound to the target. The results based primarily on RNAi should therefore be interpreted with caution if its goal is as proof-of-concept for the development of an inhibitor against the activity of the target molecule as a therapeutic (and this is indeed generally the ultimate plan for such type of studies).

Crosstalk between ERK and JNK?

A number of observations made during the course of this work also warrant further investigation. As mentioned in Chapter 3, Figure 27 showed an apparently conflicting observation between the A375 and SKMEL5 lines with respect to basal JNK phosphorylation levels. Basal JNK activity was higher in A375-PLX-R5 cells than in A375 parental cells, while SKMEL5 parental cells displayed more basal JNK activity than SKMEL5-PLX-R4 cells. The pattern was not associated with either PLX4032 resistance or changes in basal expression level of H2AX phosphorylation between parental and PLX-R cells. Rather, it appeared to be correlated with the pattern of ERK

phosphorylation levels: that is, higher ERK activation level in A375-PLX-Rs and lower ERK activity in SKMEL5-PLX-Rs compared to the parental cell line of each (Figure 25).

Interestingly, transient treatment with PLX4032 (B-Raf inhibitor) or U0126 (MEK1/2 inhibitor) decreased the phosphorylation level of not only ERK but also JNK in A375 and SKMEL5 cells (**Figure 29)**, although the known direct action of both compounds is to inhibit only the activation of ERK. Indeed, *in vitro* kinase assays of these inhibitors demonstrated a lack of inhibitory actions on JNK1/2/3 (78, 107). As therefore the observed inhibition of JNK phosphorylation is not a result of the direct action of PLX4032 or U0126, this result means that transient inhibition of ERK signaling, by inhibitors against upstream B-Raf or MEK, results in inhibition of JNK activity by an unidentified mechanism.

Constitutive activation of MEK/ERK signaling was reported to enhance JNK activity in melanoma, by "rewiring" or causing crosstalk between the ERK and JNK signaling pathways (108). In that report, constitutively-high levels of ERK activity resulting from aberrant activity of upstream components (B-Raf or N-Ras) in melanoma increased transcription and stability of c-Jun through CREB or GSK3. The regulation of c-Jun by ERK pathway was not observed in the cells without constitutively-high ERK signaling. Subsequently, c-Jun increased transcription of target genes, including RACK1, an adaptor protein that serves a platform for PKCs to phosphorylate JNK and this provided a positive feedback loop between c-Jun and JNK, which further enhanced the c-Jun activity. My current results support this model of crosstalk from ERK to JNK signaling.

Although that report picked the cell lines studied based on their high levels of ERK signaling and the presence of genomic mutation (BRAF or NRAS), the cell lines were established from the tumors harvested from different patients with distinct genetic background. In my studies, PLX-Rs and their parental cell lines can serve pairs of cell lines that differ from each other minimally in terms of genetic makeup, certainly less than melanoma lines derived from different tumors, so examination of their responses to drugs may be informative. In Figure 25, higher ERK activation level compared to parental cells in A375-PLX-Rs indicates the PLX-Rs overcame the inhibitory activity of PLX4032 and reactivated Raf/MEK/ERK signaling, whereas lower ERK activity in SKMEL5-PLX-Rs suggests they still maintain a susceptibility to PLX4032 and survive constant PLX4032 exposure by employing an alternative survival pathway independently of ERK signaling. Thus, A375-PLX-Rs represent the cells with constitutively-elevated levels of ERK signaling in comparison to parental cells. In A375-PLX-R cells with high ERK activity, basal JNK phosphorylation level is also persistently elevated, in contrast to A375 parental cells which have lower ERK activity (Figure 27).

Collectively, these observations and the published report together produced the hypothesis on a possible crosstalk between ERK and JNK (**Figure 30**): temporary inhibition of the Raf/MEK/ERK pathway leads to inhibition of JNK activation in BRAF mutant melanoma (represented by A375 and SKMEL5), while those cells that have overcome the condition of long-term inhibition of Raf/MEK/ERK signaling and acquired constitutively-high levels of ERK activation might consequently generate higher activation levels of JNK by employing a crosstalk mechanism from ERK to JNK

(represented by A375-PLX-Rs). The cells that did not acquire the condition of constantly-high ERK activation level still maintain the normal level of basal JNK phosphorylation (represented by SKMEL5-PLX-Rs).

Dual function of phospho-H2AX – DNA repair and apoptosis

H2AX, histone H2A variant X, is actually a minor subtype of the H2A family. Approximately 10% of histone H2A proteins are H2AX in normal fibroblasts, although the proportion varies in different tissues (up to 20%) (109). H2AX in its phosphorylated form (phospho-H2AX, also called γH2AX) is primarily known for its role in DNA double strand breakage (DSB) repair, and has long been utilized as an indicator of DSB. Upon DSB formation, PI3K-like kinases, ataxia telangiectasia mutated (ATM), ataxia telangiectasia and Rad3-related (ATR) and DNA-dependent protein kinase (DNA-PK), are activated and phosphorylate H2AX at Ser 139 (110). Phosphorylated H2AX is one of the first proteins recruited to DSB sites during DNA damage response, and facilitates the access of repair proteins to the site (110). H2AX also participates in DNA damage-induced chromatin remodeling by promoting the recruitment of remodeling complexes and/or other histone modifying protein complexes.

In the context of apoptosis, the earlier studies reported that H2AX phosphorylation occurs as a consequence of apoptosis. DSBs generated from DNA fragmentation during the apoptotic process were reported to produce phosphorylated H2AX (71). DNA-PK and ATM were shown to be responsible for the phosphorylation of H2AX in this process (111). However, a series of recent studies instead proposed a more

active role of phospho-H2AX in induction of apoptosis. In this scenario, phosphorylation of H2AX at Ser 139 provokes apoptosis by inducing DNA fragmentation in UV-damaged cells (70). Supporting this model, several studies reported phospho-H2AX-mediated apoptosis, some of which are involved in apoptosis induced by chemotherapeutic agents (73-76). Interestingly, immunofluorescent staining demonstrated a different distribution pattern of phospho-H2AX between the events of DSB and apoptosis (72). Phospho-H2AX was distributed throughout nuclei in apoptosis, whereas DSB-localized phospho-H2AX displayed a foci-specific pattern. Controversially, however, a pan-nuclear staining pattern of phospho-H2AX was also reported to characterize DNA single-stranded regions induced by ultraviolet C radiation, in which case H2AX is phosphorylated by ATR (109).

PKCδ inhibition by B106 treatment evoked phosphorylation of H2AX subsequent to JNK activation (Figures 14 and 15). Knockdown of PKCδ using siRNA supported this observation: JNK phosphorylation occurred by 24 hours after siRNA transfection and H2AX phosphorylation was observed at 72 hours after transfection (Figure 16). The phosphorylation of H2AX induced by B106 treatment was mitigated in the absence of JNK expression, suggesting H2AX phosphorylation occurs downstream of JNK in case of B106 exposure (Figure 17). Caspase activation caused by B106 treatment was significantly decreased in the absence of H2AX expression. Furthermore, as a direct evidence of apoptosis, DNA fragmentation was almost completely abrogated with knockdown of H2AX prior to B106 treatment (Figure 20). Collectively, these results demonstrate the importance of H2AX as an active apoptotic mediator, with functional

evidence showing it to be a necessary component of apoptosis initiated by PKCδ inhibition.

B-Raf inhibitor resistance and similarity to NRAS type

As described above, the analysis of resistance mechanism to PLX4032 showed a potential induction of the Ras/C-Raf pathway, upon which cells depend in order to survive the condition of constant inhibition of B-Raf activity by PLX4032. The possible Ras/C-Raf mediated resistance mechanism implied a resemblance between PLX4032-resistant cells and NRAS-mutated cells in their behaviors. Compared to parental cells, PLX4032-resistant cells exhibited higher levels of basal phospho-H2AX expression and more robust activation of H2AX in response to B106 treatment (Figure 27), as was seen in melanoma cells with NRAS mutations (Figures 14 and 15). These observations imply that resistance to PLX4032 potentially transforms BRAF-mutated cells into "NRAS-mutant type", at least with respect to basal levels of H2AX activity, and in response to B106 treatment. Finally, combination treatment of B106 and PLX4032 in BRAF-mutated melanoma cell lines provided at least additive anti-proliferative effects, and might inhibit the development of PLX4032 resistance.

Future Studies

Although work detailed in this dissertation clearly established the potential of PKCδ as a therapeutic target in melanomas, and the molecular mechanism of the action of PKCδ inhibition, there are several areas remaining to be explored before this targeted

approach can be further developed as a therapeutic modality. First, the selectivity of B106 as a PKCδ-selective inhibitor needs to be assessed in more extensive *in vitro* kinase assays, in which B106 is tested against a panel of kinases. While the assays performed in this project using siRNA strongly supported selectivity of B106 against PKCδ, it is still necessary to clarify the potential off-target kinases to better understand its actions, as such information might help predict possible side effects. Second, as mentioned earlier, *in vivo* efficacy needs to be confirmed when an improved B106 analogue becomes available. Alternatively, it is also useful to consider methods to enable delivery of this extremely hydrophobic compound to the tumor *in vivo*, instead of modifying the compound structure itself. Also, the effect of B106 in normal or non-tumorigenic cells, in this case normal melanocytes, has to be assessed to ensure its tumor-specificity, an essential characteristic of a potent anti-cancer therapy. In terms of further analysis of the PLX4032-resistance mechanism, resistant cells showed slightly elevated Ras activity, but this requires further validation. Among the possible assays to verify it, thorough analysis of genomic mutations in all of the RAS genes could be carried out, as there is the possibility that the elevated Ras activity is due to activating mutations of other RAS genes (KRAS or HRAS) or mutations at sites other than codon 61 (another frequently mutated codon is G12). Mutations of codon 12 are more common in KRAS, and HRAS mutations are divided almost equally between codon 12 and codon 61 (112). Although genomic mutation at codon 61 in NRAS is more commonly observed in melanoma (91), the occurrence of secondary mutations in KRAS or HRAS in the resistant lines is possible because cancerous cells sometimes survive under condition of drug treatment by

selection for mutations providing an alternative means of survival (HRAS was more commonly mutated than other RAS genes in secondary cutaneous squamous-cell carcinomas tumors in patients with melanomas treated with vemurafenib (88)).

"Marker" for action of PKCδ inhibitors

Another future direction of this project would be to identify markers that allow identification of the type of cancers in which B106 or prospective PKCδ inhibitors would perform effectively and selectively.

Melanoma is fundamentally well-suited for a therapeutic strategy pursuing cancer cell specificity by selection of a drug target molecule due to the frequency of "cancer cell-specific markers" (i.e., BRAF or NRAS mutations) or "cancer cell-specific events" (i.e., hyperactivation of the Raf/MEK pathway). Selectivity against cancer cells is already assured by the selection of the drug targets in case of B-Raf inhibitors that selectively inhibit mutant form of B-Raf or MEK inhibitors whose sensitivity is more prominent in the cells with BRAF mutations. As reasonable as the rationale behind the strategy actually is, however, targeting certain cancer cell-specific markers such as BRAF appears to provide facile opportunities for the cancer cells to develop drug resistance despite the sometimes remarkable antitumor activities produced early in the course of the treatment. While the complexity of Ras downstream signaling allows cells to have flexible and timely positive- or negative-functional regulatory options in response to changing environmental signals, it also provides for redundancy among these pathways, so that

cells can develop alternative mechanisms to compensate for any failure of the original signaling pathway, and it will remain the challenge for this type of therapeutics.

On the other hand, it is more difficult for therapeutics whose targets are not "cancer cell-specific markers" or "cancer cell-specific events", to assure cancer specificity by their targets themselves. For this reason, the synthetic lethal approach has been attracting an attention, as it provides cancer specificity without general cytotoxicity. Indeed, this is why this project started with the focus on melanomas with NRAS mutations being a "cancer cell-specific marker" and therefore synthetic lethal partner for PKCδ, inspired by previous reports. However, harboring genomic mutations in RAS genes or aberrant Ras activity may not be the relevant marker for response to B106, as B106 was revealed to be equally effective on suppression of cell growth in melanoma cell lines with BRAF and NRAS mutations. Although such a marker that can predict the response to B106 has not been identified at this point, this dissertation may be able to suggest markers to predict the mechanism of apoptosis that is induced under B106 treatment. Preliminary data showed the expression of total PKCδ protein was less abundant in NRAS mutant cells and A375- and SKMEL5-PLX-Rs than in A375 and SKMEL5 cells (**Figure 31**). On the contrary, basal phosphorylation level of H2AX was higher in melanoma cells with NRAS mutation and A375- and SKMEL5-PLX-Rs than in A375 and SKMEL5 cells (**Figures 27 and 31**). In NRAS-mutated cells and PLX4032 resistant cells, B106 treatment appears to induce more robust response in terms of H2AX activation than in A375 and SKMEL5 cells (Figures 14, 15 and 27). If higher activation levels of H2AX following B106 treatment is actually correlated with the mode of cell

growth inhibition (thus, H2AX-dependent apoptosis) and lower H2AX activation with H2AX-independent apoptosis, the observation of the basal expression levels of PKCδ or phospho-H2AX may be worth further investigation as the predictors of apoptosis after PKCδ inhibition. In order to verify such a correlation, however, much more extensive investigation is required, such as verifying the differential mode of apoptosis (H2AX-depdent or independent) between high H2AX responder and non/low H2AX responders, and applicability of this "marker" in types of cancers other than melanoma. Interestingly, imatinib mesylate, a protein kinase inhibitor, has been shown to trigger apoptosis in gastrointestinal stromal tumor cell lines through upregulation of H2AX and imatinib-mediated H2AX up-regulation correlated with imatinib sensitivity (75).

Since there is a possibility that B106 exerts apoptosis via distinct molecular mechanisms in BRAF-mutated cells compared to NRAS-mutated and B-Raf inhibitor-resistant cells, based on H2AX activation status, the prediction of the apoptosis mechanism, at least, may be helpful to predict the possible side effects related to the elevated H2AX activation. To aim for the better clinical application in the future, nonetheless, it would be beneficial to find "a marker" to predict the efficacy of compounds like B106 and tumor selectivity and this could be a next step beyond this dissertation and project.

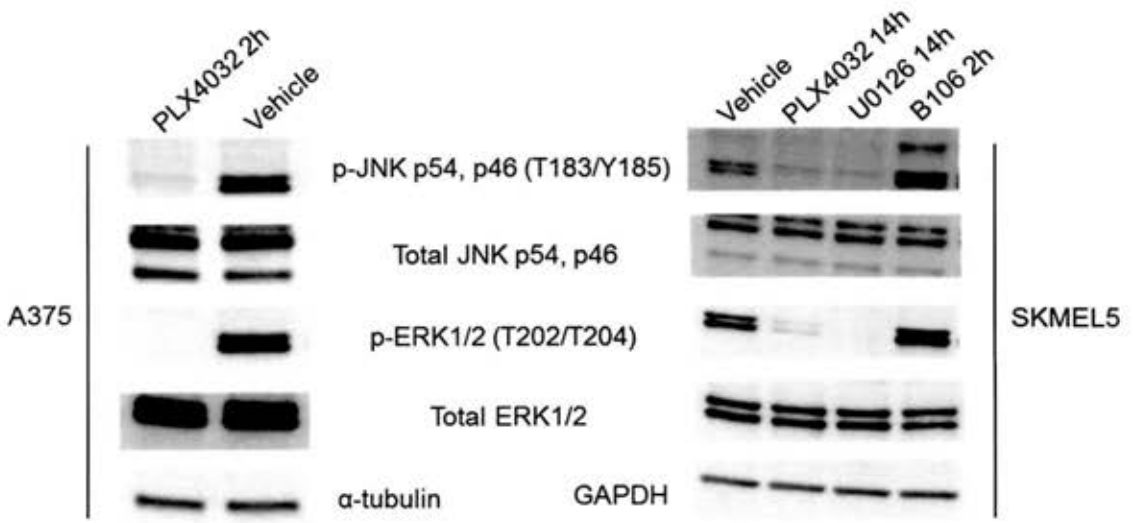

Figure 29: Inhibition of the Raf/MEK/ERK pathway transiently decreases JNK phosphorylation in A375 and SKMEL5 cells. A375 cells were treated with PLX4032 (2μM) or vehicle (DMSO) for 2 hours, and SKMEL5 cells were treated with PLX4032 (0.5μM), U0126 (5μM) or vehicle (DMSO) for 14 hours, or B106 (0.5μM) for 2 hours. Protein lysates were subjected to immunoblot analysis for phosphorylation or total expression levels of the indicated proteins. Levels of α-tubulin or GAPDH served as a loading control. The experiment was performed once for each cell line.

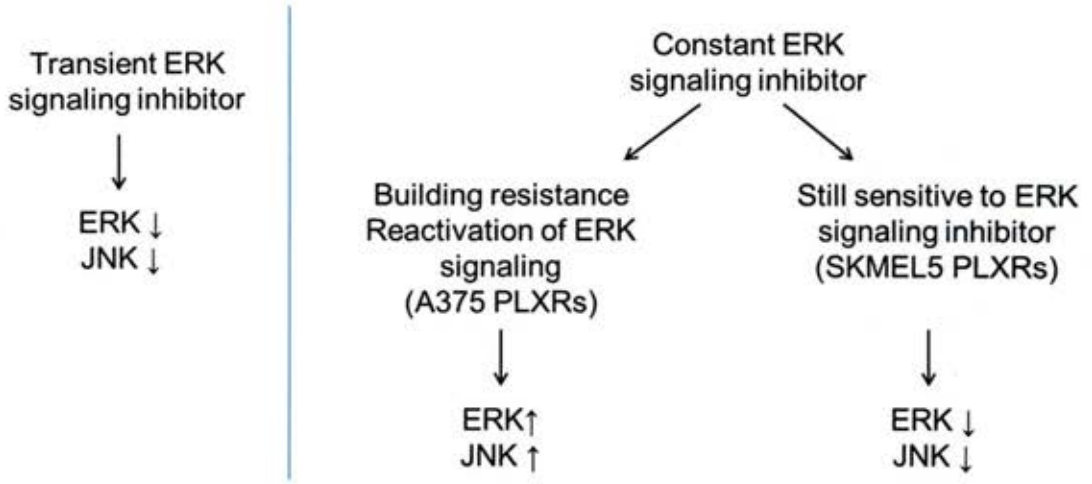

Figure 30: Hypothesis of crosstalk between ERK and JNK. (Left) Transient inhibition of ERK signaling by B-Raf inhibitors or MEK inhibitors inhibits JNK activation as well. (Right) By constant inhibition of ERK signaling, cells develop a resistance mechanism to overcome the inhibition and reactivate ERK signaling. In this case, constantly high levels of ERK activation lead to constantly high levels of JNK activation. On the other hand, those cells that did not acquire a resistant mechanism to the constant ERK inhibition still maintain their sensitivity to ERK inhibitors. As a result, the basal level of JNK activation remains normal.

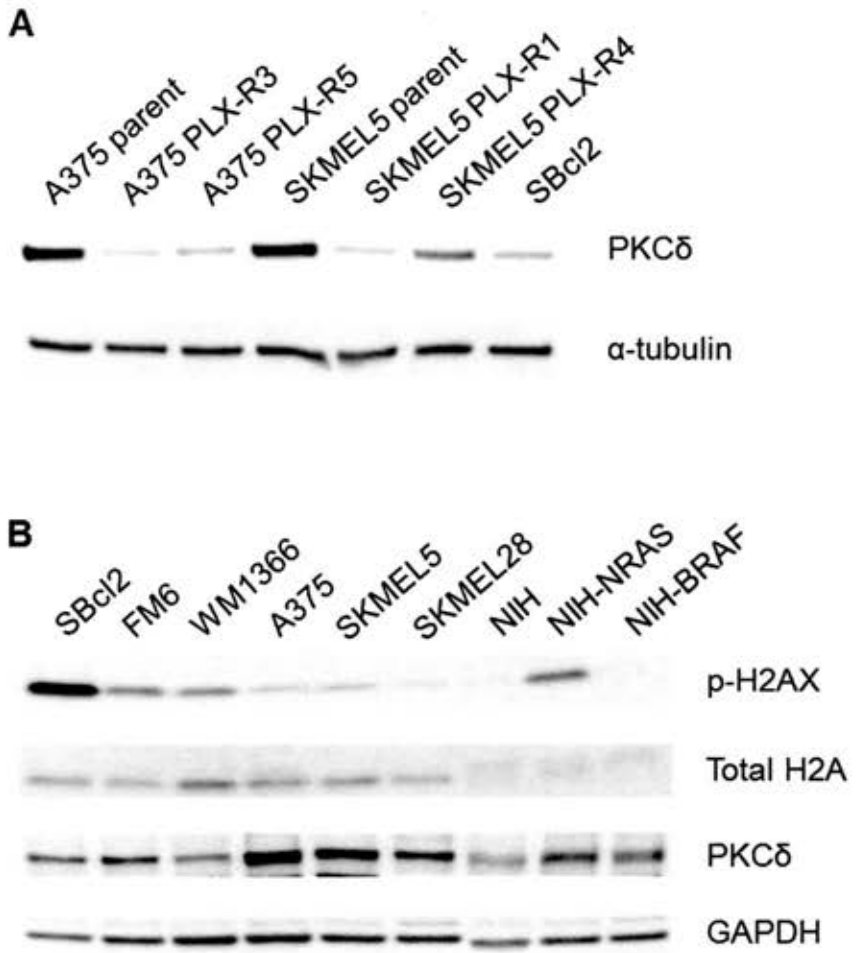

Figure 31: Comparison of basal expression levels of PKCδ and phospho-H2AX in melanoma cells lines. (A) Protein lysates from BRAF mutant cells A375 and SKMEL5 cells and their derivative PLX-R cells, and SBcl2 cells were subjected to immunoblot analysis for total expression levels of PKCδ. Levels of α-tubulin served as a loading control. The experiment was repeated twice. (B) Protein lysates from NRAS mutant cells (SBcl2, FM6 and WM1366), BRAF mutant cells (A375, SKMEL5 and SKMEL28) and NIH/3T3 and their derivatives (NIH-NRAS and NIH-BRAF) were subjected to immunoblot analysis for phosphorylation or total expression levels of the indicated proteins. Levels of GAPDH served as a loading control. The experiment was performed once.

LIST OF JOURNAL ABBREVIATIONS

Aging	Aging
Arch Immunol Ther Exp (Warsz)	Archivum Immunologiae et Therapiae Experimentalis
Biochem Pharmacol	Biochemical Pharmacology
Biochim Biophys Acta	Biochimica et Biophysica Acta
Blood	Blood
BMC Cell Biol	BMC Cell Biology
BMC Med	BMC medicine
Breast Cancer Res Treat	Breast Cancer Research and Treatment
Br J Cancer	British Journal of Cancer
Br J Pharmacol	British Journal of Pharmacology
Cancer J	The Cancer Journal
Cancer Res	Cancer Research
Cell	Cell
Cell Biochem Biophys	Cell Biochemistry and Biophysics
Cell Commun Signal	Cell Communication and Signaling
Cell Death Dis	Cell Death & Disease
Cell Signal	Cellular Signalling
	Current Gerontology and Geriatrics Research
Curr Opin Cell Biol	Current Opinion in Cell Biology
DNA Repair (Amst)	DNA Repair
Drug Resist Updat	Drug resistance updates : reviews and commentaries in antimicrobial and anticancer chemotherapy
EMBO J	The EMBO Journal
Endocr Relat Cancer	Endocrine-Related Cancer
Expert Opin Ther Targets	Expert Opinion on Therapeutic Targets
Eur J Cancer	European Journal of Cancer
Eur J Cell Biol	The European Journal of Cell Biology
FEBS Lett	FEBS letters
Free Radic Biol Med	Free Radical Biology & Medicine
Genes Cancer	Genes & Cancer
Genetics	Genetics
Genes Dev	Genes & Development
Int J Cancer	International Journal of Cancer
J Biol Chem	Journal of Biological Chemistry
J Cell Biochem	Journal of Cellular Biochemistry
J Clin Invest	The Journal of Clinical Investigation
J Immunol	The Journal of Immunology
J Orthop Res	Journal of Orthopaedic Research :

	official publication of the Orthopaedic Research Society
J Pathol	The Journal of Pathology
Lancet	Lancet
Melanoma Res	Melanoma Research
Meth Mol Biol	Methods in Molecular Biology
Mol Cancer Res	Molecular Cancer Research
Mol Cancer Ther	Molecular Cancer Therapeutics
Mol Carcinog	Molecular Carcinogenesis
Mol Cell	Molecular Cell
Mol Cell Biol	Molecular and Cellular Biology
Mini Rev Med Chem	Mini-Reviews in Medicinal Chemistry
N Engl J Med	The New England Journal of Medicine
Nat Rev Cancer	Nature Reviews. Cancer
Nature	Nature
Oncogene	Oncogene
Oncol Rep	Oncology Reports
Pancreas	Pancreas
PLoS ONE	Public Library of Science ONE
Proc Natl Acad Sci USA	Proceedings of the National Academy of Sciences of the United States of America
Science	Science
ScientificWorldJournal	TheScientificWorldJournal

REFERENCES

1. **American Cancer Society I.** 2012. Cancer Facts & Figures 2012.

2. **Finn L, Markovic SN, Joseph RW.** 2012. Therapy for metastatic melanoma: the past, present, and future. BMC Med **10:**23.

3. **Takashima A, Faller DV.** 2013. Targeting the RAS oncogene. Expert Opin Ther Targets **In Press**.

4. **Inamdar GS, Madhunapantula SV, Robertson GP.** 2010. Targeting the MAPK pathway in melanoma: why some approaches succeed and other fail. Biochem Pharmacol **80:**624-637.

5. **Kuphal S, Bosserhoff A.** 2009. Recent progress in understanding the pathology of malignant melanoma. J Pathol **219:**400-409.

6. **Kelleher FC, McArthur GA.** 2012. Targeting NRAS in melanoma. Cancer J **18:**132-136.

7. **Chapman PB, Hauschild A, Robert C, Haanen JB, Ascierto P, Larkin J, Dummer R, Garbe C, Testori A, Maio M, Hogg D, Lorigan P, Lebbe C, Jouary T, Schadendorf D, Ribas A, O'Day SJ, Sosman JA, Kirkwood JM, Eggermont AM, Dreno B, Nolop K, Li J, Nelson B, Hou J, Lee RJ, Flaherty KT, McArthur GA, Group B-S.** 2011. Improved survival with vemurafenib in melanoma with BRAF V600E mutation. N Engl J Med **364:**2507-2516.

8. **Nazarian R, Shi H, Wang Q, Kong X, Koya RC, Lee H, Chen Z, Lee MK, Attar N, Sazegar H, Chodon T, Nelson SF, McArthur G, Sosman JA, Ribas A, Lo RS.** 2010. Melanomas acquire resistance to B-RAF(V600E) inhibition by RTK or N-RAS upregulation. Nature **468:**973-977.

9. **Solit DB, Garraway LA, Pratilas CA, Sawai A, Getz G, Basso A, Ye Q, Lobo JM, She Y, Osman I, Golub TR, Sebolt-Leopold J, Sellers WR, Rosen N.** 2006. BRAF mutation predicts sensitivity to MEK inhibition. Nature **439:**358-362.

10. **Xia S, Forman LW, Faller DV.** 2007. Protein kinase C delta is required for survival of cells expressing activated p21RAS. J Biol Chem **282:**13199-13210.

11. **Leitges M, Mayr M, Braun U, Mayr U, Li C, Pfister G, Ghaffari-Tabrizi N, Baier G, Hu Y, Xu Q.** 2001. Exacerbated vein graft arteriosclerosis in protein kinase Cdelta-null mice. J Clin Invest **108:**1505-1512.

12. **Yoshida K.** 2007. PKCdelta signaling: mechanisms of DNA damage response and apoptosis. Cell Signal **19:**892-901.

13. **Zhao M, Xia L, Chen GQ.** 2012. Protein kinase cdelta in apoptosis: a brief overview. Arch Immunol Ther Exp (Warsz) **60:**361-372.

14. **Basu A, Pal D.** 2010. Two faces of protein kinase Cdelta: the contrasting roles of PKCdelta in cell survival and cell death. ScientificWorldJournal **10:**2272-2284.

15. **Liu H, Lu ZG, Miki Y, Yoshida K.** 2007. Protein kinase C delta induces transcription of the TP53 tumor suppressor gene by controlling death-promoting factor Btf in the apoptotic response to DNA damage. Mol Cell Biol **27:**8480-8491.

16. **Sitailo LA, Tibudan SS, Denning MF.** 2006. The protein kinase C delta catalytic fragment targets Mcl-1 for degradation to trigger apoptosis. J Biol Chem **281:**29703-29710.

17. **Choi SY, Kim MJ, Kang CM, Bae S, Cho CK, Soh JW, Kim JH, Kang S, Chung HY, Lee YS, Lee SJ.** 2006. Activation of Bak and Bax through c-abl-protein kinase Cdelta-p38 MAPK signaling in response to ionizing radiation in human non-small cell lung cancer cells. J Biol Chem **281:**7049-7059.

18. **Brandt B, Abou-Eladab EF, Tiedge M, Walzel H.** 2010. Role of the JNK/c-Jun/AP-1 signaling pathway in galectin-1-induced T-cell death. Cell Death Dis **1:**e23.

19. **Gomel R, Xiang C, Finniss S, Lee HK, Lu W, Okhrimenko H, Brodie C.** 2007. The localization of protein kinase Cdelta in different subcellular sites affects its proapoptotic and antiapoptotic functions and the activation of distinct downstream signaling pathways. Mol Cancer Res **5:**627-639.

20. **Yoshida K, Liu H, Miki Y.** 2006. Protein kinase C delta regulates Ser46 phosphorylation of p53 tumor suppressor in the apoptotic response to DNA damage. J Biol Chem **281:**5734-5740.

21. **Efimova T, Broome AM, Eckert RL.** 2004. Protein kinase Cdelta regulates keratinocyte death and survival by regulating activity and subcellular localization of a p38delta-extracellular signal-regulated kinase 1/2 complex. Mol Cell Biol **24:**8167-8183.

22. **Yoshida K, Miki Y, Kufe D.** 2002. Activation of SAPK/JNK signaling by protein kinase Cdelta in response to DNA damage. J Biol Chem **277:**48372-48378.

23. **Zhao KW, Li D, Zhao Q, Huang Y, Silverman RH, Sims PJ, Chen GQ.** 2005. Interferon-alpha-induced expression of phospholipid scramblase 1 through STAT1 requires the sequential activation of protein kinase Cdelta and JNK. J Biol Chem **280:**42707-42714.

24. **Das J, Ghosh J, Manna P, Sil PC.** 2010. Protective role of taurine against arsenic-induced mitochondria-dependent hepatic apoptosis via the inhibition of PKCdelta-JNK pathway. PLoS One **5:**e12602.

25. **Wang H, Xiao L, Kazanietz MG.** 2011. p23/Tmp21 associates with protein kinase Cdelta (PKCdelta) and modulates its apoptotic function. J Biol Chem **286:**15821-15831.

26. **Kim YR, Byun HS, Jeon J, Choi BL, Park KA, Won M, Zhang T, Shin S, Lee H, Oh J, Hur GM.** 2011. Apoptosis signal-regulating kinase1 is inducible by protein kinase Cdelta and contributes to phorbol ester-mediated G1 phase arrest through persistent JNK activation. Cell Biochem Biophys **61:**199-207.

27. **Yanase N, Hayashida M, Kanetaka-Naka Y, Hoshika A, Mizuguchi J.** 2012. PKC-delta mediates interferon-alpha-induced apoptosis through c-Jun NH(2)-terminal kinase activation. BMC Cell Biol **13:**7.

28. **Lomonaco SL, Kahana S, Blass M, Brody Y, Okhrimenko H, Xiang C, Finniss S, Blumberg PM, Lee HK, Brodie C.** 2008. Phosphorylation of protein kinase Cdelta on distinct tyrosine

residues induces sustained activation of Erk1/2 via down-regulation of MKP-1: role in the apoptotic effect of etoposide. J Biol Chem **283:**17731-17739.

29. **Li Z, Wang N, Fang J, Huang J, Tian F, Li C, Xie F.** 2012. Role of PKC-ERK signaling in tamoxifen-induced apoptosis and tamoxifen resistance in human breast cancer cells. Oncol Rep **27:**1879-1886.

30. **Abbas T, White D, Hui L, Yoshida K, Foster DA, Bargonetti J.** 2004. Inhibition of human p53 basal transcription by down-regulation of protein kinase Cdelta. J Biol Chem **279:**9970-9977.

31. **Perletti G, Marras E, Dondi D, Osti D, Congiu T, Ferrarese R, de Eguileor M, Tashjian AH, Jr.** 2005. p21(Waf1/Cip1) and p53 are downstream effectors of protein kinase C delta in tumor suppression and differentiation in human colon cancer cells. Int J Cancer **113:**42-53.

32. **Chew YC, Adhikary G, Wilson GM, Reece EA, Eckert RL.** 2011. Protein kinase C (PKC) delta suppresses keratinocyte proliferation by increasing p21(Cip1) level by a KLF4 transcription factor-dependent mechanism. J Biol Chem **286:**28772-28782.

33. **De Vita F, Riccardi M, Malanga D, Scrima M, De Marco C, Viglietto G.** 2012. PKC-dependent phosphorylation of p27 at T198 contributes to p27 stabilization and cell cycle arrest. Cell Cycle **11:**1583-1592.

34. **Bosco R, Melloni E, Celeghini C, Rimondi E, Vaccarezza M, Zauli G.** 2011. Fine tuning of protein kinase C (PKC) isoforms in cancer: shortening the distance from the laboratory to the bedside. Mini Rev Med Chem **11:**185-199.

35. **Clark AS, West KA, Blumberg PM, Dennis PA.** 2003. Altered protein kinase C (PKC) isoforms in non-small cell lung cancer cells: PKCdelta promotes cellular survival and chemotherapeutic resistance. Cancer Res **63:**780-786.

36. **Mauro LV, Grossoni VC, Urtreger AJ, Yang C, Colombo LL, Morandi A, Pallotta MG, Kazanietz MG, Bal de Kier Joffe ED, Puricelli LL.** 2010. PKC Delta (PKCdelta) promotes tumoral progression of human ductal pancreatic cancer. Pancreas **39:**e31-41.

37. **Ringshausen I, Schneller F, Bogner C, Hipp S, Duyster J, Peschel C, Decker T.** 2002. Constitutively activated phosphatidylinositol-3 kinase (PI-3K) is involved in the defect of apoptosis in B-CLL: association with protein kinase Cdelta. Blood **100:**3741-3748.

38. **McCracken MA, Miraglia LJ, McKay RA, Strobl JS.** 2003. Protein kinase C delta is a prosurvival factor in human breast tumor cell lines. Mol Cancer Ther **2:**273-281.

39. **McKiernan E, O'Brien K, Grebenchtchikov N, Geurts-Moespot A, Sieuwerts AM, Martens JW, Magdolen V, Evoy D, McDermott E, Crown J, Sweep FC, Duffy MJ.** 2008. Protein kinase Cdelta expression in breast cancer as measured by real-time PCR, western blotting and ELISA. Br J Cancer **99:**1644-1650.

40. **Baudot AD, Jeandel PY, Mouska X, Maurer U, Tartare-Deckert S, Raynaud SD, Cassuto JP, Ticchioni M, Deckert M.** 2009. The tyrosine kinase Syk regulates the survival of chronic lymphocytic leukemia B cells through PKCdelta and proteasome-dependent regulation of Mcl-1 expression. Oncogene **28:**3261-3273.

41. **Lonne GK, Masoumi KC, Lennartsson J, Larsson C.** 2009. Protein kinase Cdelta supports survival of MDA-MB-231 breast cancer cells by suppressing the ERK1/2 pathway. J Biol Chem **284:**33456-33465.

42. **Wang Q, Zhou Y, Wang X, Evers BM.** 2006. Glycogen synthase kinase-3 is a negative regulator of extracellular signal-regulated kinase. Oncogene **25:**43-50.

43. **Grossoni VC, Falbo KB, Kazanietz MG, de Kier Joffe ED, Urtreger AJ.** 2007. Protein kinase C delta enhances proliferation and survival of murine mammary cells. Mol Carcinog **46:**381-390.

44. **Muscella A, Urso L, Calabriso N, Vetrugno C, Rochira A, Storelli C, Marsigliante S.** 2009. Anti-apoptotic effects of protein kinase C-delta and c-fos in cisplatin-treated thyroid cells. Br J Pharmacol **156:**751-763.

45. **Wang Q, Wang X, Evers BM.** 2003. Induction of cIAP-2 in human colon cancer cells through PKC delta/NF-kappa B. J Biol Chem **278:**51091-51099.

46. **Wang Q, Wang X, Zhou Y, Evers BM.** 2006. PKCdelta-mediated regulation of FLIP expression in human colon cancer cells. Int J Cancer **118:**326-334.

47. **Zhu T, Chen L, Du W, Tsuji T, Chen C.** 2010. Synthetic Lethality Induced by Loss of PKC delta and Mutated Ras. Genes Cancer **1:**142-151.

48. **Ranta F, Leveringhaus J, Theilig D, Schulz-Raffelt G, Hennige AM, Hildebrand DG, Handrick R, Jendrossek V, Bosch F, Schulze-Osthoff K, Haring HU, Ullrich S.** 2011. Protein kinase C delta (PKCdelta) affects proliferation of insulin-secreting cells by promoting nuclear extrusion of the cell cycle inhibitor p21Cip1/WAF1. PLoS One **6:**e28828.

49. **La Porta CA, Di Dio A, Porro D, Comolli R.** 2000. Overexpression of novel protein kinase C delta in BL6 murine melanoma cells inhibits the proliferative capacity in vitro but enhances the metastatic potential in vivo. Melanoma Res **10:**93-102.

50. **Putnam AJ, Schulz VV, Freiter EM, Bill HM, Miranti CK.** 2009. Src, PKCalpha, and PKCdelta are required for alphavbeta3 integrin-mediated metastatic melanoma invasion. Cell Commun Signal **7:**10.

51. **Diaz Bessone MI, Berardi DE, Campodonico PB, Todaro LB, Lothstein L, Bal de Kier Joffe ED, Urtreger AJ.** 2011. Involvement of PKC delta (PKCdelta) in the resistance against different doxorubicin analogs. Breast Cancer Res Treat **126:**577-587.

52. **Zhang J, Liu N, Zhang J, Liu S, Liu Y, Zheng D.** 2005. PKCdelta protects human breast tumor MCF-7 cells against tumor necrosis factor-related apoptosis-inducing ligand-mediated apoptosis. J Cell Biochem **96:**522-532.

53. **Dobzhansky T, Krimbas C, Krimbas MG.** 1960. Genetics of Natural Populations. Xxix. Is the Genetic Load in Drosophila Pseudoobscura a Mutational or a Balanced Load? Genetics **45:**741-753.

54. **Hartwell LH, Szankasi P, Roberts CJ, Murray AW, Friend SH.** 1997. Integrating genetic approaches into the discovery of anticancer drugs. Science **278:**1064-1068.

55. **Kaelin WG, Jr.** 2005. The concept of synthetic lethality in the context of anticancer therapy. Nat Rev Cancer **5:**689-698.

56. **Solimini NL, Luo J, Elledge SJ.** 2007. Non-oncogene addiction and the stress phenotype of cancer cells. Cell **130:**986-988.

57. **Xia S, Chen Z, Forman LW, Faller DV.** 2009. PKCdelta survival signaling in cells containing an activated p21Ras protein requires PDK1. Cell Signal **21:**502-508.

58. **Chen Z, Forman LW, Miller KA, English B, Takashima A, Bohacek RA, Williams RM, Faller DV.** 2011. Protein kinase Cdelta inactivation inhibits cellular proliferation and decreases survival in human neuroendocrine tumors. Endocr Relat Cancer **18:**759-771.

59. **Soltoff SP.** 2007. Rottlerin: an inappropriate and ineffective inhibitor of PKCdelta. Trends Pharmacol Sci **28:**453-458.

60. **Soloff RS, Katayama C, Lin MY, Feramisco JR, Hedrick SM.** 2004. Targeted deletion of protein kinase C lambda reveals a distribution of functions between the two atypical protein kinase C isoforms. J Immunol **173:**3250-3260.

61. **Favaloro B, Allocati N, Graziano V, Di Ilio C, De Laurenzi V.** 2012. Role of apoptosis in disease. Aging (Albany NY) **4:**330-349.

62. **Alberts B.** 2002. Molecular biology of the cell, 4th ed. Garland Science, New York.

63. **Johnson GL, Nakamura K.** 2007. The c-jun kinase/stress-activated pathway: regulation, function and role in human disease. Biochim Biophys Acta **1773:**1341-1348.

64. **Chauhan D, Hideshima T, Treon S, Teoh G, Raje N, Yoshihimito S, Tai YT, Li W, Fan J, DeCaprio J, Anderson KC.** 1999. Functional interaction between retinoblastoma protein and stress-activated protein kinase in multiple myeloma cells. Cancer Res **59:**1192-1195.

65. **Shen HM, Liu ZG.** 2006. JNK signaling pathway is a key modulator in cell death mediated by reactive oxygen and nitrogen species. Free Radic Biol Med **40:**928-939.

66. **Weston CR, Davis RJ.** 2007. The JNK signal transduction pathway. Curr Opin Cell Biol **19:**142-149.

67. **Keshet Y, Seger R.** 2010. The MAP kinase signaling cascades: a system of hundreds of components regulates a diverse array of physiological functions. Methods Mol Biol **661:**3-38.

68. **Bode AM, Dong Z.** 2007. The functional contrariety of JNK. Mol Carcinog **46:**591-598.

69. **Haeusgen W, Herdegen T, Waetzig V.** 2011. The bottleneck of JNK signaling: molecular and functional characteristics of MKK4 and MKK7. Eur J Cell Biol **90:**536-544.

70. **Lu C, Zhu F, Cho YY, Tang F, Zykova T, Ma WY, Bode AM, Dong Z.** 2006. Cell apoptosis: requirement of H2AX in DNA ladder formation, but not for the activation of caspase-3. Mol Cell **23:**121-132.

71. **Rogakou EP, Nieves-Neira W, Boon C, Pommier Y, Bonner WM.** 2000. Initiation of DNA fragmentation during apoptosis induces phosphorylation of H2AX histone at serine 139. J Biol Chem **275:**9390-9395.

72. **de Feraudy S, Revet I, Bezrookove V, Feeney L, Cleaver JE.** 2010. A minority of foci or pan-nuclear apoptotic staining of gammaH2AX in the S phase after UV damage contain DNA double-strand breaks. Proc Natl Acad Sci U S A **107:**6870-6875.

73. **Jane EP, Pollack IF.** 2010. Enzastaurin induces H2AX phosphorylation to regulate apoptosis via MAPK signalling in malignant glioma cells. Eur J Cancer **46:**412-419.

74. **Lee YY, Yu YB, Gunawardena HP, Xie L, Chen X.** 2012. BCLAF1 is a radiation-induced H2AX-interacting partner involved in gammaH2AX-mediated regulation of apoptosis and DNA repair. Cell Death Dis **3:**e359.

75. **Liu Y, Tseng M, Perdreau SA, Rossi F, Antonescu C, Besmer P, Fletcher JA, Duensing S, Duensing A.** 2007. Histone H2AX is a mediator of gastrointestinal stromal tumor cell apoptosis following treatment with imatinib mesylate. Cancer Res **67:**2685-2692.

76. **Wen W, Zhu F, Zhang J, Keum YS, Zykova T, Yao K, Peng C, Zheng D, Cho YY, Ma WY, Bode AM, Dong Z.** 2010. MST1 promotes apoptosis through phosphorylation of histone H2AX. J Biol Chem **285:**39108-39116.

77. **Davies H, Bignell GR, Cox C, Stephens P, Edkins S, Clegg S, Teague J, Woffendin H, Garnett MJ, Bottomley W, Davis N, Dicks E, Ewing R, Floyd Y, Gray K, Hall S, Hawes R, Hughes J, Kosmidou V, Menzies A, Mould C, Parker A, Stevens C, Watt S, Hooper S, Wilson R, Jayatilake H, Gusterson BA, Cooper C, Shipley J, Hargrave D, Pritchard-Jones K, Maitland N, Chenevix-Trench G, Riggins GJ, Bigner DD, Palmieri G, Cossu A, Flanagan A, Nicholson A, Ho JW, Leung SY, Yuen ST, Weber BL, Seigler HF, Darrow TL, Paterson H, Marais R, Marshall CJ, Wooster R, Stratton MR, Futreal PA.** 2002. Mutations of the BRAF gene in human cancer. Nature **417:**949-954.

78. **Tsai J, Lee JT, Wang W, Zhang J, Cho H, Mamo S, Bremer R, Gillette S, Kong J, Haass NK, Sproesser K, Li L, Smalley KS, Fong D, Zhu YL, Marimuthu A, Nguyen H, Lam B, Liu J, Cheung I, Rice J, Suzuki Y, Luu C, Settachatgul C, Shellooe R, Cantwell J, Kim SH, Schlessinger J, Zhang KY, West BL, Powell B, Habets G, Zhang C, Ibrahim PN, Hirth P, Artis DR, Herlyn M, Bollag G.** 2008. Discovery of a selective inhibitor of oncogenic B-Raf kinase with potent antimelanoma activity. Proc Natl Acad Sci U S A **105:**3041-3046.

79. **Flaherty KT, Puzanov I, Kim KB, Ribas A, McArthur GA, Sosman JA, O'Dwyer PJ, Lee RJ, Grippo JF, Nolop K, Chapman PB.** 2010. Inhibition of mutated, activated BRAF in metastatic melanoma. The New England journal of medicine **363:**809-819.

80. **Hauschild A, Grob JJ, Demidov LV, Jouary T, Gutzmer R, Millward M, Rutkowski P, Blank CU, Miller WH, Jr., Kaempgen E, Martin-Algarra S, Karaszewska B, Mauch C, Chiarion-Sileni V, Martin AM, Swann S, Haney P, Mirakhur B, Guckert ME, Goodman V, Chapman PB.** 2012. Dabrafenib in BRAF-mutated metastatic melanoma: a multicentre, open-label, phase 3 randomised controlled trial. Lancet **380:**358-365.

81. **Villanueva J, Vultur A, Lee JT, Somasundaram R, Fukunaga-Kalabis M, Cipolla AK, Wubbenhorst B, Xu X, Gimotty PA, Kee D, Santiago-Walker AE, Letrero R, D'Andrea K, Pushparajan A, Hayden JE, Brown KD, Laquerre S, McArthur GA, Sosman JA, Nathanson**

KL, Herlyn M. 2010. Acquired resistance to BRAF inhibitors mediated by a RAF kinase switch in melanoma can be overcome by cotargeting MEK and IGF-1R/PI3K. Cancer Cell **18:**683-695.

82. **Montagut C, Sharma SV, Shioda T, McDermott U, Ulman M, Ulkus LE, Dias-Santagata D, Stubbs H, Lee DY, Singh A, Drew L, Haber DA, Settleman J.** 2008. Elevated CRAF as a potential mechanism of acquired resistance to BRAF inhibition in melanoma. Cancer Res **68:**4853-4861.

83. **Johannessen CM, Boehm JS, Kim SY, Thomas SR, Wardwell L, Johnson LA, Emery CM, Stransky N, Cogdill AP, Barretina J, Caponigro G, Hieronymus H, Murray RR, Salehi-Ashtiani K, Hill DE, Vidal M, Zhao JJ, Yang X, Alkan O, Kim S, Harris JL, Wilson CJ, Myer VE, Finan PM, Root DE, Roberts TM, Golub T, Flaherty KT, Dummer R, Weber BL, Sellers WR, Schlegel R, Wargo JA, Hahn WC, Garraway LA.** 2010. COT drives resistance to RAF inhibition through MAP kinase pathway reactivation. Nature **468:**968-972.

84. **Hatzivassiliou G, Song K, Yen I, Brandhuber BJ, Anderson DJ, Alvarado R, Ludlam MJ, Stokoe D, Gloor SL, Vigers G, Morales T, Aliagas I, Liu B, Sideris S, Hoeflich KP, Jaiswal BS, Seshagiri S, Koeppen H, Belvin M, Friedman LS, Malek S.** 2010. RAF inhibitors prime wild-type RAF to activate the MAPK pathway and enhance growth. Nature **464:**431-435.

85. **Heidorn SJ, Milagre C, Whittaker S, Nourry A, Niculescu-Duvas I, Dhomen N, Hussain J, Reis-Filho JS, Springer CJ, Pritchard C, Marais R.** 2010. Kinase-dead BRAF and oncogenic RAS cooperate to drive tumor progression through CRAF. Cell **140:**209-221.

86. **Kaplan FM, Shao Y, Mayberry MM, Aplin AE.** 2011. Hyperactivation of MEK-ERK1/2 signaling and resistance to apoptosis induced by the oncogenic B-RAF inhibitor, PLX4720, in mutant N-RAS melanoma cells. Oncogene **30:**366-371.

87. **Poulikakos PI, Zhang C, Bollag G, Shokat KM, Rosen N.** 2010. RAF inhibitors transactivate RAF dimers and ERK signalling in cells with wild-type BRAF. Nature **464:**427-430.

88. **Su F, Viros A, Milagre C, Trunzer K, Bollag G, Spleiss O, Reis-Filho JS, Kong X, Koya RC, Flaherty KT, Chapman PB, Kim MJ, Hayward R, Martin M, Yang H, Wang Q, Hilton H, Hang JS, Noe J, Lambros M, Geyer F, Dhomen N, Niculescu-Duvaz I, Zambon A, Niculescu-Duvaz D, Preece N, Robert L, Otte NJ, Mok S, Kee D, Ma Y, Zhang C, Habets G, Burton EA, Wong B, Nguyen H, Kockx M, Andries L, Lestini B, Nolop KB, Lee RJ, Joe AK, Troy JL, Gonzalez R, Hutson TE, Puzanov I, Chmielowski B, Springer CJ, McArthur GA, Sosman JA, Lo RS, Ribas A, Marais R.** 2012. RAS mutations in cutaneous squamous-cell carcinomas in patients treated with BRAF inhibitors. N Engl J Med **366:**207-215.

89. **Callahan MK, Rampal R, Harding JJ, Klimek VM, Chung YR, Merghoub T, Wolchok JD, Solit DB, Rosen N, Abdel-Wahab O, Levine RL, Chapman PB.** 2012. Progression of RAS-mutant leukemia during RAF inhibitor treatment. N Engl J Med **367:**2316-2321.

90. **Symonds JM, Ohm AM, Carter CJ, Heasley LE, Boyle TA, Franklin WA, Reyland ME.** 2011. Protein kinase C delta is a downstream effector of oncogenic K-ras in lung tumors. Cancer Res **71:**2087-2097.

91. **Fernandez-Medarde A, Santos E.** 2011. Ras in cancer and developmental diseases. Genes Cancer **2:**344-358.

92. **Hibi M, Lin A, Smeal T, Minden A, Karin M.** 1993. Identification of an oncoprotein- and UV-responsive protein kinase that binds and potentiates the c-Jun activation domain. Genes Dev **7:**2135-2148.

93. **Derijard B, Hibi M, Wu IH, Barrett T, Su B, Deng T, Karin M, Davis RJ.** 1994. JNK1: a protein kinase stimulated by UV light and Ha-Ras that binds and phosphorylates the c-Jun activation domain. Cell **76:**1025-1037.

94. **Donovan N, Becker EB, Konishi Y, Bonni A.** 2002. JNK phosphorylation and activation of BAD couples the stress-activated signaling pathway to the cell death machinery. J Biol Chem **277:**40944-40949.

95. **Wang XT, Pei DS, Xu J, Guan QH, Sun YF, Liu XM, Zhang GY.** 2007. Opposing effects of Bad phosphorylation at two distinct sites by Akt1 and JNK1/2 on ischemic brain injury. Cell Signal **19:**1844-1856.

96. **Gross A, McDonnell JM, Korsmeyer SJ.** 1999. BCL-2 family members and the mitochondria in apoptosis. Genes Dev **13:**1899-1911.

97. **Srivastava RK, Mi QS, Hardwick JM, Longo DL.** 1999. Deletion of the loop region of Bcl-2 completely blocks paclitaxel-induced apoptosis. Proc Natl Acad Sci U S A **96:**3775-3780.

98. **Yamamoto K, Ichijo H, Korsmeyer SJ.** 1999. BCL-2 is phosphorylated and inactivated by an ASK1/Jun N-terminal protein kinase pathway normally activated at G(2)/M. Mol Cell Biol **19:**8469-8478.

99. **Tsuruta F, Sunayama J, Mori Y, Hattori S, Shimizu S, Tsujimoto Y, Yoshioka K, Masuyama N, Gotoh Y.** 2004. JNK promotes Bax translocation to mitochondria through phosphorylation of 14-3-3 proteins. EMBO J **23:**1889-1899.

100. **Madesh M, Antonsson B, Srinivasula SM, Alnemri ES, Hajnoczky G.** 2002. Rapid kinetics of tBid-induced cytochrome c and Smac/DIABLO release and mitochondrial depolarization. J Biol Chem **277:**5651-5659.

101. **Deng Y, Ren X, Yang L, Lin Y, Wu X.** 2003. A JNK-dependent pathway is required for TNFalpha-induced apoptosis. Cell **115:**61-70.

102. **Turjanski AG, Vaque JP, Gutkind JS.** 2007. MAP kinases and the control of nuclear events. Oncogene **26:**3240-3253.

103. **Fan M, Chambers TC.** 2001. Role of mitogen-activated protein kinases in the response of tumor cells to chemotherapy. Drug Resist Updat **4:**253-267.

104. **Tournier C, Hess P, Yang DD, Xu J, Turner TK, Nimnual A, Bar-Sagi D, Jones SN, Flavell RA, Davis RJ.** 2000. Requirement of JNK for stress-induced activation of the cytochrome c-mediated death pathway. Science **288:**870-874.

105. **Lee LF, Li G, Templeton DJ, Ting JP.** 1998. Paclitaxel (Taxol)-induced gene expression and cell death are both mediated by the activation of c-Jun NH2-terminal kinase (JNK/SAPK). J Biol Chem **273:**28253-28260.

106. **Koyama T, Mikami T, Koyama T, Imakiire A, Yamamoto K, Toyota H, Mizuguchi J.** 2006. Apoptosis induced by chemotherapeutic agents involves c-Jun N-terminal kinase activation in sarcoma cell lines. J Orthop Res **24:**1153-1162.

107. **Favata MF, Horiuchi KY, Manos EJ, Daulerio AJ, Stradley DA, Feeser WS, Van Dyk DE, Pitts WJ, Earl RA, Hobbs F, Copeland RA, Magolda RL, Scherle PA, Trzaskos JM.** 1998. Identification of a novel inhibitor of mitogen-activated protein kinase kinase. J Biol Chem **273:**18623-18632.

108. **Lopez-Bergami P, Huang C, Goydos JS, Yip D, Bar-Eli M, Herlyn M, Smalley KS, Mahale A, Eroshkin A, Aaronson S, Ronai Z.** 2007. Rewired ERK-JNK signaling pathways in melanoma. Cancer Cell **11:**447-460.

109. **Bonner WM, Redon CE, Dickey JS, Nakamura AJ, Sedelnikova OA, Solier S, Pommier Y.** 2008. GammaH2AX and cancer. Nat Rev Cancer **8:**957-967.

110. **Yuan J, Adamski R, Chen J.** 2010. Focus on histone variant H2AX: to be or not to be. FEBS Lett **584:**3717-3724.

111. **Mukherjee B, Kessinger C, Kobayashi J, Chen BP, Chen DJ, Chatterjee A, Burma S.** 2006. DNA-PK phosphorylates histone H2AX during apoptotic DNA fragmentation in mammalian cells. DNA Repair (Amst) **5:**575-590.

112. **Prior IA, Lewis PD, Mattos C.** 2012. A comprehensive survey of Ras mutations in cancer. Cancer Res **72:**2457-2467.

CIRRICULUM VITAE

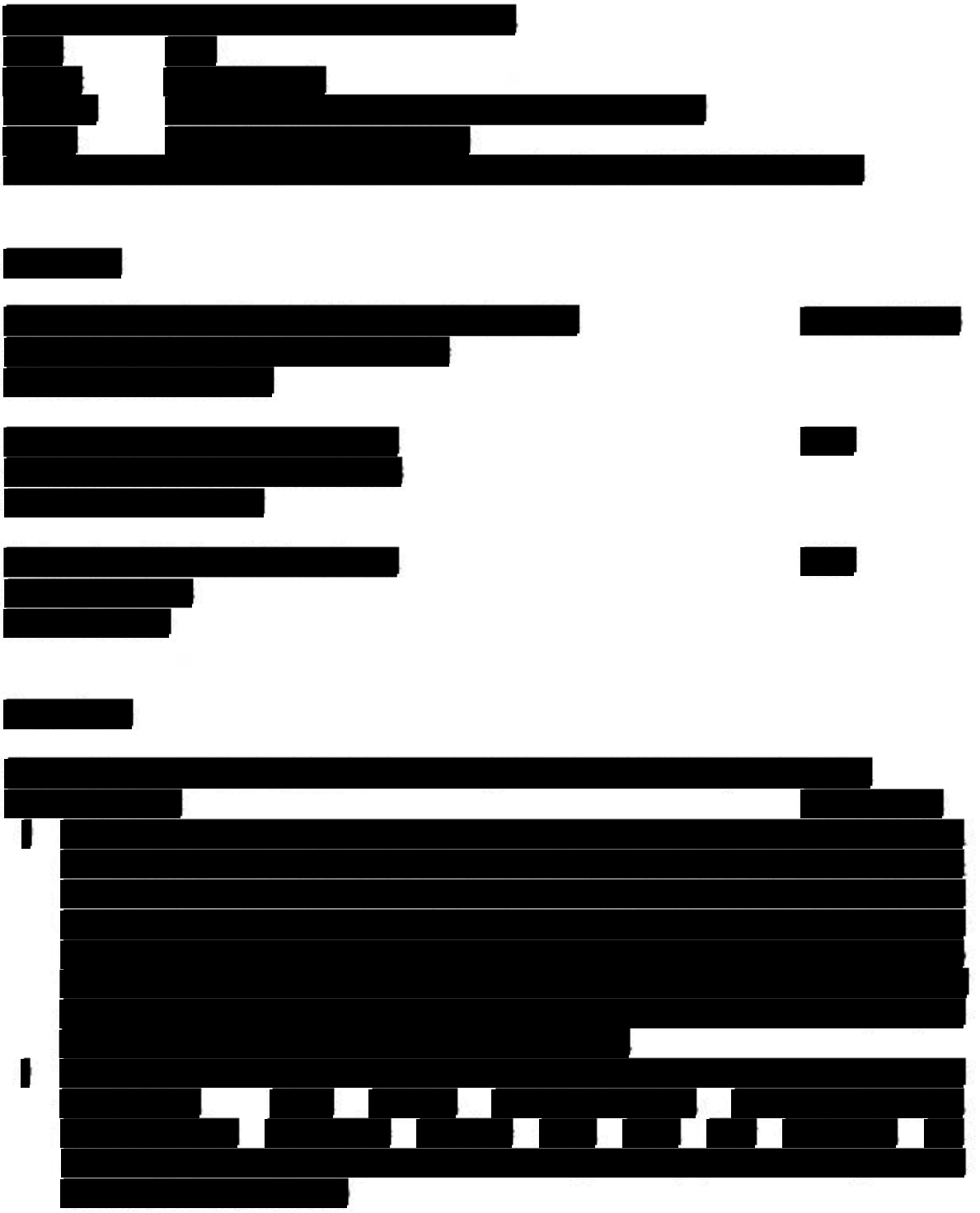

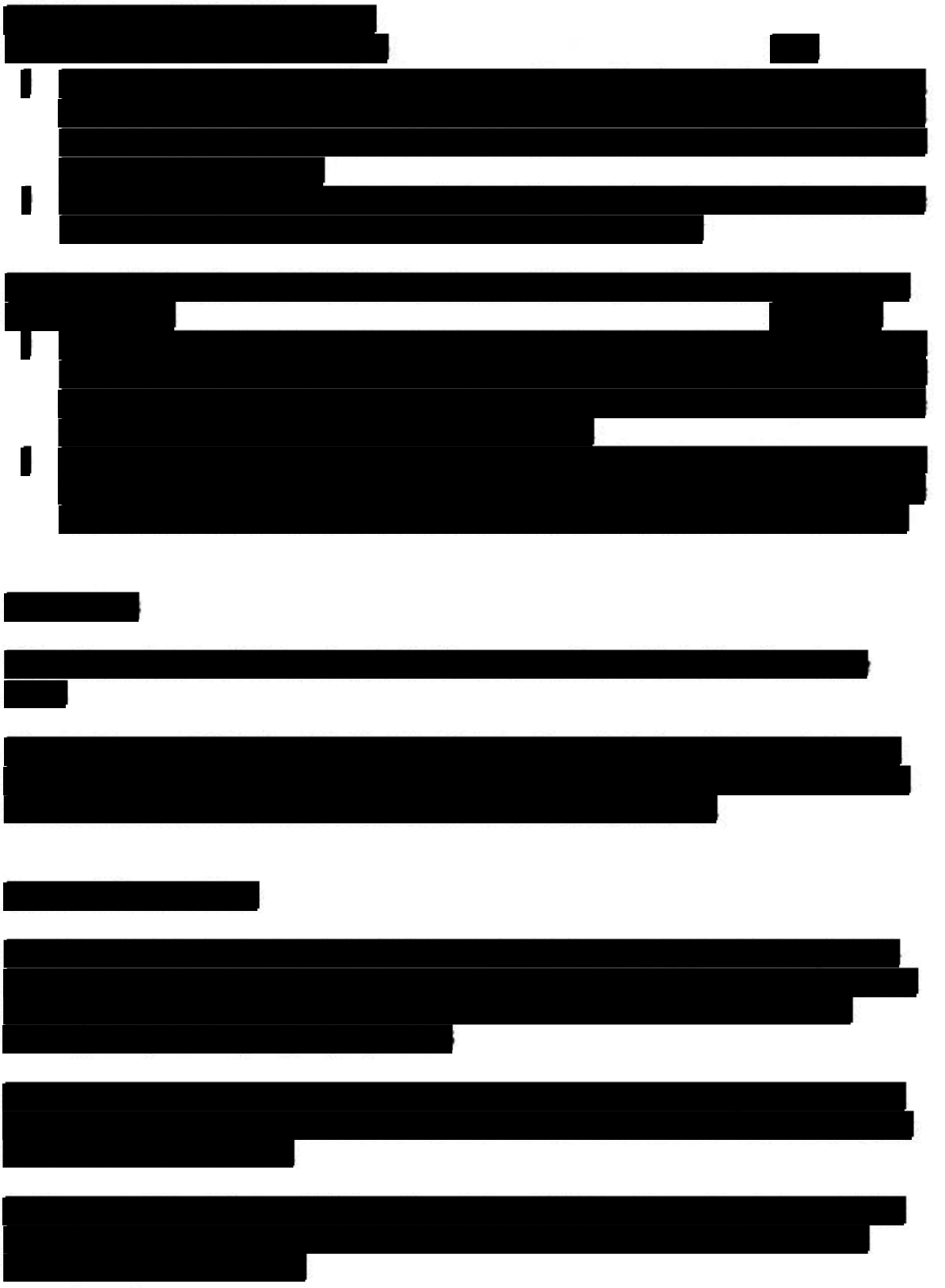

[redacted]

[redacted]

[redacted]

[redacted]